

Time-dependent Assessment of the Human Lumbar Spine in Response to Flexion
Exposures: *In Vivo* Measurement and Modeling

Nima Toosizadeh

Dissertation submitted to the faculty of the Virginia Polytechnic Institute and State University in
partial fulfillment of the requirements for the degree of

Doctor of Philosophy

In

Industrial and Systems Engineering

Maury A. Nussbaum, Chair

Michael J. Agnew

Michael L. Madigan

Robert H. Sturges

Robert L. West

Feb 8, 2013

Blacksburg, Virginia

Keywords: Lumbar spine; Prolonged flexion; Repetitive flexion; Viscoelastic modeling;
Biomechanics

UMI Number: 3585848

All rights reserved

INFORMATION TO ALL USERS

The quality of this reproduction is dependent upon the quality of the copy submitted.

In the unlikely event that the author did not send a complete manuscript and there are missing pages, these will be noted. Also, if material had to be removed, a note will indicate the deletion.



UMI 3585848

Published by ProQuest LLC (2014). Copyright in the Dissertation held by the Author.

Microform Edition © ProQuest LLC.

All rights reserved. This work is protected against unauthorized copying under Title 17, United States Code



ProQuest LLC.
789 East Eisenhower Parkway
P.O. Box 1346
Ann Arbor, MI 48106 - 1346

Time-dependent Assessment of the Human Lumbar Spine in Response to Flexion Exposures:

In Vivo Measurement and Modeling

Nima Toosizadeh

ABSTRACT

Among several work-related injuries, low back disorders (LBDs) are the leading cause of lost workdays, and with annual treatment costs in excess of \$10 billion in the US. Epidemiological evidence has indicated that prolonged and/or repetitive non-neutral postures, such as trunk flexion, are commonly associated with an increased risk of LBDs. Trunk flexion can result in viscoelastic deformations of soft tissues and subsequent mechanical and neuromuscular alterations of the trunk, and may thereby increase LBD risk. While viscoelastic behaviors of isolated spinal motion segments and muscles have been extensively investigated, *in vivo* viscoelastic responses of the trunk have not, particularly in response to flexion exposures. Further, most biomechanical efforts at understanding occupational LBDS have not considered the influence of flexion exposures on spine loads.

Four studies were completed to characterize viscoelastic deformation of the trunk in response several flexion exposures and to develop and evaluate a computational model of the human trunk that accounts for time-dependent characteristics of soft tissues. Participants were exposed to prolonged flexion at different trunk angles and external moments, and repetitive trunk flexion with different external moments and flexion rates. Viscoelastic properties were quantified using laboratory experiments and viscoelastic models. A multi-segment model of the upper body was developed and evaluated, and then used to estimate muscle forces and spine loads during simulated lifting tasks before and after prolonged trunk flexion at a constant angle and constant external moment. Material properties from the earlier experiments were used to evaluate/calibrate the model.

Experimental results indicated important effects of flexion angle, external moment, and flexion rate on trunk viscoelastic behaviors. Material properties from fitted Kelvin-solid models differed with flexion angle and external moment. Nonlinear viscoelastic behavior of the trunk tissues was evident, and predictive performance was enhanced using Kelvin-solid models with ≥ 2

retardation/relaxation time constants. Predictions using the multi-segment model suggested increases in spine loads following prolonged flexion exposures, primarily as a consequence of additional muscle activity. As a whole, these results help to characterize the effects of trunk flexion exposures on trunk biomechanics, contribute to more effective estimates of load distribution among passive and active components, enhance our understanding of LBD etiology, and may facilitate future controls/interventions.

Acknowledgments

This dissertation would not have been possible without the guidance and the help of several individuals over the last four years. First and foremost, I appreciate my advisor Dr. Maury Nussbaum for his continuous guidance and support. I have learned not only technical research methods but also a new vision for problem solving, which will help me in my professional career in future. I also appreciate my committee members, Dr. Michael Agnew, Dr. Michael Madigan, Dr. Robert Sturges, and Dr. Robert West for their support during my PhD coursework and their feedback on this dissertation.

I thank all members of the Industrial Ergonomics and Biomechanics Lab, especially Dr. Babak Bazrgari, Dr. Brad Hendershot, and Khoirul Muslim. I had a really great time working and collaborating with them. I thank Randy Waldron for his help with designing and constructing the experimental equipment used in this research.

To my family: Thank you for your help and support, although you were million miles away, you never stop encouraging me in every aspect of my life. And to my best friend Yasamin Khorramzadeh, thank you for everything. It was a great pleasure having you as a support during my study here at Virginia Tech.

Table of Contents

1 Introduction	1
1.1 Low Back Disorders (LBDs) and Risk Factors	1
1.2 Potential Mechanism of LBD Risk due to Flexion Exposures	2
1.3 Measuring the Viscoelastic Properties of the Spine	4
1.4 Modeling Viscoelastic Behaviors	5
1.5 Aims and Chapter Organization	7
1.6 References	8
2 Load-relaxation Properties of the Human Trunk in Response to Prolonged Flexion: Measuring and Modeling the Effect of Flexion Angle	13
Abstract	13
2.1 Introduction.....	15
2.2 Methods.....	17
2.3 Results.....	25
2.4 Discussion.....	30
2.5 References.....	37
3 Creep Deformation of the Human Trunk in Response to Prolonged and Repetitive Flexion: Measuring and Modeling the Effect of External Moment and Flexion Rate	42
Abstract	42
3.1 Introduction.....	43
3.2 Methods: Prolonged Flexion.....	45
3.2.1 Participants.....	45
3.2.2 Experimental design and procedures	45
3.2.3 Outcome measures	48
3.2.4 Viscoelastic models	49
3.2.5 Data analysis	51
3.3 Results: Prolonged Flexion.....	51
3.4 Methods: Repetitive Flexion.....	55
3.4.1 Participants.....	55
3.4.2 Experimental design and procedure.....	55
3.4.3 Outcome measures	56
3.4.4 Viscoelastic models	57
3.4.5 Data analysis	58
3.5 Results: Repetitive Flexion.....	58
3.6 Discussion.....	59
3.6.1 Prolonged trunk flexion	59
3.6.2 Repetitive trunk flexion	63
3.6.3 Limitations, implications, and conclusions.....	63
3.7 References.....	65

4 Prolonged Trunk Flexion can Increase Spine Loads During a Subsequent Lifting Task: An Investigation of the Effects of Trunk Flexion Duration and Angle using a Sagittaly Symmetric Viscoelastic Spine Model	68
Abstract	68
4.1 Introduction.....	69
4.2 Methods.....	71
4.2.1 Modeling approach	71
4.2.2 Model calibration and evaluation	75
4.2.3 Prolonged flexion exposures.....	76
4.3 Results	77
4.3.1 Calibration and evaluation results	77
4.3.2 Results from prolonged flexion exposures	78
4.4 Discussion.....	79
4.5 Appendix.....	86
4.6 References.....	88
5 Trunk Tissue Creep Can Increase Spine Forces During a Subsequent Lifting Task: An Investigation of the Effects of Trunk Flexion on Spine Mechanical Behaviors Using Experimental and Viscoelastic Modeling Approaches	93
Abstract	93
5.1 Introduction.....	95
5.2 Methods.....	97
5.2.1 Modeling approach	98
5.2.2 Model calibration and evaluation	99
5.2.3 Flexion/lifting kinematics	99
5.2.4 Flexion/lifting simulations	102
5.3 Results	102
5.3.1 Experiment results: kinematics and nEMG	102
5.3.2 Model-based results: creep, spine forces, and muscle forces	104
5.4 Discussion.....	106
5.5 References.....	111
6 Conclusions	114
6.1 Effects of task conditions on trunk viscoelastic behaviors	114
6.2 Characterizing trunk viscoelastic behaviors using Kelvin-solid models	115
6.3 Changes in spine loads due to prolonged trunk flexion	115
6.4 Limitations and future direction.....	116
6.5 Summary.....	117
Appendix A	118

List of Figures

Figure 2.1: Experimental setup for load-relaxation test (60% FR angle condition illustrated).....	20
Figure 2.2 Illustration of a hysteresis loop. The highlighted area (ΔE) denotes the dissipated energy; NZ in flexion (extension) is the distance between point A (point B) and the neutral posture. Target lumbar flexion angle = 30, 40, 60, 80, or 100% FR.	21
Figure 2.3: Kelvin-solid models: (a) SLS model (b) Prony Series model. Each spring and damper in series represents a Maxwell model. For clarity, linear rather than rotational components are illustrated.	23
Figure 2.4: Effects of lumbar flexion angles on direct outcome measures: (a) initial moment, (b) moment drop, and (c) percentage change in normalized NZ. Post-hoc groupings are indicated by brackets and letters, and best-fit exponential relationships are provided.....	26
Figure 2.5: Mean measures of viscoelastic model prediction quality: (a) R^2 and (b): root-mean-square errors (RMSE)	27
Figure 2.6: Effects of lumbar flexion angle on SLS model parameters: (a): stiffness of Maxwell component = K_1 , (b): parallel stiffness = K_2 , (c): relaxation time constant = T , and (d): instantaneous stiffness = $K_1 + K_2$. Post-hoc groupings are indicated by brackets and letters, and best-fit relationships (linear or exponential) are provided.....	28
Figure 2.7: Fast and slow phases of moment drop during the load-relaxation period. Representative data are shown, and which indicate the advantage of the Prony Series over SLS model for predicting measured behaviors. Results are for a 100% FR exposure	35
Figure 3.1: Experimental setup for creep testing (condition with 42 N of extra load is illustrated), including placement of inertial measurement units (IMUs)	46
Figure 3.2: Sample results, indicating lumbar flexion angle during creep exposure and recovery, and selected outcome measures. Experimental data are illustrated in grey for an exposure with 85 N of extra load	48
Figure 3.3: Illustration of two Kelvin-solid models: GK (top), and SNS (bottom). Each spring and damper combination in parallel represents a Kelvin model. For clarity, linear rather than rotational components are illustrated	50

- Figure 3.4: Effects of external moment, induced using extra loads (at the wrists), on initial and creep angles. Post-hoc groupings are indicated by brackets and letters, and best-fit exponential relationships are provided. Mean values of extra loads (across genders) are presented52
- Figure 3.5: Effects of external moment on SNS model parameters for both genders: a) stiffness of Kelvin component (K_1); b) in-series (instantaneous) stiffness (K_2); and c) damping of Kelvin component (C). Best-fit relationships (linear or exponential) are provided53
- Figure 3.6: Representative data showing fast and slow phases of creep and recovery, and the, relative advantage of the GK vs. SNS models for predicting behaviors. Experimental results are mean values for exposures involving the largest external moment (i.e., largest extra load)54
- Figure 3.7: Predicted recovered angles using the GK and SNS models. Mean values of extra loads (across genders) are presented55
- Figure 3.8: Representative results illustrating lumbar flexion angle during cumulative creep, and selected outcome measures. Experimental data are illustrated in grey for a prolonged flexion exposure with 85 N of extra load and 4 flex/min rate57
- Figure 3.9: A cycle of external moment history for repetitive flexion at 4 flex/min rate. A similar moment history was applied for 2 and 3 flex/min rates, with longer rest periods58
- Figure 3.10: Effects of external moment and flexion rate on cumulative creep. Values are given for both experimental and model-predicted results. Mean values of extra load (across genders) are presented59
- Figure 4.1: Multi-segment model in an upright posture. *Global muscles* – ICPT: iliocostalis lumborum pars thoracic, LGPT: longissimus thoracis pars thoracic. *Local muscles* – ICPL: iliocostalis lumborum pars lumborum, LGPL: longissimus thoracis pars lumborum, MF: multifidus, and QL: quadratus lumborum. Hands and arms are not illustrated in this figure, and the figure is not to scale72
- Figure 4.2: SNS model representation of intervertebral discs and passive muscles. Here, K_1 and C are the respective stiffness and damping of a torsional/linear spring and damper components in series (Maxwell component), and K_2 is the stiffness of a parallel torsional/linear spring (Roylance, 2001). K_1 and C represent viscous responses to deformation, K_2 is the steady-state stiffness once the material is totally relaxed, and $K_1 + K_2$ is the instantaneous stiffness. The moment-time equation for the SNS model at a

constant flexion angle of θ_0 is $M(t) = \theta_0 \left(K_2 + K_1 e^{-\frac{K_1 t}{C}} \right)$ 74

Figure 4.3: Peak intradiscal pressure at L4/L5 in several tasks from an *in vivo* experiment (Wilke et al., 2001) and predicted by the current model. Model predictions were made under different conditions of muscle wrapping and specified levels of abdominal muscle (RA, EO, and IO) co-activity78

Figure 4.4: Increases in peak load, peak axial stiffness, and absorbed energy at L5/S1, following trunk flexion exposures of different durations and angles (as a % of flexion-relaxation angle = FR)79

Figure 4.5: Elastic properties of lumbar motion segments in (a) axial compression, and (b) sagittal rotation88

Figure 5.1: SNS model representation of intervertebral discs and passive muscles. Here, K_1 and C are the respective stiffness and damping of a torsional/linear spring and damper components in parallel (Kelvin component), and K_2 is the stiffness of a parallel torsional/linear spring (Royleance, 2001). K_1 and C represent viscous responses to deformation, $K_1 + K_2$ is the steady-state stiffness once the material is totally relaxed, and K_2 is the instantaneous stiffness. The creep angle-time equation for the SNS model at a constant external moment of M_0 is: $\theta(t) = \frac{M_0}{K_1} \left(\frac{K_1 + K_2}{K_2} - e^{-\frac{t}{\tau}} \right)$ 98

Figure 5.2: Changes in peak relative flexion of lumbar motion segments during lifting tasks performed before and after creep exposure. The symbol * indicates a significant post-exposure change103

Figure 5.3: Increase in muscle activity (nEMG) during lifting tasks performed before and after creep exposure. The symbol * indicates a significant post-exposure change103

Figure 5.4: Increases in predicted peak compression force (a) and antero-posterior shear force (b) during lifting tasks performed before and after creep exposures; the latter predictions were done using identical and modified kinematics105

List of Tables

Table 2.1: Mean (SD) values of estimated parameters for different viscoelastic models with respect to lumbar flexion angle (SLS model parameters are shown in Figure 2.6).....	28
Table 2.2: Dimensionless sensitivity coefficients for the four models with respect to initial moment and moment drop.	29
Table 3.1: Mean (SD) values of participant age and anthropometry in the two trunk flexion experiment.....	45
Table 3.2: Effects of external moment and gender on direct and derived outcome measures following prolonged flexion. The symbol * indicates a significant effect	52
Table 3.3: Effects of external moment and flexion rate on direct outcome measures following repetitive flexion. The symbol * indicates a significant effect	59
Table 4.1: Estimated relationships between viscous (K_1 and C) and elastic (K_2) components of spinal motion segments and muscles in the model	74
Table 4.2: Predicted reactive moments, and changes in compression and antero-posterior shear forces and muscle forces (passive and active) when performing lifting task prior to (Pre) and immediately following (Post) a simulated flexion exposure of 16 min at 100%FR angle. Peak values are reported at each spinal level, for lifting 180N. Muscles are listed at the level of insertion. (See Figure 1 caption for a list of muscles.).	81
Table 4.3: Mass centers (z): vertical locations of mass centers with respect to S1 in the vertical direction, Mass centers (x): horizontal distance from corresponding vertebral centers in the antero-posterior direction, with positive indicating posterior to S1.....	86
Table 4.4: Physiological cross section area (PCSA), and muscle origins and insertions. “z” and “x” values are vertical and horizontal locations with respect to S1, with positive indicating superior and posterior to S1, respectively. PCSA values from this table were multiplied by two to account for bilateral muscle pairs.....	87
Table 5.1: Estimated relationships between viscous (K_1 and C) and elastic (K_2) components of spinal motion segments and muscles used in the biomechanical model	99
Table 5.2: Predicted changes in peak passive and active muscle forces (all values in Newton) during lifting tasks performed prior to (Pre) and immediately following (Post) a simulated 6-minute creep exposure. Muscles are listed at the level of origin.....	104

1 Introduction

1.1 Low Back Disorders (LBDs) and Risk Factors

LBDs are one of the most frequent type of injuries, with a lifetime probability of occurrence that may be as high as 80% (Rubin 2007). LBDs are costly in terms of both direct treatment expenses (e.g. physician service, medication and hospital stays) and indirect personal costs (e.g. absenteeism and decreased productivity) (Dagenais et al., 2008). Health care expenditures for treatment for spine-related problems in the United States alone accounted for approximately \$86 billion from 1997 to 2006 (Martin et al., 2009). In addition, the total number of people seeking treatment for spinal problems in the United States increased from 14.8 million in 1997 to 21.9 million in 2006, leading to an average 7.0% increase in expenditures per year (Martin et al., 2009). These data draw attention to the need for more investigation on the potential risk factors of LBDs and prevention strategies for reducing back injuries.

Diverse LBD risk factors have been identified, and which can be divided into physical, psychological, and individual (e.g. gender, age and smoking) causes. Roughly 37% of LBDs are attributed to physical (occupational) risk factors (Punnett et al., 2005), and among these, trunk flexion exposures and lifting are important. A large number of both daily and occupational tasks require prolonged and/or repetitive trunk flexion. Occupationally, there is strong evidence to suggest that trunk flexion can increase the risk of a LBD (Hatipkarasulu et al., 2011; Hoogendoorn et al., 1999; Kuiper et al., 1999,). For example, a prospective cohort study found an increase in risk of LBDs among workers who worked with their trunk at a minimum of 60° of flexion for more than 5% of the day, and for workers who lifted a load of at least 25 kg more than 15 times per working day (Hoogendoorn et al., 2000). On the other hand, a review by

Roffey, et al., (2010) concluded that there is not sufficient evidence for a causal role of non-neutral spine postures, such as spine flexion, when it is considered independent of other factors (Roffey et al., 2010). Accordingly, it is difficult to evaluate the effect of an individual exposure or factor, since there are close interactions between different exposures/factors (Manek and MacGregor 2005) and since no single method is available for evaluating risks in diverse occupational tasks (Nelson and Hughes 2009). As such, the combination of different factors (e.g. trunk flexion exposure and lifting) may be more predictive of LBDs than individual factors. To investigate these interrelations, and to improve our understandings of LBD causalities, there is thus value in assessing the potential interactions, or inter-dependencies, between distinct risk factors.

1.2 Potential Mechanism of LBD Risk due to Flexion Exposure

From a mechanical viewpoint, all components of the vertebral column show time-dependent behavior when exposed to prolonged loadings (Phillips et al., 2004; Pollintine et al., 2010; Wang et al., 1997). Ligaments, collagen fibers, and passive components of muscles act as viscoelastic materials due to a gradual rearrangement of collagen fibers (Oliver and Twomey 1995).

Intervertebral discs respond to an applied load by exuding fluid both from the nucleus and the annulus through the endplates (Silva et al., 2005). Over time, the gradual deformation of bony tissues (cortical and trabecular) caused by micro-cracking of the bone matrix, can lead to creep of collagen fibers (Pollintine et al., 2009). As such, prolonged or repetitive trunk flexion results in viscoelastic deformation of soft tissues, and consequently a laxity of the trunk as a whole.

Based on previous studies on humans, trunk stiffness can decrease up to 39% after 16 min of flexion (Hendershot et al., 2011). Such changes in stiffness properties are also denoted as

reductions in “intrinsic” stiffness. As the intrinsic stiffness of the spine decreases, equilibrating any external moment and maintaining stability is typically compensated by additional activation of muscles (Hodges et al., 2009; Olson et al., 2009; Shin and Mirka 2007, Shin et al., 2009). Such compensatory muscle activation, in turn, can cause additional (or increased) loads on joints and other soft tissues. As such, even small changes in the passive stiffness of motion segments can result in substantial changes in spine load, due to the fact that the moment arms of paraspinal muscles are relatively small.

Trunk flexion exposures can also cause alterations in trunk neuromuscular behaviors. The efficiency of the mechanoreceptors in ligaments and other soft tissues can be affected by stretching, as in trunk flexion exposures, leading to impaired force distribution among muscle fascicles and compromised reflexive responses (Cholewicki et al., 2005; Rogers and Granata 2006; Solomonow 2011; Stubbs et al., 1998). Reflex response has an important role in controlling the stability of the spine, and can achieve this with less energy expenditure compared to co-contraction of the torso musculature (Franklin and Granata 2007; Moorhouse and Granata 2007). Thus, with a deterioration of reflexive mechanism of the spine, additional muscle-generated forces are imposed on spinal motion segments, and which may contribute to LBD development.

These are two main proposed pathways by which LBDs are thought to be caused by flexion exposures and stretching of soft tissues. These pathways suggest that when evaluating an occupational task, such as lifting, there is a need for measuring the effects of prior spinal exposures (e.g., postures). Accounting for such “history dependence” may aid in the

development of method that provide more accurate estimations of spine loads and potential LBD risks for diverse occupational tasks. The following section summarizes existing approaches and major results from studies that have measured and modeled the viscoelastic behavior of soft tissues. In this summary, existing research gap(s) are identified in some areas.

1.3 Measuring the Viscoelastic Properties of the Spine

Many empirical studies have explored the viscoelastic responses of spinal motion segments and muscles. These studies have involved *in vitro* measurements of axial creep (Burns et al., 1984; Kazarian 1975; Keller et al., 1987; Pollintine et al., 2010) and flexion/extension creep (Little and Khalsa 2005; Oliver and Twomey 1995; Twomey and Taylor 1982; Twomey and Taylor 1983), as well as *in vivo* measurements of whole-body creep (Brown 1992; Hedman and Fernie 1995; McGill and Kurutz 2006). A few experiments have also addressed the load-relaxation response of thoracolumbar segments using cadaver motion segments (Adams and Dolan 1996; Holmes and Hukins 1996; Johannessen et al., 2004; Little and Khalsa 2005). Many studies have also determined the viscoelastic properties of muscle, using both *in vitro* (Abbott and Lowy 1957; Glantz 1974; Truong 1974; Greven and Hohorst 1975; Linke and Leake 2004; Sanjeevi 1982; Taylor et al., 1990) and *in vivo* (Best et al., 1994; Hawkins et al., 2009; Magnusson et al., 1995; Magnusson et al., 1996; Magnusson et al., 2000; Ryan et al., 2010; Ryan et al., 2011) measurements, in response to creep, load-relaxation, and cyclic loadings. These studies have provided a fundamental understanding of the time-dependent response of trunk soft tissues, which is of substantial biomechanical and clinical importance and utility. However, there are some gaps in these investigations that need to be addressed before a viscoelastic model of the spine can be developed.

Most measurements of viscoelastic properties of the spine have been performed on cadaver motion segments. A primary limitation of *in vitro* experiments is the lack of metabolic processes of intervertebral discs, respiration, circulation and muscle activity, which can influence measurements of viscoelastic properties in prolonged tests (Hult et al., 1995; Keller et al., 1990). While tissue properties obtained from *in vitro* studies are useful for estimating elastic and viscous behaviors, they should be adjusted using *in vivo* measurements on the intact human spine to derive more accurate properties for biomechanical models. Further, there is evidence of nonlinear viscoelastic behaviors of trunk soft tissues (Hult et al., 1995; Troyer and Puttlitz 2011). Nonlinear viscoelasticity can be demonstrated, for example, as a different creep response at different magnitudes of loading, or by different load-relaxation responses at different magnitudes of displacement (Findley et al., 1989). Some experiments have assessed the nonlinearity in elastic response of spinal motion segments (Guan et al., 2007; Panjabi et al., 1994); however, evaluating the nonlinearity in viscoelastic behavior at different magnitudes of loading/displacement has not been broadly reported. Thus, there is a need to explore the viscoelastic properties of the trunk in more detail, to attain a better understanding of time-dependent behaviors due to prolonged and repetitive loadings.

1.4 Modeling Viscoelastic Behaviors

Several approaches have been developed and applied to model the viscoelastic behavior of soft tissues. One of the most common approaches is based on the equation of creep or load-relaxation for a viscoelastic material. In this approach, Kelvin-solid models have been used typically, to characterize the force-time or displacement-time responses of a spinal motion segment (Alfrey and Doty 1945; Burns et al., 1984; Holmes and Hukins 1996; Johannessen et

al., 2004; Keller et al., 1987; Keller and Nathan 1999; Pollintine et al., 2010). Among different types of Kelvin-solid models, the standard linear solid (SLS) model has generated acceptable predictions of viscoelastic responses under quasi-static conditions (Groth and Granata 2008). However, when this model was applied to dynamic loadings it showed several limitations (Li et al., 1995). Groth and Granata (2008) improved the SLS model by adding a nonlinear component and use the resulting standard nonlinear solid (SNS) model to develop predictions of dynamic responses of the intervertebral joint. This addition, though, was made only for elastic behavior in the model. In the same way, a model of the viscoelastic behavior of a motion segment can be refined, by measuring and employing time-dependent properties obtained in response to a range of loadings/displacements. These properties, though, are yet to be established and implemented in biomechanical models to improve estimates of both dynamic and static responses.

In another approach (Argoubi and Shirazi-Adl 1996), a poroelastic material was modeled, consisting of a fully saturated porous medium (solid matrix skeleton) and an interstitial fluid (pore fluid). Several studies have applied this type of approach to intervertebral discs, to measure/predict creep and load-relaxation behaviors (Ehlers et al., 2009; Riches et al., 2002; Wu and Chen 1996). Using poroelastic material properties for intervertebral discs can provide comprehensive information regarding biomechanical behaviors, such as fluid loss, pore pressure and strain/stress in each component of intervertebral discs (Schmidt et al., 2010). Yet, most of these detailed aspects are not relevant to or required for purposes of occupational task evaluation, and models based on this approach can lead to lengthy computational run-times for spine load calculations. Thus, implementing less complicated models, such as the Kelvin-solid models, is likely sufficient to predict time-dependent force-displacement behaviors of the spine. By

maintaining a balance between model detail and computational efficiency, a usable and effective model is likely to be obtainable for task evaluation. Although biomechanical models of the spine have been extensively reported, there remains a need for a time-dependent model to evaluate the noted interrelationships between different LBD risk factors.

1.5 Aims and Chapter Organization

The main goal of the current research was to develop and evaluate a computational model of the human upper body, with emphasis on the lumbar spine, and that accounts for time-dependent characteristics of human trunk tissues. The central hypothesis was that prolonged and repetitive trunk flexion can increase the risk of LBDs by increasing spine loads. It was also hypothesized that the trunk exhibits nonlinear viscoelastic behaviors. To evaluate these hypotheses, *in vivo* experimental studies and biomechanical modeling efforts were conducted to quantify trunk viscoelastic behavior in response to flexion exposures; a viscoelastic model of the trunk was developed and evaluated, and the effects of diverse flexion exposures on spine loads during a lifting task were investigated using the viscoelastic model.

Two laboratory and two modeling studies were completed. In the first two studies, trunk viscoelastic properties were measured in response to prolonged and repetitive flexion exposures at several flexion angles, external moments, and flexion rates. The third and fourth studies developed and evaluated a viscoelastic model using results from the first two. Then, the model was used to estimate time-dependent changes in spine load, during a lifting task, as a result of several flexion exposures. This dissertation is organized with one chapter for each study. Chapter 2 describes measuring and modeling of load-relaxation properties of the human trunk in

response to prolonged flexion at different flexion angles. Chapter 3 describes measuring and modeling of creep deformation of the human trunk in response to prolonged and repetitive flexion at different external moments and flexion rates. Chapter 4 examines the effect of prolonged trunk flexion at a constant flexion angle on spine loads during a lifting task. Chapter 5 investigates the effect of prolonged trunk flexion at constant external moment on spine loads during a lifting task. In the latter two Chapters, a viscoelastic model was developed and used to estimate time-dependent changes in spine load. A summary of the results from all studies and several implications are presented in Chapter 6.

1.6 References

- Abbott, B., Lowy, J., 1957. Stress relaxation in muscle. *Proc. R. Soc. Lond. B. Biol. Sci.*, 146, 281-288.
- Adams, M., Dolan, P., 1996. Time-dependent changes in the lumbar spine's resistance to bending. *Clinical Biomechanics*, 11, 194-200.
- Alfrey, T., Doty, P., 1945. The methods of specifying the properties of viscoelastic materials. *Journal of Applied Physics*, 16, 700-713.
- Argoubi, M., Shirazi-Adl, A., 1996. Poroelastic creep response analysis of a lumbar motion segment in compression. *J. Biomech.*, 29, 1331-1339.
- Best, T.M., Mcelhaney, J., Garrett Jr, W.E., Myers, B.S., 1994. Characterization of the passive responses of live skeletal muscle using the quasi-linear theory of viscoelasticity. *J. Biomech.*, 27, 413-419.
- Burns, M., Kaleps, I., Kazarian, L., 1984. Analysis of compressive creep behavior of the vertebral unit subjected to a uniform axial loading using exact parametric solution equations of kelvin-solid models--part i. *Human intervertebral joints. J. Biomech.*, 17, 113-115, 117-130.
- Cholewicki, J., Silfies, S.P., Shah, R.A., Greene, H.S., Reeves, N.P., Alvi, K., Goldberg, B., 2005. Delayed trunk muscle reflex responses increase the risk of low back injuries. *Spine*, 30, 2614-2620.
- Dagenais, S., Caro, J., Haldeman, S., 2008. A systematic review of low back pain cost of illness studies in the united states and internationally. *The spine journal: official journal of the North American Spine Society*, 8, 8-20.
- Ehlers, W., Karajan, N., Markert, B., 2009. An extended biphasic model for charged hydrated tissues with application to the intervertebral disc. *Biomechanics and modeling in mechanobiology*, 8, 233-251.
- Findley, W.N., Lai, J.S., Onaran, K., 1989. *Creep and relaxation of nonlinear viscoelastic materials: With an introduction to linear viscoelasticity*, Dover Publications.

- Franklin, T.C., Granata, K.P., 2007. Role of reflex gain and reflex delay in spinal stability—a dynamic simulation. *J. Biomech.*, 40, 1762-1767.
- Glantz, S.A., 1974. A constitutive equation for the passive properties of muscle. *J. Biomech.*, 7, 137-145.
- Greven, K., Hohorst, B., 1975. Creep after loading in relaxed and contracted (kcl or k2so4 depolarized) smooth muscle (taenia coli of the guinea pig). *Pflugers Arch.*, 359, 111-125.
- Groth, K.M., Granata, K.P., 2008. The viscoelastic standard nonlinear solid model: Predicting the response of the lumbar intervertebral disk to low-frequency vibrations. *J. Biomech. Eng.*, 130, 031005.
- Guan, Y., Yoganandan, N., Moore, J., Pintar, F.A., Zhang, J., Maiman, D.J., Laud, P., 2007. Moment-rotation responses of the human lumbosacral spinal column. *J. Biomech.*, 40, 1975-1980.
- Hatipkarasulu, G.S., Aghazadeh, F., Nimbarte, A.D., 2011. Loading and recovery behavior of the human lumbar spine under static flexion. *Work*, 38, 111-122.
- Hawkins, D., Lum, C., Gaydos, D., Dunning, R., 2009. Dynamic creep and pre-conditioning of the achilles tendon in-vivo. *J. Biomech.*, 42, 2813-2817.
- Hedman, T.P., Fernie, G.R., 1995. In vivo measurement of lumbar spinal creep in two seated postures using magnetic resonance imaging. *Spine*, 20 (2), 178.
- Hendershot, B., Bazrgari, B., Muslim, K., Toosizadeh, N., Nussbaum, M.A., Madigan, M.L., 2011. Disturbance and recovery of trunk stiffness and reflexive muscle responses following prolonged trunk flexion: Influences of flexion angle and duration. *Clin. Biomech.*, 26, 250-256.
- Hodges, P., Van Den Hoorn, W., Dawson, A., Cholewicki, J., 2009. Changes in the mechanical properties of the trunk in low back pain may be associated with recurrence. *J. Biomech.*, 42, 61-66.
- Holmes, A., Hukins, D., 1996. Analysis of load-relaxation in compressed segments of lumbar spine. *Med. Eng. Phys.*, 18, 99-104.
- Hoogendoorn, W.E., Bongers, P.M., De Vet, H.C.W., Douwes, M., Koes, B.W., Miedema, M.C., Ariëns, G.a.M., Bouter, L.M., 2000. Flexion and rotation of the trunk and lifting at work are risk factors for low back pain: Results of a prospective cohort study. *Spine*, 25, 3087-3092.
- Hoogendoorn, W.E., Van Poppel, M.N.M., Bongers, P.M., Koes, B.W., Bouter, L.M., 1999. Physical load during work and leisure time as risk factors for back pain. *Scand. J. Work. Environ. Health*, 25, 387-403.
- Hult, E., Ekström, L., Kaigle, A., Holm, S., Hansson, T., 1995. In vivo measurement of spinal column viscoelasticity—an animal model. *Proc Inst Mech Eng H*, 209, 105-110.
- Johannessen, W., Vresilovic, E.J., Wright, A.C., Elliott, D.M., 2004. Intervertebral disc mechanics are restored following cyclic loading and unloaded recovery. *Ann. Biomed. Eng.*, 32, 70-76.
- Kazarian, L., 1975. Creep characteristics of the human spinal column. *Orthop Clin North Am*, 6, 3-18.
- Keller, T., Spengler, D., Hansson, T., 1987. Mechanical behavior of the human lumbar spine. I. Creep analysis during static compressive loading. *J. Orthop. Res.*, 5, 467-478.
- Keller, T.S., Holm, S.H., Hansson, T.H., Spengler, D., 1990. The dependence of intervertebral disc mechanical properties on physiologic conditions. *Spine*, 15, 751-761.

- Keller, T.S., Nathan, M., 1999. Height change caused by creep in intervertebral discs: A sagittal plane model. *J Spinal Disord Tech*, 12, 313-324.
- Kuiper, J.I., Burdorf, A., Verbeek, J.H.a.M., Frings-Dresen, M.H.W., Van Der Beek, A.J., Viikari-Juntura, E.R.A., 1999. Epidemiologic evidence on manual materials handling as a risk factor for back disorders: A systematic review. *Int J Ind Ergon*, 24, 389-404.
- Kurutz, M., 2006. In vivo age-and sex-related creep of human lumbar motion segments and discs in pure centric tension. *J. Biomech.*, 39, 1180-1190.
- Li, S., Patwardhan, A.G., Amirouche, F.M.L., Havey, R., Meade, K.P., 1995. Limitations of the standard linear solid model of intervertebral discs subject to prolonged loading and low-frequency vibration in axial compression. *J. Biomech.*, 28, 779-790.
- Linke, W.A., Leake, M.C., 2004. Multiple sources of passive stress relaxation in muscle fibres. *Phys. Med. Biol.*, 49, 3613-3827.
- Little, J.S., Khalsa, P.S., 2005. Human lumbar spine creep during cyclic and static flexion: Creep rate, biomechanics, and facet joint capsule strain. *Ann. Biomed. Eng.*, 33, 391-401.
- Magnusson, S., Simonsen, E., Dyhre-Poulsen, P., Aagaard, P., Mohr, T., Kjaer, M., 1996. Viscoelastic stress relaxation during static stretch in human skeletal muscle in the absence of emg activity. *Scand. J. Med. Sci. Sports*, 6, 323-328.
- Magnusson, S., Simonsen, E.B., Aagaard, P., Gleim, G., Mchugh, M., Kjaer, M., 1995. Viscoelastic response to repeated static stretching in the human hamstring muscle. *Scand. J. Med. Sci. Sports*, 5, 342-347.
- Magnusson, S.P., Aagaard, P., Nielson, J.J., 2000. Passive energy return after repeated stretches of the hamstring muscle-tendon unit. *Med. Sci. Sports Exerc.*, 32, 1160-1164.
- Manek, N.J., Macgregor, A., 2005. Epidemiology of back disorders: Prevalence, risk factors, and prognosis. *Curr. Opin. Rheumatol.*, 17, 134-140.
- Martin, B.I., Turner, J.A., Mirza, S.K., Lee, M.J., Comstock, B.A., Deyo, R.A., 2009. Trends in health care expenditures, utilization, and health status among us adults with spine problems, 1997–2006. *Spine*, 34, 2077-2084.
- Mcgill, S., Brown, S., 1992. Creep response of the lumbar spine to prolonged full flexion. *Clin. Biomech.*, 7, 43-46.
- Moorhouse, K.M., Granata, K.P., 2007. Role of reflex dynamics in spinal stability: Intrinsic muscle stiffness alone is insufficient for stability. *J. Biomech.*, 40, 1058-1065.
- Nelson, N.A., Hughes, R.E., 2009. Quantifying relationships between selected work-related risk factors and back pain: A systematic review of objective biomechanical measures and cost-related health outcomes. *International Journal of Industrial Ergonomics*, 39, 202-210.
- Oliver, M., Twomey, L., 1995. Extension creep in the lumbar spine. *Clin. Biomech.*, 10, 363-368.
- Olson, M.W., Li, L., Solomonow, M., 2009. Interaction of viscoelastic tissue compliance with lumbar muscles during passive cyclic flexion–extension. *J. Electromyogr. Kinesiol.*, 19, 30-38.
- Panjabi, M., Oxland, T., Yamamoto, I., Crisco, J., 1994. Mechanical behavior of the human lumbar and lumbosacral spine as shown by three-dimensional load-displacement curves. *J. Bone Joint Surg. Am.*, 76, 413-424.
- Phillips, C., Repperger, D., Neidhard-Doll, A., Reynolds, D., 2004. Biomimetic model of skeletal muscle isometric contraction: I. An energetic-viscoelastic model for the skeletal muscle isometric force twitch. *Comput. Biol. Med.*, 34, 307-322.

- Pollintine, P., Luo, J., Offa-Jones, B., Dolan, P., Adams, M.A., 2009. Bone creep can cause progressive vertebral deformity. *Bone*, 45, 466-472.
- Pollintine, P., Van Tunen, M.S.L.M., Luo, J., Brown, M.D., Dolan, P., Adams, M.A., 2010. Time-dependent compressive deformation of the ageing spine: Relevance to spinal stenosis. *Spine*, 35, 386-394.
- Punnett, L., Prüss-Ütün, A., Nelson, D.I., Fingerhut, M.A., Leigh, J., Tak, S.W., Phillips, S., 2005. Estimating the global burden of low back pain attributable to combined occupational exposures. *Am. J. Ind. Med.*, 48, 459-469.
- Riches, P., Dhillon, N., Lotz, J., Woods, A., McNally, D., 2002. The internal mechanics of the intervertebral disc under cyclic loading. *J. Biomech.*, 35, 1263-1271.
- Roffey, D.M., Wai, E.K., Bishop, P., Kwon, B.K., Dagenais, S., 2010. Causal assessment of awkward occupational postures and low back pain: Results of a systematic review. *Spine J*, 10, 89-99.
- Rogers, E.L., Granata, K.P., 2006. Disturbed paraspinal reflex following prolonged flexion-relaxation and recovery. *Spine*, 31, 839-845.
- Rubin, D.I., 2007. Epidemiology and risk factors for spine pain. *Neurol. Clin.*, 25, 353-371.
- Ryan, E., Herda, T., Costa, P., Walter, A., Cramer, J., 2011. Dynamics of viscoelastic creep during repeated stretches. *Scand. J. Med. Sci. Sports*, 22, 179-184.
- Ryan, E.D., Herda, T.J., Costa, P.B., Walter, A.A., Hoge, K.M., Stout, J.R., Cramer, J.T., 2010. Viscoelastic creep in the human skeletal muscle-tendon unit. *Eur. J. Appl. Physiol.*, 108, 207-211.
- Sanjeevi, R., 1982. A viscoelastic model for the mechanical properties of biological materials. *J. Biomech.*, 15, 107-109.
- Schmidt, H., Shirazi-Adl, A., Galbusera, F., Wilke, H.J., 2010. Response analysis of the lumbar spine during regular daily activities—a finite element analysis. *J. Biomech.*, 43, 1849-1856.
- Shin, G., D'souza, C., Liu, Y.H., 2009. Creep and fatigue development in the low back in static flexion. *Spine*, 34, 1873-1878.
- Shin, G., Mirka, G.A., 2007. An in vivo assessment of the low back response to prolonged flexion: Interplay between active and passive tissues. *Clin. Biomech.*, 22, 965-971.
- Silva, P., Crozier, S., Veidt, M., Percy, M.J., 2005. An experimental and finite element poroelastic creep response analysis of an intervertebral hydrogel disc model in axial compression. *Journal of Materials Science: Materials in Medicine*, 16, 663-669.
- Solomonow, M., 2011. Neuromuscular manifestations of viscoelastic tissue degradation following high and low risk repetitive lumbar flexion. *J. Electromyogr. Kinesiol.*, 22, 155-175.
- Stubbs, M., Harris, M., Solomonow, M., Zhou, B., Lu, Y., Baratta, R., 1998. Ligamentomuscular protective reflex in the lumbar spine of the feline. *J. Electromyogr. Kinesiol.*, 8, 197-204.
- Taylor, D.C., Dalton, J.D., Seaber, A.V., Garrett, W.E., 1990. Viscoelastic properties of muscle-tendon units. *Am. J. Sports Med.*, 18, 300-309.
- Troyer, K.L., Puttlitz, C.M., 2011. Human cervical spine ligaments exhibit fully nonlinear viscoelastic behavior. *Acta biomaterialia*, 7, 700-709.
- Truong, X., 1974. Viscoelastic wave propagation and rheologic properties of skeletal muscle. *Am. J. Physiol.*, 226, 256-264.

- Twomey, L., Taylor, J., 1982. Flexion creep deformation and hysteresis in the lumbar vertebral column. *Spine*, 7, 116-122.
- Twomey, L., Taylor, J., 1983. Sagittal movements of the human lumbar vertebral column: A quantitative study of the role of the posterior vertebral elements. *Arch. Phys. Med. Rehabil.*, 64, 322-325.
- Wang, J., Parnianpour, M., Shirazi-Adl, A., Engin, A., 1997. Failure criterion of collagen fiber: Viscoelastic behavior simulated by using load control data. *Theor. Appl. Frac. Mech.*, 27, 1-12.
- Wu, J., Chen, J., 1996. Clarification of the mechanical behaviour of spinal motion segments through a three-dimensional poroelastic mixed finite element model. *Med. Eng. Phys.*, 18, 215-224.

2 Load-relaxation Properties of the Human Trunk in Response to Prolonged Flexion: Measuring and Modeling the Effect of Flexion Angle

Nima Toosizadeh, Maury A. Nussbaum, Babak Bazrgari, and Michael L. Madigan

Abstract

Experimental studies suggest that prolonged trunk flexion reduces passive support of the spine. To understand alterations of the synergy between active and passive tissues following such loadings, several studies have assessed the time-dependent behavior of passive tissues including those within spinal motion segments and muscles. Yet, there remain limitations regarding load-relaxation of the lumbar spine in response to flexion exposures and the influence of different flexion angles. Ten healthy participants were exposed for 16 min to each of five magnitudes of lumbar flexion specified relative to individual flexion-relaxation angles (i.e., 30, 40, 60, 80, and 100%), during which lumbar flexion angle and trunk moment were recorded. Outcome measures were initial trunk moment, moment drop, parameters of four viscoelastic models (i.e., Standard Linear Solid model, the Prony Series, Schapery's Theory, and the Modified Superposition Method), and changes in neutral zone and viscoelastic state following exposure. There were significant effects of flexion angle on initial moment, moment drop, changes in normalized neutral zone, and some parameters of the Standard Linear Solid model. Initial moment, moment drop, and changes in normalized neutral zone increased exponentially with flexion angle. Kelvin-solid models produced better predictions of temporal behaviors. Observed responses to trunk flexion suggest nonlinearity in viscoelastic properties, and which likely reflected viscoelastic behaviors of spinal (lumbar) motion segments. Flexion induced changes in viscous properties and neutral zone imply an increase in internal loads and perhaps increased risk of low

back disorders. Kelvin-solid models, especially the Prony Series model appeared to be more effective at modeling load-relaxation of the trunk.

2.1 Introduction

Trunk flexion exposures, whether prolonged or cyclic, result in viscoelastic deformation of passive tissues in the posterior trunk and consequently a reduction in trunk stiffness (Hendershot et al., 2011; Kazarian 1975). A decrease in passive trunk stiffness can be compensated by extra activation of muscles (McCook et al., 2009; Olson et al., 2009; Shin and Mirka 2007, Shin et al., 2009), which may cause additional loads on joints and other soft tissues (Bazrgari and Shirazi-Adl 2007). Moreover, extra activation of muscles may increase metabolic cost and consequently contribute to muscle fatigue (Adams and Dolan 1995, Shin et al., 2009). Since the risk of low back disorders (LBDs) may be associated with excessive spinal loads and muscle fatigue (Bakker et al., 2009; Brereton and McGill 1999; Burdorf and Sorock 1997), an accurate assessment of the time-dependent changes in load partitioning among passive trunk tissues and active muscles is of importance in investigating the risk of LBDs.

Determining the distribution of loads among passive and active components of the human trunk, typically using a biomechanical model, requires a realistic representation of time-dependent passive properties. A number of experiments have assessed the time-dependent behavior of passive trunk tissues. Many *in vitro* studies have focused on the viscoelastic properties of spinal motion segments, especially in flexion/extension (Adams and Dolan 1996; Little and Khalsa 2005; Oliver and Twomey 1995; Twomey and Taylor 1982; Twomey and Taylor 1983). Several other studies have determined the viscoelastic properties of muscle using both *in vitro* (Abbott and Lowy 1957; Glantz 1974, Truong 1974; Greven et al., 1976; Linke and Leake 2004; Sanjeevi 1982; Taylor et al., 1990) and *in vivo* (Best et al., 1994; Hawkins et al., 2009; Magnusson et al., 1995; Magnusson et al., 1996; Magnusson et al., 2000; Ryan et al., 2010; Ryan

et al., 2011) measurements. Furthermore, in an *in vivo* study by McGill and Brown (1992), the whole-trunk creep was measured for prolonged flexion exposures.

While these studies have provided a fundamental understanding of the time-dependent responses of trunk tissues, some limitations still exist. Most measurements of the viscoelastic properties of the spine have been performed on cadaver motion segments. The main limitation of these *in vitro* experiments is the lack of metabolic processes of intervertebral discs, respiration, circulation and muscle activity, which are influential in prolonged tests (Hult et al., 1995; Keller et al., 1990). Many occupational tasks require prolonged trunk flexion at a constant angle (load-relaxation); however, no studies to our knowledge have measured load-relaxation of the lumbar spine *in vivo* in response to flexion exposures. Previous reports show that load-relaxation behavior of soft tissues is not directly correlated to creep response (Purslow et al., 1998; Thornton et al., 1997), which indicates that load-relaxation is not simply the inverse of creep responses and that they should be determined separately. Furthermore, there is evidence of nonlinear viscoelastic behaviors for spinal soft tissues and motion segments (Hult et al., 1995; Toosizadeh et al., 2010; Troyer and Puttlitz 2011). However, it is unknown how such nonlinearity in viscoelastic behavior is influenced by different magnitudes of loading/displacement.

Hence, the main purpose of this study was to quantify the load-relaxation responses of the human trunk during prolonged flexed postures. Load-relaxation responses were measured *in vivo* at several trunk flexion angles and then fit using a range of viscoelastic models. Based on previous evidence of nonlinear viscoelastic behavior of trunk soft tissues (Hult et al., 1995; Toosizadeh et

al., 2010; Troyer and Puttlitz 2011), we hypothesized that the whole trunk would exhibit nonlinear viscoelastic responses to prolonged flexion and that these responses would depend on the specific flexion angle. Several different approaches, based on equations of creep deformation or load-relaxation, have been previously developed to model the viscoelastic behavior of soft tissues. These include Kelvin-solid models, Schapery's Theory, and the Modified Superposition method (Ambrosetti-Giudici et al., 2010; Burns et al., 1984; Keller and Nathan 1999; Machiraju et al., 2006; Provenzano et al., 2002,). Among different types of Kelvin-solid models, the standard linear solid (SLS) and Prony Series models have given the best predictions of viscoelastic responses under quasi-static conditions (Groth and Granata 2008; Machiraju et al., 2006). However, these models have never been used to predict the load-relaxation response of the whole trunk. As such, the second purpose of the current study was to evaluate different viscoelastic modeling approaches for characterizing these responses. We hypothesized that available viscoelastic models would have differing success in characterizing these responses, with better predictions from Kelvin-solid models.

2.2 Methods

Ten healthy young adults with no self-reported history of low-back pain participated after completing informed consent procedures approved by the Virginia Tech Institutional Review Board. Participants included five males with mean (SD) age, stature, and body mass of 24.4 (4.2) yr, 179.9 (6.9) cm, and 71. (7.3) kg, respectively; corresponding values for the five females were 23.8 (2.6) yr, 164.4 (3.9) cm, and 57.9 (5.1) kg. A relatively young set of participants (from 18-29yr) was included to avoid potential influences related to age.

Each participant completed five experimental sessions, one for each of five levels of trunk flexion including 30, 40, 60, 80, and 100% of the flexion-relaxation (FR) angle (see below). These flexion levels were used to cover a wide range of potential exposures, and the lower level was increased to 30% of FR angle based on pilot results that indicated exposure to 20% of FR angle was insufficient to capture viscoelastic properties. At least three days separated consecutive sessions, and the presentation order was counterbalanced using 5×5 Latin Squares (one for each gender). Sessions were conducted before 9:00 am to minimize effects of cumulative daily loading.

Lumbar flexion angle was measured using inertial measurement units (IMUs: Xsens Technologies XM-B-XB3, Enschede, Netherlands). IMUs were placed on the skin using medical-grade, double-sided tape, over the spinous processes of T12 and S1, and sampled at 100 Hz. Electromyography (EMG) of the Longissimus and Rectus Abdominus muscles was collected using bipolar Ag/AgCl surface electrodes and previously reported electrode placements (Hendershot et al., 2011; McGill 1991). Raw EMG data were preamplified (×100) near the collection site, and signals were then bandpass filtered (10-500 Hz) and amplified in hardware (Measurement System Inc., Ann Arbor, MI, USA) before being sampled at 1000 Hz.

After instrumentation, each participant stood in a rigid metal frame and straps were used to restrain the pelvis and lower limbs. In a preliminary session for each participant, FR angle was measured using procedures similar to an earlier study (Hendershot et al., 2011). Briefly, participants flexed their trunk slowly to full passive trunk flexion (~5 sec) and slowly returned to the upright standing posture (~5 sec). FR angle was defined as the trunk flexion angle, near the

end of the range-of-motion, with minimal EMG. FR angle measurements were done three times, and the largest FR angle from the three trials was used as the reference for specifying flexion exposures in the experimental sessions. To minimize within-subject variability in FR angles due to creep-dependent changes (Shin et al., 2009), FR angles were desired at a relatively fixed level of creep deformation. This was achieved by inducing near-maximal (asymptotic) creep deformation of the trunk prior to obtaining FR angles. Specifically, participants adopted full passive trunk flexion for four minutes, which was expected to induce > 90% of maximal creep (McGill and Brown 1992).

While standing in the rigid frame with their pelvis restrained, participants were exposed to trunk flexion by rotating the pelvis and lower extremities forward/upward to induce trunk flexion (Figure 2.1), thereby stretching the passive lumbar tissues and producing an external extension moment. A footrest with adjustable height was used under the feet to position the L5/S1 joint at the frame's rotational axis. Participants' trunks were constrained at the T8 level using a rigid harness-rod assembly, which ensured that the trunk was maintained roughly upright. While the lower extremities were raised (loading phase), during the flexion exposure (load-relaxation phase), and while the lower extremities were lowered (unloading phase), forces due to passive tissues stretching were measured continuously (1000 Hz) using a load cell (Interface SM2000, Scottsdale, AZ, USA) on the harness-rod assembly. EMG measures (as described above) were used as biofeedback to minimize voluntary muscle activation throughout these procedures, thus ensuring that measures were predominantly reflecting passive tissue properties. Participants also maintained a consistent head posture (facing forward and looking at a monitor). Flexion

exposures lasted 16 minutes, which was considered sufficient to capture the majority of load-relaxation (Toosizadeh et al., 2010) and also be well tolerated by participants.

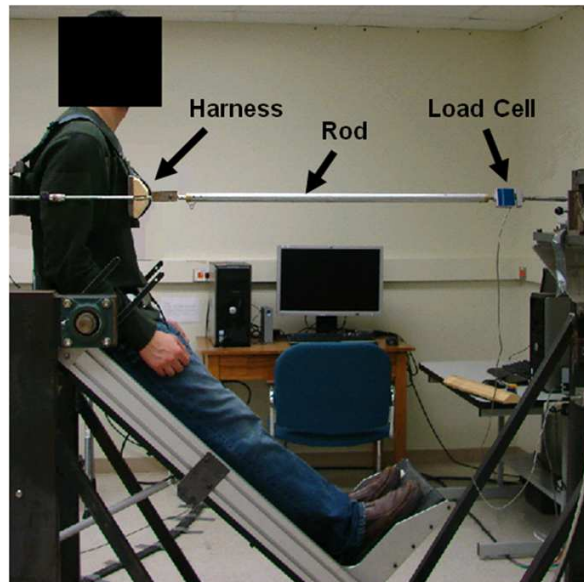


Figure 2.1: Experimental setup for load-relaxation test (60% FR angle condition illustrated).

Several direct or derived outcome measures were obtained for the trunk: 1) initial moment, 2) moment drop, 3) neutral zone (NZ), 4) viscoelastic state, and 5) viscoelastic model parameters characterizing the viscoelastic (load-relaxation) behaviors. Initially, the exposure periods were divided into the three phases noted above (loading, load-relaxation, and unloading). Trunk moments were determined from the measured force (load cell) and associated moment arm (measured vertical distance between the rod and L5/S1 center of rotation). Three-second windows at the start and end of the load-relaxation phase were used to calculate the initial moment and moment drop. Loading (flexion) and unloading (extension) phases were used to estimate the NZ (Figure 2.2), a region over which little resistance exists against external forces or moments (Panjabi 1992). The NZ was defined specifically as the portion of the trunk range of

motion around the neutral (upright) posture where the slope of the flexion angle-moment curve was $< 0.1 \text{ Nm/deg}$ and the passive moment was $< 7 \text{ Nm}$ (Scannell and McGill 2003). For each participant, the NZ range was divided by the FR angle to yield a normalized NZ for each flexion exposure, and the percentage change from the pre-exposure value was obtained.

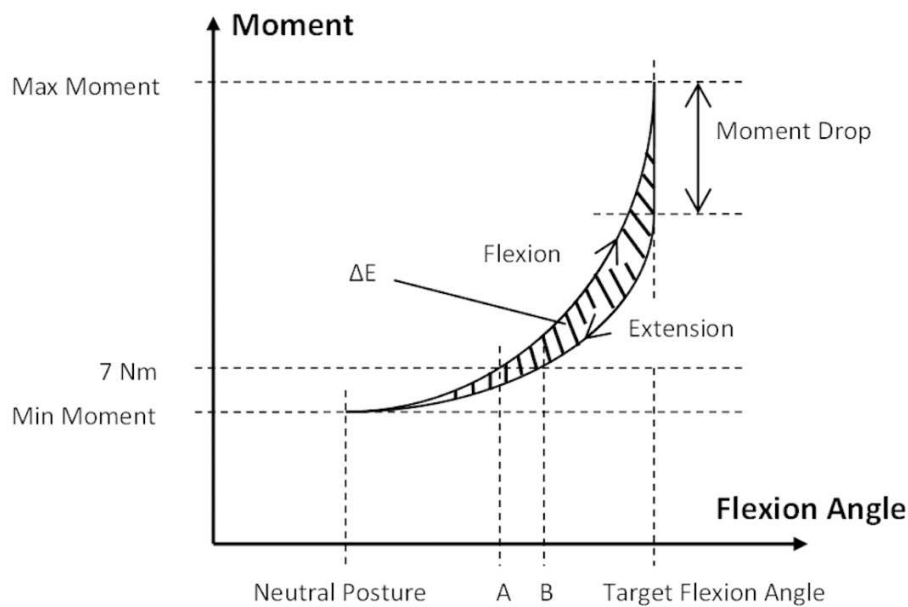


Figure 2.2 Illustration of a hysteresis loop. The highlighted area (ΔE) denotes the dissipated energy; NZ in flexion (extension) is the distance between point A (point B) and the neutral posture. Target lumbar flexion angle = 30, 40, 60, 80, or 100% FR.

Total energies for flexion (E_1) and extension (E_2) were calculated from areas under the flexion-angle-moment curves in the loading and unloading phases, respectively, and these used to determine absorbed energy: $\Delta E = E_1 - E_2$ (Figure 2.2). Subsequently, the ratio of hysteresis/energy input (RE), which describes the viscoelastic state (Koeller et al., 1986), was estimated as $\Delta E/E_1$. For a pure elastic material, $RE = 0$, and for a pure viscous material $RE = 1$ (Koeller et al., 1986; Yahia et al., 1991).

To characterize trunk viscoelastic behaviors, four common types of viscoelastic models of varying complexity were used, with the load-relaxation equations for each provided below:

Standard Linear Solid (SLS) model (Figure 2.3):

$$M(t) = \theta_0 \left(K_2 + K_1 e^{-\frac{K_1 t}{C}} \right) \quad (2.1)$$

where K_1 and C are, respectively, stiffness and damping of torsional spring and damper components in series (Maxwell component), and K_2 is the stiffness of a parallel torsional spring (Roylance 2001). K_1 and C represent viscous responses to deformation, and K_2 is the steady-state stiffness once the material is totally relaxed. $K_1 + K_2$ is the instantaneous stiffness, and the relaxation time constant $\left(T = \frac{C}{K_1} \right)$ shows the rate of moment relaxation.

Prony Series (Figure 2.3):

$$M(t) = \theta_0 \left(J_0 + \sum_{i=1}^n J_i e^{-\frac{t}{\tau_i}} \right) \quad (2.2)$$

where J_i , and τ_i ($\tau_i = \frac{J_i}{\eta_i}$) are respective stiffness and relaxation time constants from each spring and damper in the i^{th} Maxwell component of the Wiechert model. J_0 is the steady-state stiffness once the material is totally relaxed, and n is the number of Maxwell components in the model (Machiraju et al., 2006). Here, values of $n = 2, 3,$ and 4 were considered.

Schapery's Theory:

$$M(t) = h_e K_e \theta_0 + h_2 C \theta_0 t^{-n} \quad (2.3)$$

where h_e and h_2 are angle-dependent constants, K_e is the torsional stiffness at equilibrium (final data point), and C and n are constants that derived by curve fitting (Provenzano et al., 2002; Strganac and Golden 1996).

Modified Superposition Method:

$$M(t) = K_0 \theta_0 t^{-gn_0} \tag{2.4}$$

where g is an angle-dependent constant, K_0 is the torsional stiffness at the beginning of load-relaxation, and n_0 is the initial relaxation rate obtained by curve fitting (Ambrosetti-Giudici et al., 2010; Provenzano et al., 2002,).

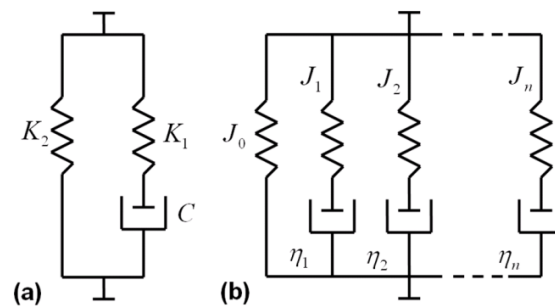


Figure 2.3: Kelvin-solid models: (a) SLS model (b) Prony Series model. Each spring and damper in series represents a Maxwell model. For clarity, linear rather than rotational components are illustrated.

These equations (models) were derived assuming a constant flexion angle = θ_0 and using established procedures (Provenzano et al., 2002; Roylance 2001; Wenbo et al., 2001,). Model parameters were estimated for each exposure (i.e., each participant in each flexion angle) by minimizing least-squared errors in predicted moments within the load-relaxation phase. Subsequently, model prediction quality was evaluated using the mean, across participants, of coefficients of determination (R^2) and root-mean-square errors (RMSE) obtained for each

exposure. Model prediction quality using the Prony Series model was comparable using $n = 2$, 3, and 4, and thus the simplest equation (i.e., $n = 2$) was used in the remainder of this work.

After testing for normality of distribution, separate mixed-factor, repeated-measures analyses of variance (ANOVAs) were performed to evaluate the effects of flexion angle and gender on each of the direct and derived measures. Only the relevant SLS model parameters (K_1 , K_2 , C , T , and $K_1 + K_2$) were analyzed in this way, to assess potential nonlinearity in elastic and viscous properties, since their interpretation is relatively straightforward versus parameters within the other models. Post-hoc comparisons between flexion exposure levels were done, where relevant, using Tukey's HSD. Effects of flexion angle on direct outcome measures (i.e., initial moment, moment drop and changes in NZ) were also explored using linear and nonlinear curve fits to mean values, and these were evaluated based on coefficients of determination (R^2). As several such curves should logically include the origin (e.g., zero flexion yields zero moment), the origin was included as an additional data point. However, SLS model parameter values near 0% FR were not extrapolated, since in this region (i.e., the NZ) rotational stiffness is substantially smaller than elsewhere (Scannell and McGill 2003; Thompson et al., 2003). Statistical significance was concluded when $p < 0.05$, all analyses were performed using JMP (Version 9, SAS Institute Inc., Cary, NC, USA), and all summary statistics are given as means (SD). Incomplete data were available for four trials involving 30% FR exposures, during which clear moment changes over time were not evident, and results from one 100% FR trial were excluded as clear outliers (studentized residuals).

A sensitivity analysis was performed to assess the effects of each model parameter with respect to describing viscoelastic behavior of the trunk. Sensitivity coefficients were calculated as (Lehman and Stark 1982):

$$S = \frac{\Delta b / b_0}{\Delta p / p_0} \quad (2.5)$$

where b_0 is the nominal value (mean value across all trials) of a relevant outcome measure (i.e., moment drop and initial angle), and p_0 is a given model parameter; Δp is the range of the model parameter across all trials; and, Δb is the range in the predicted outcome measure (i.e., change in moment drop or initial moment prediction) that results from changing the given model parameter over Δp while all other model parameters are kept at their nominal values. All model-based calculations were performed in MATLABTM (MathWorks, Natick, MA, USA).

2.3 Results

There were significant effects of lumbar flexion angle on initial moment ($F_{(4,25)} = 29.51, P < 0.0001$), moment drop ($F_{(4,23)} = 9.08, P < 0.0001$), and changes in normalized NZ ($F_{(4,21)} = 5.82, P < 0.0025$). All three measures increased with lumbar flexion angle (Figure 2.4), and each of the relationships with lumbar flexion angle was well characterized by exponential functions ($R^2 > 0.93$). Viscoelastic state (RE) overall was 0.42 (0.15), indicating a mix of elastic and viscous behaviors, and was not affected by lumbar flexion angle ($F_{(4,22)} = 0.39, P = 0.81$). Gender had no main or interactive effects on any of these outcome measures ($P > 0.11$).

The different models exhibited different levels of prediction quality (as based on R^2 and RMSE) and some levels of dependency on lumbar flexion angle (Figure 2.5). Overall differences in R^2 and RMSE between the SLS and Prony Series models were negligible (8 and 5%, respectively),

and these two exponential models produced better predictions than the two power models (i.e., Schapery's Theory and the Modified Superposition Method). While RMSE were consistent across lumbar flexion angles, R^2 generally increased with angle for each model.

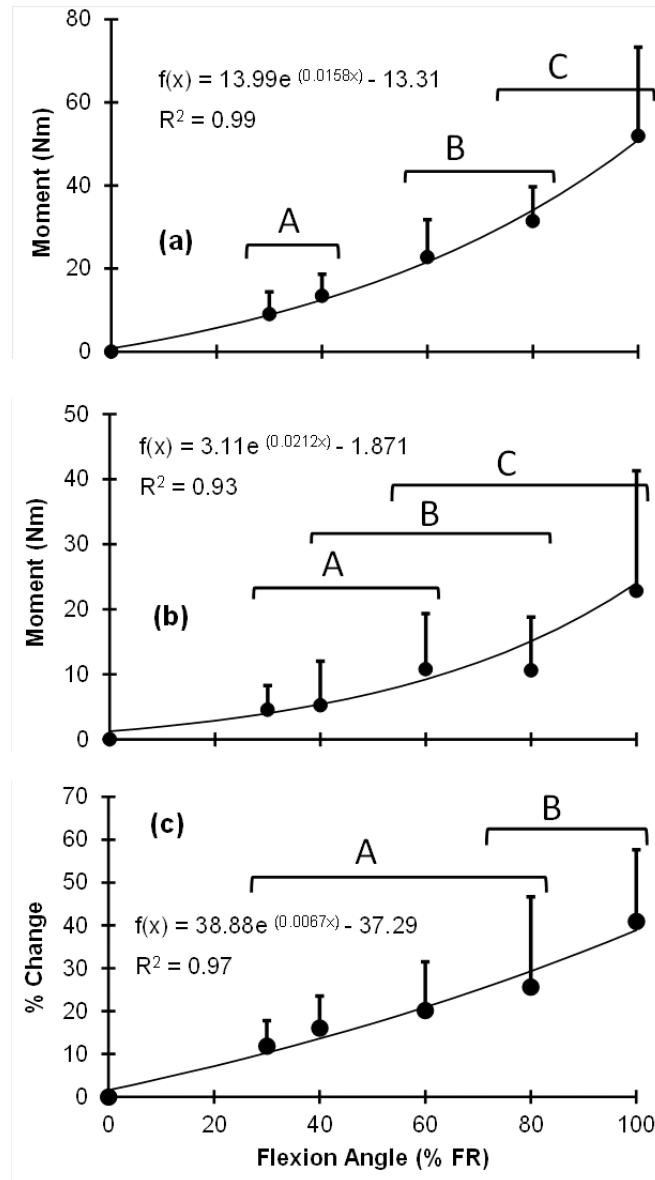


Figure 2.4: Effects of lumbar flexion angles on direct outcome measures: (a) initial moment, (b) moment drop, and (c) percentage change in normalized NZ. Post-hoc groupings are indicated by brackets and letters, and best-fit exponential relationships are provided.

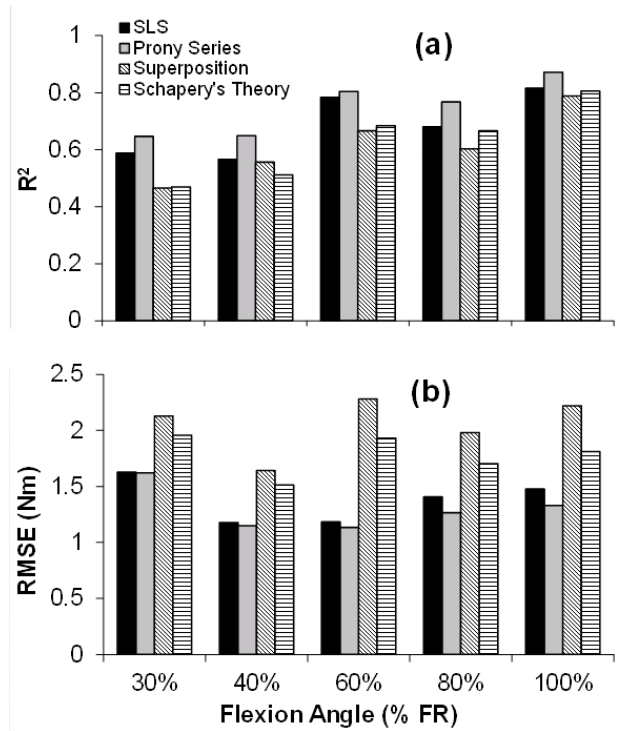


Figure 2.5: Mean measures of viscoelastic model prediction quality: (a) R^2 and (b): root-mean-square errors (RMSE).

Lumbar flexion angle significantly affected the K_1 ($F_{(4,24)} = 3.84, P = 0.0154$), and ($F_{(4,23)} = 6.96, P = 0.0008$) parameters within the SLS model; K_1 decreased and K_2 increased with lumbar flexion angle (Figure 2.6). C , T , and $K_1 + K_2$, in contrast, were not affected by lumbar flexion angle ($P > 0.10$), and gender had no main or interactive effects on any of the SLS model parameters ($P > 0.07$). T and $K_1 + K_2$ tended to increase with lumbar flexion angle, while C remained quite consistent across all lumbar flexion angles with mean (SD) = 111 (107) Nms/deg. Parameters obtained for the other models at specified lumbar flexion angles are presented in Table 2.1.

Table 2.1: Mean (SD) values of estimated parameters for different viscoelastic models with respect to lumbar flexion angle (SLS model parameters are shown in Figure 2.6)

Model parameters (Units)	Lumbar flexion angle (percentage of FR angle)				
	30%	40%	60%	80%	100%
Prony Series					
J_0 (Nm/deg)	0.07 (0.14)	0.19 (0.12)	0.19 (0.23)	0.24 (0.28)	0.23 (0.25)
J_1 (Nm/deg)	0.40 (0.36)	0.25 (0.30)	0.49 (0.46)	0.36 (0.38)	0.36 (0.24)
J_2 (Nm/deg)	0.10 (0.19)	0.17 (0.28)	0.21 (0.17)	0.21 (0.26)	0.34 (0.38)
τ_1 (sec)	12.6 (15.4)	20.6 (17.3)	7.6 (12.1)	9.8 (10.3)	8.8 (11.1)
τ_2 (sec)	1058.4 (1352.5)	1030.6 (704.7)	764.4 (632.5)	1690.6 (1323.1)	1704.5 (1491.3)
Schapery's Theory					
$h_e K_e$ (Nm/deg)	0.15 (0.01)	0.15 (0.01)	0.26 (0.01)	0.23 (0.01)	0.54 (0.01)
$h_2 C$ (Nm/deg×sec)	0.62 (0.54)	0.62 (0.54)	0.74 (0.58)	0.60 (0.34)	0.68 (0.42)
n (dimensionless)	0.28 (0.40)	0.42 (0.57)	0.32 (0.23)	0.24 (0.25)	0.23 (0.16)
Modified Superposition					
K_0 (Nm/deg×sec)	0.522 (0.272)	0.524 (0.265)	0.560 (0.232)	0.564 (0.227)	0.749 (0.386)
gn_0 (dimensionless)	0.29 (0.39)	0.09 (0.12)	0.09 (0.07)	0.07 (0.06)	0.06 (0.03)

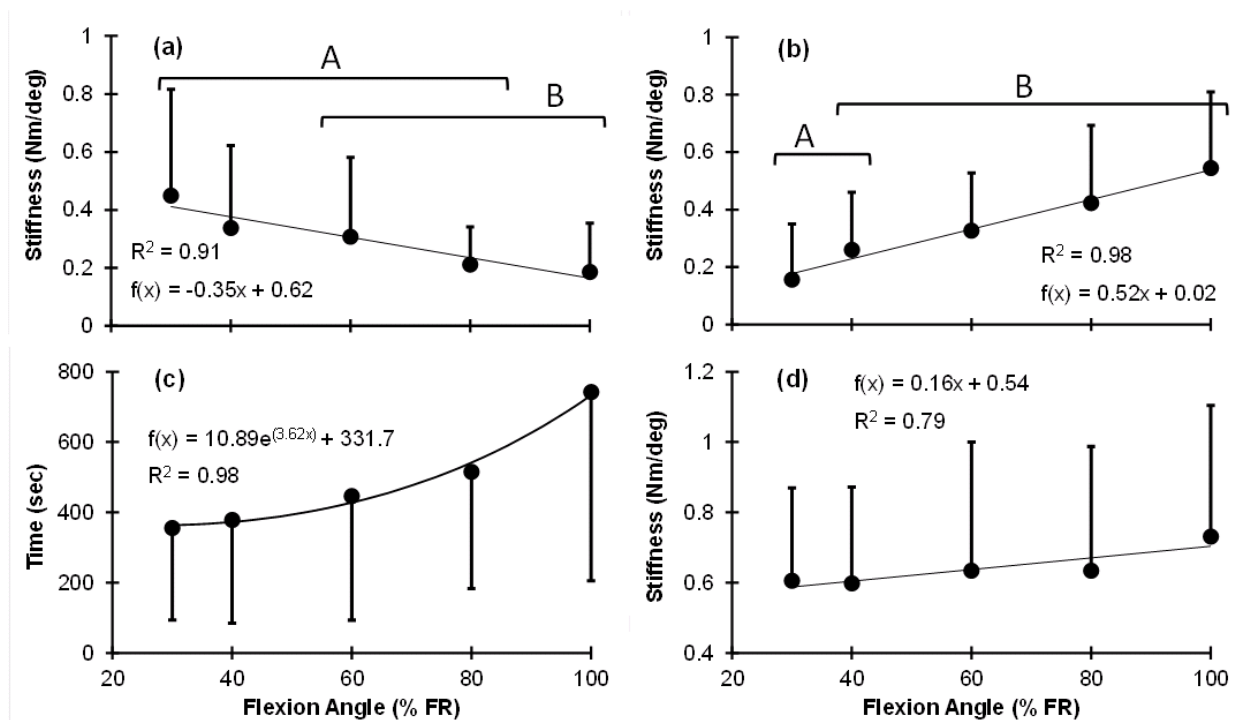


Figure 2.6: Effects of lumbar flexion angle on SLS model parameters: (a): stiffness of Maxwell component = K_1 , (b): parallel stiffness = K_2 , (c): relaxation time constant = T , and (d): instantaneous stiffness = $K_1 + K_2$. Post-hoc groupings are indicated by brackets and letters, and best-fit relationships (linear or exponential) are provided.

From the sensitivity analyses, several dependencies were evident (Table 2.2). Some parameters (K_2 , J_0 , and h_e) were purely related to elastic behavior (initial moment), while others (T , τ_1 , τ_2 , n , and gn_0) were purely related to viscous responses (moment drop) of soft tissues. The remaining parameters (K_1 , J_1 , J_2 , h_2 , and K_0) were related to both elastic and viscous behaviors. Of note, the moment drop sensitivity coefficient of τ_1 (i.e., the smaller relaxation time constant in the Prony Series model) was several orders of magnitude smaller than that of τ_2 (i.e., the larger relaxation time constant); hence, the larger relaxation time constant describes more of the moment drop.

Table 2.2: Dimensionless sensitivity coefficients for the four models with respect to initial moment and moment drop

Model parameters	Sensitivity coefficient	
	Initial moment	Moment drop
SLS model		
K_2	0.66	0.00
K_1	0.31	0.67
T	0.00	0.14
Prony Series		
J_0	0.27	0.00
J_1	0.52	1.27
J_2	0.29	0.38
τ_1	0.00	2.5 e-5
τ_2	0.00	0.09
Schapery's Theory		
$h_e K_e$	0.36	0.00
$h_2 C$	0.95	2.03
n	0.00	0.03
Modified Superposition		
K_0	0.84	1.15
gn_0	0.00	0.24

2.4 Discussion

Nonlinearity in both elastic and viscous properties of the trunk was clearly evident. This was apparent both from nonlinear changes in initial moment and moment drop with lumbar flexion angle and the angle-dependency of SLS model parameters (K_1 and K_2). Here, exponential increase in moment drop and K_1 reduction with lumbar flexion angle demonstrated nonlinearity in the viscous behavior of the trunk. Moreover, relaxation rate (T) increased with lumbar flexion angle (Figure 2.6). Although this change was not significant, it suggests that more time is required for the initial moment to relax at larger lumbar flexion angles. While there is previous evidence of nonlinear viscoelastic behaviors of spinal soft tissues (Hult et al., 1995, Troyer and Puttlitz 2011), the current work presents new evidence for nonlinearity in the whole trunk. The flexion distribution among thorax and lumbar components was not controlled here. However, and as suggested by previous work (Arjmand and Shirazi-Adl 2005; Nussbaum and Chaffin 1996), and our direct measurement of lumbar angle most of the flexion likely occurred in the lumbar spine.

Estimated elastic and viscous properties here are comparable with previous reports. For elastic behavior, the magnitudes of initial moment versus lumbar flexion angle (i.e., instantaneous moment-angle relationship) were similar to those in previous studies (McGill et al., 1994, Parkinson et al., 2004). Changes in the initial moment (and $K_1 + K_2$) with lumbar flexion angle also showed the same nonlinear moment-angle relationship that has been found earlier (Guan et al., 2007; Panjabi et al., 1994). For viscous behavior, the mean (SD) value of moment drop during load-relaxation periods was 41 (22)% across all five exposure conditions. Earlier *in vitro* studies reported a ~ 48% reduction in flexion reactive moment of lumbar spine motion segments

(Adams and Dolan 1996) and ~ 27% reduction in passive muscle force (Best et al., 1994; Sanjeevi 1982; Sarver et al., 2003) after 16 minutes of loading. (Approximate values were derived using interpolation.) Moreover, the current mean (SD) value of the required time for a 90% drop relative to the initial moment was 5.9 (3.7) minutes, similar to values of ~ 5 minutes for spinal motion segments and ~ 9 minutes for passive muscles (Sarver et al., 2003).

According to observed values of moment drop and relaxation duration, it is possible to infer which tissue components of the trunk are predominant in providing viscous behavior. We consider two parallel systems to be responsible for generating the reactive moment: 1) spinal motion segments (i.e., vertebrae, disc, facets and ligaments), and 2) passive tissues integrated within muscle units (i.e., tendon, epimysium, perimysium, and endomysium). Optimal lengths of the active force-length relationship of trunk-extensor muscles occur at lumbar angles close to full flexion (Keller and Roy 2002; Raschke and Chaffin 1996; Roy et al., 2003), and passive tension developed in muscles typically starts at/near this optimal length and increases as length increases. However, other studies have indicated smaller lumbar flexion angles corresponding to the peak trunk extension moment (Chaffin et al., 1991; Kumar et al., 1995), and this discrepancy may be related to differences in experimental methods used and between individuals (i.e., different ages or genders). Thus, at less extreme lumbar flexion angles (30-100% of FR angle) the contribution of passive muscle forces was assumed to be relatively small. In this study, mean maximum flexion exposure during load-relaxation (100% of FR) was equal to 87% of the mean full lumbar flexion angle. Accordingly, it was expected that spinal motion segments (rather than passive muscle stiffness) were predominant in providing the measured reactive moment. This was also supported by the fact that measured initial moments here are comparable with

previously reported values for isolated spinal motion segments (without muscles) (Adams and Dolan 1996; Stokes and Gardner-Morse 2003). As such, for angles smaller than FR, a majority of the moment drop should thus result from viscoelastic behavior of spinal motion segments. Of note, this reduction in stiffness should be compensated by additional muscle activities, such as when performing a task following a prolonged period of flexion. Extrapolating from the current research and previous modeling results (Bazrgari and Shirazi-Adl 2007), this extra muscle activity could substantially increase the internal load on the spine, up to ~ 600 N in extreme cases. Results here, though, were not sufficient to explain in detail the passive moment allocation among different components of spinal motion segments. For instance, ligaments might contribute to passive moment in trunk flexion exposures, and consequently to the passive moment drop during the load-relaxation period. As such, a reduction in ligament forces can reduce the imposed forces on spinal motion segments. However, it was beyond the scope of the current study to explore the force/moment distribution among different passive components within spinal motion segments.

When the trunk is flexed, passive tissues resist the external moment, yet this resistance is small for deformations near the NZ (Thompson et al., 2003). Panjabi (2003) suggested that an increase in the NZ reflects instability and an increased LBD risk, and it may also be a sensitive parameter for defining the onset of spinal injuries (Oxland et al., 1992). According to Yamamoto et al., (1989), the NZ for flexion is 8.8 degrees for the L1-S1 spine, which is comparable to the current mean (SD) of 10.5 (5.5) degree here prior to flexion exposure. Rotational displacements of other spinal motion segments superior to the lumbar vertebrae likely account for the difference between the NZ measures in the current *in vivo* study and previous *in vitro* studies. In agreement

with the effect of lumbar flexion angle on viscoelastic behavior, pre- and post-exposure NZ differences increased exponentially with lumbar flexion angle. Previous *in vivo* studies have reported an increase in spinal motion segment laxity after prolonged and cyclic flexion (Solomonow et al., 2001, Youssef et al., 2008). These studies measured the neuromuscular neutral zone (NNZ), which is the amount of rotational displacement applied to the lumbar spine before muscle activity increases the stiffness of the intervertebral joints. Though NNZ and NZ might be different in magnitude (Solomonow et al., 2001), it is expected that they are closely related to each other, and results from the current study confirmed that flexion exposures increase the NZ as well. However, the present results regarding a nonlinear increase in NZ changes with lumbar flexion angle have not, to our knowledge, been previously quantified. An increase in NZ following prolonged flexion exposure suggests that the LBD risk may increase as well, and that the increase in LBD risk depends on the extent of lumbar flexion angle involved.

Comparing moment-angle curves before and after flexion exposures demonstrated that trunk soft tissues generated lower reactive moments for an identical lumbar flexion angle after exposures. This phenomenon of a hysteresis loop during loading and unloading has been shown in previous *in vitro* studies on soft tissues. In these, RE values have been reported equal to ~ 0.2 for intervertebral discs under axial compression (Gay et al., 2006), and between 0.1 and 0.59 for spinal ligaments in load-relaxation (Yahia et al., 1991). However, no evidence could be found regarding RE for flexion exposure of the whole trunk, especially at different lumbar flexion angles. Here, an almost constant RE value of 0.42 (0.15) was found at different lumbar flexion angles, with no clear increasing or decreasing trend, suggesting an identical viscoelastic state for the whole trunk over a wide range of lumbar flexion angles. Because both elastic and viscous

properties change with lumbar flexion angle, these RE outcomes do not contradict our earlier results regarding nonlinearity in viscoelastic properties. Rather, the RE results suggest that elastic and viscous properties change in parallel and such that the overall viscoelastic state of the trunk is independent of lumbar flexion angle.

Assessing differences related to gender was not a main focus of this study, and which was likely underpowered in this respect. Indeed, no significant differences were evident, though some suggestive results were found. Overall, males exhibited greater flexion stiffness, with 15% higher initial moments, 6% lower maximum lumbar flexion angles, and 7% lower FR angles. The same qualitative difference in stiffness between genders was observed from the SLS model, where $K_1 + K_2$ was 6% greater among males. In partial agreement with our findings, greater flexibility in females has been previously reported for trunk flexion (Bazrgari et al., 2011; Brown et al., 2002; McClure et al., 1998).

We evaluated different viscoelastic modeling approaches in terms of their ability to characterize the load-relaxation responses of the human trunk. Both the Prony Series and SLS models, using exponential equations, were more effective for describing viscoelastic behavior of the trunk than the two power models. Predictions from these two exponential models, however, differed slightly in how they described the immediate moment drop (i.e., at the beginning of the load-relaxation period). From inspection of load-relaxation graphs, distinct fast and slow phases can be identified in most, with the transition occurring in roughly the first 30-60 seconds of exposure (representative data shown in Figure 2.7). These two phases are more easily distinguishable when exposure was to larger lumbar flexion angles. Similar dual-phase results have been

reported for the creep behavior of spinal motion segments (Burns et al., 1984), with two specific creep rates: fast-rate creep, immediately after loading (from 0 to 1 minute of exposure); and slow-rate creep for the remaining exposure duration (from 1 to 480 minutes of exposure). Hence, the Prony Series model, with two relaxation time constants (τ_1 and τ_2), may be more appropriate than the SLS model for predicting load-relaxation behavior, especially in response to larger lumbar flexion angles (see also Figure 2.5, which showed larger RMSE differences between the two models with increasing lumbar flexion angle). Results from the sensitivity analysis confirmed the benefits of adding an additional, shorter relaxation time constant (τ_1) in the Prony Series model, though the sensitivity coefficient of τ_1 was quite small.

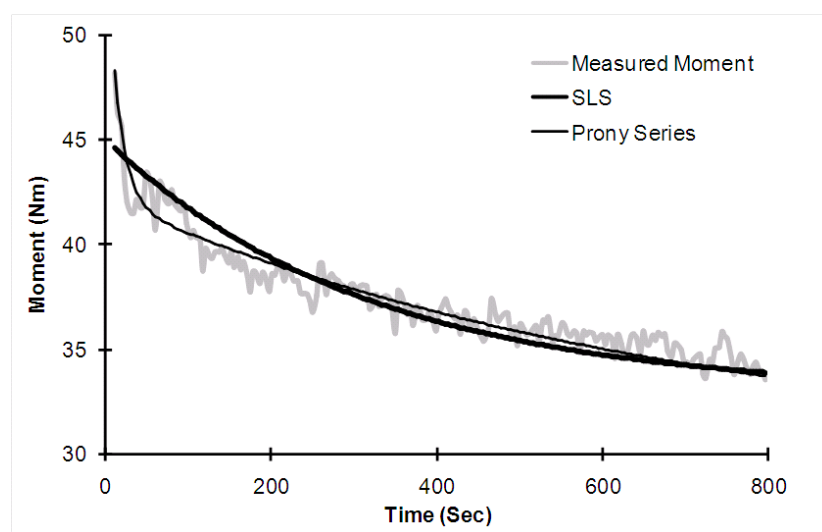


Figure 2.7: Fast and slow phases of moment drop during the load-relaxation period. Representative data are shown, and which indicate the advantage of the Prony Series over the SLS model for predicting measured behaviors. Results are for a 100% FR exposure.

An important potential limitation of the current study is related to the (in) accuracy in measuring *in vivo* viscoelastic properties. It is challenging to measure viscoelastic properties *in vivo*, with two of the more substantial problems related to the relatively modest changes in moment during

load-relaxation and the unavoidable presence of uncontrolled body movements. The former was particularly problematic for small exposure angles, and as noted earlier four trials involving 30% FR exposures were discarded due to insufficiency in capturing viscoelastic properties. These effects account, at least in part, for the larger variability within each exposure (larger RMSE) compared to *in vitro* studies. To minimize the latter source of error, voluntary movements were controlled (to the extent feasible) during data collection, both visually and using EMG. Additional analysis of the EMG data was done, and mean values of raw EMG data were not significantly different between the first and the last minute of load-relaxation (from paired t-tests, $P = 0.45$ and $P = 0.25$ for the extensors and flexors, respectively). Both EMG values, though, decreased slightly (less than ~5%) over the exposure period, perhaps due to a decrease in co-contraction with prolonged exposure. This decrease in muscle activity, in any case, likely led to some overestimation of moment drop and underestimation of viscous stiffness (K_1). Further, the gluteal muscles have a primary role in hip and trunk extension, and an important effect in spine stability during gait (McGill 2007). The activity of these muscles, however, was not monitored during the present study due to limitations in placing the electrodes.

In summary, the current work can facilitate a better understanding of how the load distribution among passive and active trunk components changes during prolonged flexion exposures. The current experimental setup isolated the effects of lumbar flexion angle independent of variation in gravitational loads and trunk muscle activity; specified lumbar flexion angles were achieved by raising participants' legs, rather than by having participants maintain forward flexion of the trunk. Any variability or potential confounding induced by muscle activity, inaccurate posture maintenance, or fatigue was thereby minimized. The results described an angle-dependent and

nonlinear relaxation behavior of the human trunk. Measured load-relaxation more likely arose from viscoelastic behavior of spinal motion segments, rather than passive muscles. Furthermore, viscoelastic responses were characterized using different types of models and material properties were derived, for which Kelvin-solid models more efficiently described load-relaxation behavior than other models. Such viscoelastic material properties can be used to predict trunk behaviors and lumbar mechanics in response to prolonged flexion exposures, for example by incorporation within larger-scale biomechanical models. In the occupational domain, diverse tasks involve prolonged exposure to flexed postures; as such, the current results may help in future efforts to control work-related LBDs.

2.5 References

- Abbott, B., Lowy, J., 1957. Stress relaxation in muscle. *Proc. R. Soc. Lond. B. Biol. Sci.*, 146, 281-288.
- Adams, M., Dolan, P., 1995. Recent advances and their clinical in lumbar spinal mechanics significance. *Clin. Biomech.*, 10, 3-19.
- Adams, M., Dolan, P., 1996. Time-dependent changes in the lumbar spine's resistance to bending. *Clin. Biomech.*, 11, 194-200.
- Ambrosetti-Giudici, S., Gédet, P., Ferguson, S.J., Chegini, S., Burger, J., 2010. Viscoelastic properties of the ovine posterior spinal ligaments are strain dependent. *Clin. Biomech.*, 25, 97-102.
- Arjmand, N., Shirazi-Adl, A., 2005. Biomechanics of changes in lumbar posture in static lifting. *Spine*, 30, 2637-2648.
- Bakker, E.W.P., Verhagen, A.P., Van Trijffel, E., Lucas, C., Koes, B.W., 2009. Spinal mechanical load as a risk factor for low back pain: A systematic review of prospective cohort studies. *Spine*, 34, E281-E293.
- Bazrgari, B., Hendershot, B., Muslim, K., Toosizadeh, N., Nussbaum, M.A., Madigan, M.L., 2011. Disturbance and recovery of trunk mechanical and neuromuscular behaviours following prolonged trunk flexion: Influences of duration and external load on creep-induced effects. *Ergonomics*, 54, 1043-1052.
- Bazrgari, B., Shirazi-Adl, A., 2007. Spinal stability and role of passive stiffness in dynamic squat and stoop lifts. *Computer Methods in Biomechanics and Biomedical Engineering*, 10, 351-360.
- Best, T.M., Mcelhaney, J., Garrett Jr, W.E., Myers, B.S., 1994. Characterization of the passive responses of live skeletal muscle using the quasi-linear theory of viscoelasticity. *J. Biomech.*, 27, 413-419.

- Brereton, L.C., McGill, S.M., 1999. Effects of physical fatigue and cognitive challenges on the potential for low back injury. *Hum Mov Sci*, 18, 839-857.
- Brown, M.D., Holmes, D.C., Heiner, A.D., Wehman, K.F., 2002. Intraoperative measurement of lumbar spine motion segment stiffness. *Spine*, 27, 954-958.
- Burdorf, A., Sorock, G., 1997. Positive and negative evidence of risk factors for back disorders. *Scand. J. Work. Environ. Health*, 23, 243-256.
- Burns, M., Kaleps, I., Kazarian, L., 1984. Analysis of compressive creep behavior of the vertebral unit subjected to a uniform axial loading using exact parametric solution equations of kelvin-solid models--part i. Human intervertebral joints. *J. Biomech.*, 17, 113-130.
- Chaffin, D.B., Andersson, G., Martin, B.J., 1991. *Occupational biomechanics*: Wiley New York.
- Gay, R.E., Ilharreborde, B., Zhao, K., Zhao, C., An, K.N., 2006. Sagittal plane motion in the human lumbar spine: Comparison of the in vitro quasistatic neutral zone and dynamic motion parameters. *Clin. Biomech.*, 21, 914-919.
- Glantz, S.A., 1974. A constitutive equation for the passive properties of muscle. *J. Biomech.*, 7, 137-145.
- Greven, K., Rudolph, K., Hohorst, B., 1976. Creep after loading in the relaxed and contracted smooth muscle (taenia coli of the guinea pig) under various osmotic conditions. *Pflugers Arch.*, 362, 255-260.
- Groth, K.M., Granata, K.P., 2008. The viscoelastic standard nonlinear solid model: Predicting the response of the lumbar intervertebral disk to low-frequency vibrations. *J. Biomech. Eng.*, 130, 031005.
- Guan, Y., Yoganandan, N., Moore, J., Pintar, F.A., Zhang, J., Maiman, D.J., Laud, P., 2007. Moment-rotation responses of the human lumbosacral spinal column. *J. Biomech.*, 40, 1975-1980.
- Hawkins, D., Lum, C., Gaydos, D., Dunning, R., 2009. Dynamic creep and pre-conditioning of the achilles tendon in-vivo. *J. Biomech.*, 42, 2813-2817.
- Hendershot, B., Bazrgari, B., Muslim, K., Toosizadeh, N., Nussbaum, M.A., Madigan, M.L., 2011. Disturbance and recovery of trunk stiffness and reflexive muscle responses following prolonged trunk flexion: Influences of flexion angle and duration. *Clin. Biomech.*, 26, 250-256.
- Hult, E., Ekström, L., Kaigle, A., Holm, S., Hansson, T., 1995. In vivo measurement of spinal column viscoelasticity—an animal model. *Proc Inst Mech Eng H*, 209 (2), 105-110.
- Kazarian, L., 1975. Creep characteristics of the human spinal column. *Orthop. Clin. North Am.*, 6, 3-18.
- Keller, T.S., Holm, S.H., Hansson, T.H., Spengler, D., 1990. The dependence of intervertebral disc mechanical properties on physiologic conditions. *Spine*, 15, 751-761.
- Keller, T.S., Nathan, M., 1999. Height change caused by creep in intervertebral discs: A sagittal plane model. *J Spinal Disord Tech*, 12, 313-324.
- Keller, T.S., Roy, A.L., 2002. Posture-dependent isometric trunk extension and flexion strength in normal male and female subjects. *J Spinal Disord Tech*, 15, 312-318.
- Koeller, W., Muehlhaus, S., Meier, W., Hartmann, F., 1986. Biomechanical properties of human intervertebral discs subjected to axial dynamic compression--influence of age and degeneration. *J. Biomech.*, 19, 807-816.
- Kumar, S., Dufresne, R.M., Schoor, T.V., 1995. Human trunk strength profile in flexion and extension. *Spine*, 20, 160-168.

- Lehman, S.L., Stark, L.W., 1982. Three algorithms for interpreting models consisting of ordinary differential equations: Sensitivity coefficients, sensitivity functions, global optimization. *Math. Biosci.*, 62, 107-122.
- Linke, W.A., Leake, M.C., 2004. Multiple sources of passive stress relaxation in muscle fibres. *Phys. Med. Biol.*, 49, 3613-3827.
- Little, J.S., Khalsa, P.S., 2005. Human lumbar spine creep during cyclic and static flexion: Creep rate, biomechanics, and facet joint capsule strain. *Ann. Biomed. Eng.*, 33, 391-401.
- Machiraju, C., Phan, A.V., Pearsall, A., Madanagopal, S., 2006. Viscoelastic studies of human subscapularis tendon: Relaxation test and a wiechert model. *Comput. Methods Programs Biomed.*, 83, 29-33.
- Magnusson, S., Simonsen, E., Dyhre-Poulsen, P., Aagaard, P., Mohr, T., Kjaer, M., 1996. Viscoelastic stress relaxation during static stretch in human skeletal muscle in the absence of emg activity. *Scand. J. Med. Sci. Sports*, 6, 323-328.
- Magnusson, S., Simonsen, E.B., Aagaard, P., Gleim, G., Mchugh, M., Kjaer, M., 1995. Viscoelastic response to repeated static stretching in the human hamstring muscle. *Scand. J. Med. Sci. Sports*, 5, 342-347.
- Magnusson, S.P., Aagaard, P., Nielson, J.J., 2000. Passive energy return after repeated stretches of the hamstring muscle-tendon unit. *Med. Sci. Sports Exerc.*, 32, 1160-1164.
- Mcclure, P., Siegler, S., Nobilini, R., 1998. Three-dimensional flexibility characteristics of the human cervical spine in vivo. *Spine*, 23, 216-223.
- Mccook, D.T., Vicenzino, B., Hodges, P.W., 2009. Activity of deep abdominal muscles increases during submaximal flexion and extension efforts but antagonist co-contraction remains unchanged. *J. Electromyogr. Kinesiol.*, 19, 754-762.
- Mcgill, S., 2007. *Low back disorders: Evidence-based prevention and rehabilitation: Human Kinetics Publishers.*
- Mcgill, S., Brown, S., 1992. Creep response of the lumbar spine to prolonged full flexion. *Clin. Biomech.*, 7, 43-46.
- Mcgill, S., Seguin, J., Bennett, G., 1994. Passive stiffness of the lumbar torso in flexion, extension, lateral bending, and axial rotation. Effect of belt wearing and breath holding. *Spine*, 19, 696-704.
- Mcgill, S.M., 1991. Electromyographic activity of the abdominal and low back musculature during the generation of isometric and dynamic axial trunk torque: Implications for lumbar mechanics. *J. Orthop. Res.*, 9, 91-103.
- Nussbaum, M., Chaffin, D., 1996. Development and evaluation of a scalable and deformable geometric model of the human torso. *Clin. Biomech.*, 11, 25-34.
- Oliver, M., Twomey, L., 1995. Extension creep in the lumbar spine. *Clin. Biomech.*, 10, 363-368.
- Olson, M.W., Li, L., Solomonow, M., 2009. Interaction of viscoelastic tissue compliance with lumbar muscles during passive cyclic flexion-extension. *J. Electromyogr. Kinesiol.*, 19, 30-38.
- Oxland, T.R., Lin, R.M., Panjabi, M.M., 1992. Three-dimensional mechanical properties of the thoracolumbar junction. *J. Orthop. Res.*, 10, 573-580.
- Panjabi, M., Oxland, T., Yamamoto, I., Crisco, J., 1994. Mechanical behavior of the human lumbar and lumbosacral spine as shown by three-dimensional load-displacement curves. *J. Bone Joint Surg. Am.*, 76, 413-424.

- Panjabi, M.M., 1992. The stabilizing system of the spine. Part ii. Neutral zone and instability hypothesis. *J. Spinal Disord.*, 5, 390-396.
- Panjabi, M.M., 2003. Clinical spinal instability and low back pain. *J. Electromyogr. Kinesiol.*, 13, 371-379.
- Parkinson, R.J., Beach, T.a.C., Callaghan, J.P., 2004. The time-varying response of the in vivo lumbar spine to dynamic repetitive flexion. *Clin. Biomech.*, 19, 330-336.
- Provenzano, P., Lakes, R., Corr, D., Vanderby, R., 2002. Application of nonlinear viscoelastic models to describe ligament behavior. *Biomech Model Mechanobiol*, 1, 45-57.
- Purslow, P.P., Wess, T., Hukins, D., 1998. Collagen orientation and molecular spacing during creep and stress-relaxation in soft connective tissues. *J. Exp. Biol.*, 201, 135-142.
- Raschke, U., Chaffin, D.B., 1996. Support for a linear length-tension relation of the torso extensor muscles: An investigation of the length and velocity emg-force relationships. *J. Biomech.*, 29, 1597-1604.
- Roy, A., Keller, T., Colloca, C., 2003. Posture-dependent trunk extensor emg activity during maximum isometrics exertions in normal male and female subjects. *J. Electromyogr. Kinesiol.*, 13, 469-476.
- Roylance, D., 2001. Engineering viscoelasticity. Department of materials science and engineering. Massachusetts Institute of Technology. Cambridge, MA, 2139, 24.
- Ryan, E., Herda, T., Costa, P., Walter, A., Cramer, J., 2011. Dynamics of viscoelastic creep during repeated stretches. *Scand. J. Med. Sci. Sports*, 22, 179-184.
- Ryan, E.D., Herda, T.J., Costa, P.B., Walter, A.A., Hoge, K.M., Stout, J.R., Cramer, J.T., 2010. Viscoelastic creep in the human skeletal muscle-tendon unit. *Eur. J. Appl. Physiol.*, 108, 207-211.
- Sanjeevi, R., 1982. A viscoelastic model for the mechanical properties of biological materials. *J. Biomech.*, 15, 107-109.
- Sarver, J.J., Robinson, P.S., Elliott, D.M., 2003. Methods for quasi-linear viscoelastic modeling of soft tissue: Application to incremental stress-relaxation experiments. *J. Biomech. Eng.*, 125, 754.
- Scannell, J.P., McGill, S.M., 2003. Lumbar posture—should it, and can it, be modified? A study of passive tissue stiffness and lumbar position during activities of daily living. *Phys. Ther.*, 83, 907-917.
- Shin, G., D'souza, C., Liu, Y.H., 2009. Creep and fatigue development in the low back in static flexion. *Spine*, 34, 1873-1878.
- Shin, G., Mirka, G.A., 2007. An in vivo assessment of the low back response to prolonged flexion: Interplay between active and passive tissues. *Clin. Biomech.*, 22, 965-971.
- Solomonow, M., Eversull, E., He Zhou, B., Baratta, R.V., Zhu, M.P., 2001. Neuromuscular neutral zones associated with viscoelastic hysteresis during cyclic lumbar flexion. *Spine*, 26, E314-E324.
- Stokes, I.a.F., Gardner-Morse, M., 2003. Spinal stiffness increases with axial load: Another stabilizing consequence of muscle action. *J. Electromyogr. Kinesiol.*, 13, 397-402.
- Strganac, T.W., Golden, H.J., 1996. Predictions of nonlinear viscoelastic behavior using a hybrid approach. *Int J Solids Struct*, 33, 4561-4570.
- Taylor, D.C., Dalton, J.D., Seaber, A.V., Garrett, W.E., 1990. Viscoelastic properties of muscle-tendon units. *Am. J. Sports Med.*, 18, 300-309.

- Thompson, R.E., Barker, T.M., Percy, M.J., 2003. Defining the neutral zone of sheep intervertebral joints during dynamic motions: An in vitro study. *Clin. Biomech.*, 18, 89-98.
- Thornton, G., Oliynyk, A., Frank, C., Shrive, N., 1997. Ligament creep cannot be predicted from stress relaxation at low stress: A biomechanical study of the rabbit medial collateral ligament. *J. Orthop. Res.*, 15, 652-656.
- Toosizadeh, N., Bazrgari, B., Hendershot, B., Muslim, K., Nussbaum, M.A., 2010. In vivo load-relaxation of the trunk with prolonged flexion. *ASB*, Providence RI.
- Troyer, K.L., Puttlitz, C.M., 2011. Human cervical spine ligaments exhibit fully nonlinear viscoelastic behavior. *Acta biomaterialia*, 7, 700-709.
- Truong, X., 1974. Viscoelastic wave propagation and rheologic properties of skeletal muscle. *Am. J. Physiol.*, 226, 256-264.
- Twomey, L., Taylor, J., 1982. Flexion creep deformation and hysteresis in the lumbar vertebral column. *Spine*, 7, 116-122.
- Twomey, L., Taylor, J., 1983. Sagittal movements of the human lumbar vertebral column: A quantitative study of the role of the posterior vertebral elements. *Arch. Phys. Med. Rehabil.*, 64, 322-325.
- Wenbo, L., Ting-Qing, Y., Qunli, A., 2001. Time-temperature-stress equivalence and its application to nonlinear viscoelastic materials. *Acta Mechanica Solida Sinica*, 14, 195-199.
- Yahia, L., Audet, J., Drouin, G., 1991. Rheological properties of the human lumbar spine ligaments. *J. Biomed. Eng.*, 13, 399-406.
- Yamamoto, I., Panjabi, M.M., Crisco, T., Oxland, T., 1989. Three-dimensional movements of the whole lumbar spine and lumbosacral joint. *Spine*, 14, 1256-1260.
- Youssef, J., Davidson, B., Zhou, B.H., Lu, Y., Patel, V., Solomonow, M., 2008. Neuromuscular Neutral zones response to static lumbar flexion: Muscular stability compensator. *Clin. Biomech.*, 23, 870-880.

3 Creep Deformation of the Human Trunk in Response to Prolonged and Repetitive Flexion: Measuring and Modeling the Effect of External Moment and Flexion Rate

Nima Toosizadeh and Maury A. Nussbaum

Abstract

While viscoelastic responses of isolated trunk soft tissues have been characterized in earlier studies, the effects of external moment and flexion rate on these responses in the intact human trunk are largely unknown. Two experiments were conducted to measure trunk viscoelastic behaviors, one involving prolonged flexion with several external moments and the other repetitive trunk flexion with different external moments and flexion rates. Direct outcome measures included initial trunk angle, creep angle, and residual/cumulative creep. Viscoelastic behaviors in both experiments were characterized using different Kelvin-solid models. For prolonged flexion, external moment significantly affected initial angle, creep angle, and viscoelastic model parameters, while residual creep remained unchanged. For repetitive flexion, cumulative creep angle significantly increased with both external moment and flexion rate. Nonlinear viscoelastic behavior of the trunk was evident in both experiments, which also indicated better predictive performance using Kelvin-solid models with ≥ 2 retardation time constants. Understanding trunk viscoelastic behaviors in response to flexion exposures can help in future modeling and in assessing how such exposures alter the synergy between active and passive trunk tissues.

3.1 Introduction

Time-dependent behaviors of trunk soft tissues, especially in response to flexion/extension exposures, have been characterized in several studies. These include measurements of viscoelastic properties of spinal motion segments (Little and Khalsa 2005; Twomey and Taylor 1982), and passive muscle components (Hawkins et al., 2009; Magnusson et al., 2000; Ryan et al., 2011). Further, creep in the human trunk has been measured *in vivo* during prolonged and repetitive flexion exposures, and creep/recovery behaviors have been assessed in feline spines. While these studies have provided a fundamental understanding of the time-dependent responses of trunk tissues, some limitations remain. Most measurements of spine viscoelastic properties have been performed on cadaveric material, and these *in vitro* experiments do not account for metabolic processes that are influential in prolonged tests (Hult et al., 1995; Keller et al., 1990). Moreover, there is evidence for nonlinear viscoelastic behavior of trunk soft tissues (Hult et al., 1995; Toosizadeh et al., 2012; Troyer and Puttlitz 2011). In the few *in vivo* studies that measured viscoelastic properties in trunk flexion, creep deformations were measured with only one or two external moment magnitudes. As such, *in vivo* creep deformations of the human trunk to prolonged and repetitive flexion, and the dependency of these responses to diverse loading magnitudes/rates, are still unknown.

One important application of information regarding trunk viscoelastic behavior is in assessing work-related low back disorder (WRLBD) risk. Epidemiological studies indicate an increased risk of WRLBDs due to prolonged or repetitive trunk flexion, especially when these exposures are followed by a demanding task such as lifting (Hoogendoorn et al., 2000; Prado-Leon et al., 2005; Punnett et al., 1991). A potential mechanism involved is viscoelastic deformation of

passive tissues in the posterior trunk and a subsequent reduction in trunk passive stiffness (Bazrgari et al., 2011; Olson et al., 2009; Parkinson et al., 2004; Solomonow 2011; Toosizadeh et al., 2012). Trunk passive stiffness along with muscle activity (i.e., reflexive and voluntary contractions) contribute to trunk equilibrium and stability (Panjabi 1992; Reeves et al., 2007). A reduction in trunk passive stiffness might be compensated by additional muscle activity, which can increase the loading on spinal motion segments, increase metabolic cost, and contribute to muscle fatigue (Adams and Dolan 1995; Shin et al., 2009). Since WRLBD risk may be associated with spinal loads and muscle fatigue (Bakker et al., 2009; Brereton and McGill 1999; Burdorf and Sorock 1997), describing time-dependent changes in load partitioning among active and passive trunk tissues can help in understanding this risk.

In the current work, creep deformation and recovery were measured *in vivo* in response to several external moments during prolonged flexion exposures (Experiment 1), and to several external moments and to several rates of repetitive trunk flexion (Experiment 2). Given the noted evidence of nonlinear viscoelastic behavior of trunk soft tissues, we hypothesized (1) that the whole trunk would exhibit nonlinear viscoelastic responses to flexion exposures. We also hypothesized (2) that the recovery of mechanical properties would depend on the external moment during exposure. Kelvin-solid models, specifically the Generalized Kelvin (GK) and standard nonlinear solid (SNS) models, have given the best predictions of viscoelastic responses under quasi-static conditions (Groth and Granata 2008; Machiraju et al., 2006), and the same models were used here to predict creep deformations of the whole trunk. We hypothesized (3) that these viscoelastic models would have differing success in characterizing these responses.

3.2 Methods: Prolonged Flexion

3.2.1 Participants

Ten healthy young adults (Table 3.1), with no self-reported history of low-back pain, participated after completing informed consent procedures approved by the Virginia Tech Institutional Review Board. In both experiments, relatively young participants (range = 19-28 yr) were included to avoid potential influences related to age.

Table 3.1: Mean (SD) values of participant age and anthropometry in the two trunk flexion experiment.

<i>Prolonged Flexion</i>	Number	Age (yr)	Stature (cm)	Body mass (kg)
All	10	24 (4)	174.5 (9.8)	71.3 (10.7)
Male	5	24 (4)	182.7 (4.0)	79.8 (5.5)
Female	5	24 (3)	166.3 (5.5)	62.7 (6.7)
<i>Repetitive Flexion</i>				
All	12	24 (5)	174.8 (7.7)	70.9 (5.8)
Male	6	25 (4)	179.6 (5.9)	74.2 (4.1)
Female	6	24 (3)	170.0 (6.5)	67.6 (5.5)

3.2.2 Experimental design and procedures

Prolonged trunk flexion exposures were performed to investigate the effect of external moment on viscoelastic properties. Participants stood in a rigid frame, and straps were used to restrain the pelvis and lower limbs. For conditions involving extra loads (see below), two weights were attached to participants' wrists (Figure 3.1). To quantify viscoelastic deformation during flexion exposure, lumbar flexion angle was measured using inertial measurement units (IMUs: Xsens Technologies XM-B-XB3, Enschede, Netherlands). IMUs were placed on the skin using medical-grade, double-sided tape, over the spinous processes of T12 and S1, and sampled at 100 Hz. Electromyography (EMG) of the erector spinae (at the L1 and L3 levels), rectus abdominus,

and external oblique muscles was collected bilaterally using bipolar Ag/AgCl surface electrodes, with electrode placements as previously reported (Toosizadeh et al., 2012). Raw EMG data were preamplified (x100) near the collection site, bandpass filtered (10-500 Hz) and amplified in hardware (Measurement System Inc., Ann Arbor, MI, USA), and sampled at 1000 Hz.

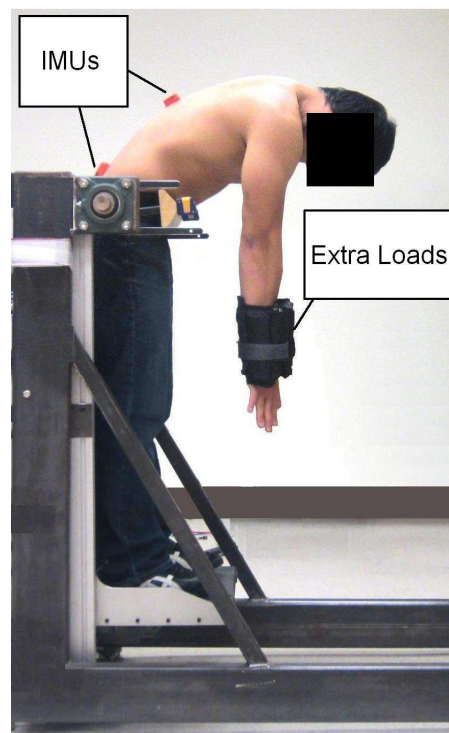


Figure 3.1: Experimental setup for creep testing (condition with 42 N of extra load is illustrated), including placement of inertial measurement units (IMUs).

The effect of moment on viscoelastic behaviors during prolonged flexion was assessed using five levels of external moment induced by extra loads of 0, 21, 42, 63, and 84 N for males and 0, 13.5, 27, 40.5, and 54 N for females. The maximum load for males was set to represent the mean weight handled in a high-risk manual material handling task (Marras et al., 1993), and the maximum load for females was adjusted based on relative lifting capacities between genders (Mital 1984, Snook and Ciriello 1991). Prolonged flexion exposures were completed in sessions

on different days and with ≥ 3 days between consecutive sessions. The presentation order was counterbalanced using 5×5 Latin Squares (one for each gender), and sessions were conducted before 9:00 am to minimize the effects of cumulative daily loading. Prolonged creep deformation was induced by participant's flexing their trunk slowly to full passive trunk flexion (~ 3 sec), remaining in this flexed posture (6 min), and then slowly returning to the upright standing posture (~ 3 sec). During full flexion, participants were asked to face downward, looking at a mark on the floor, and with their arms hanging vertically. These procedures were intended to minimize changes in trunk angle and external moments due to body movements. EMG measures (as described above) were used as biofeedback to minimize voluntary muscle activation, thus ensuring that measures were predominantly reflecting passive tissue properties. Six minutes of full flexion was considered sufficient for estimating viscoelastic properties (McGill and Brown 1992). Longer periods were not used to avoid soreness in the biceps femoris and paraspinal muscles and consequent involuntary body movements.

Following each prolonged exposure, additional flexion tasks were completed to measure the recovery of trunk viscoelastic properties. Since the recovery phase has a rate about half that of creep deformation (McGill and Brown 1992), 12 minutes of recovery were used, during which participants adopted full passive flexion every 20 seconds. This involved the same procedures as above, though the flexed posture was maintained for only 1 sec. Maximum lumbar angle during each post-exposure flexion was recorded to characterize recovery. The rate of three flexions/min was selected based on pilot results, as sufficient to capture rapid initial recovery behaviors but also to avoid excessive creep deformation due to repetitive trunk flexion. Moreover, to account for potential influences of repetitive flexion during recovery, cumulative creep due to repetitive

flexion was quantified in the subsequent experiment (described below) and was subtracted from the current results.

3.2.3 Outcome measures

Several direct and derived (model-based, described below) outcome measures were obtained: initial angle, creep angle, residual creep, and viscoelastic model parameters during creep. Three-second windows at the start and end of each prolonged flexion were used to calculate initial and creep angles. Residual creep was defined as the difference between the mean of the last two full flexion angles in the recovery phase and the initial pre-creep angle (Figure 3.2).

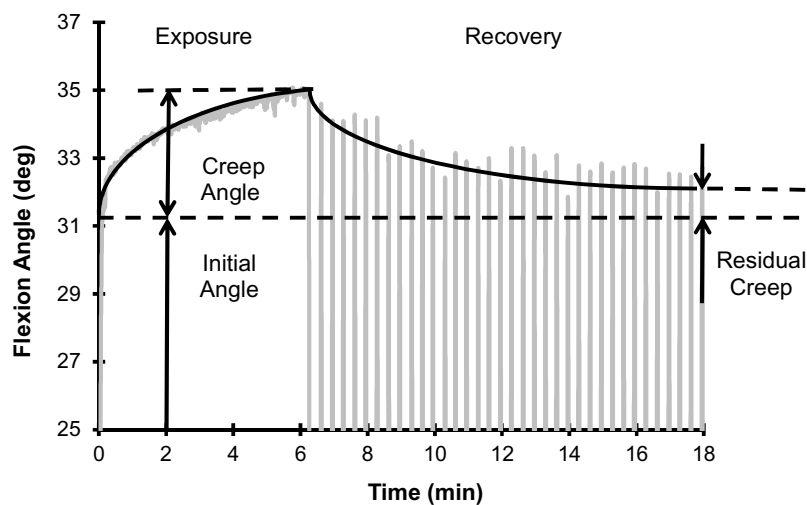


Figure 3.2: Sample results, indicating lumbar flexion angle during creep exposure and recovery, and selected outcome measures. Experimental data are illustrated in grey for an exposure with 85 N of extra load.

3.2.4 Viscoelastic models

To characterize trunk creep deformation in response to prolonged flexion, two common types of Kelvin-solid models (i.e., GK and SNS models) of differing complexity were used (Figure 3.3).

The creep equation for the GK model is (Findley et al., 1989):

$$\theta(t) = M_0 \sum_{i=1}^n \frac{1}{J_i} \left(1 - e^{-\frac{t}{\tau_i}} \right) + \frac{M_0}{J_0} \quad (3.1)$$

where J_i and τ_i ($\tau_i = \frac{\eta_i}{J_i}$) respectively are stiffness and retardation time constants in the i^{th}

Kelvin component; n is the number of Kelvin components (set to $n = 2, 3$ and 4); and J_0 is the stiffness of an in-series torsional spring representing instantaneous deformation. Here, M_0 is the external moment, and was considered constant during prolonged flexion exposure since changes due to creep deformation are negligible (McGill and Brown 1992). A multi-segment model was used to estimate the external moment at the L2-L3 level (~ middle of the lumbar spine) for each participant in each loading condition. To determine the moment arms of upper body segments (head, neck, upper extremities, thoracic and lumbar spine), the relative sagittal rotation of each motion segment (T12-L1 through L5-S1) was estimated using available material properties (Bazrgari et al., 2008; Guan et al., 2007; Panjabi et al., 1994), and the thorax, neck, and head were considered as one rigid body (Arjmand and Shirazi-Adl 2005; Nussbaum and Chaffin 1996). Mass and mass center locations for model segments were derived and scaled based on participant body mass and stature (Bazrgari et al., 2008; De Leva 1996).

With $n = 1$, the GK model is simplified to the SNS model introduced by Groth and Granata, (2008). This has the same structure as the SLS model, yet spring and damper components have nonlinear force-length or force-velocity properties. The creep equation for the SNS model is:

$$\theta(t) = \frac{M_0}{K_1} \left(\frac{K_1 + K_2}{K_2} - e^{-\frac{t}{T}} \right) \quad (3.2)$$

where K_1 and C are stiffness and damping of torsional spring and damper components in parallel, and K_2 is the stiffness of an in-series torsional spring (Figure 3.3). K_1 and C represent viscous responses to deformation, and K_2 the instantaneous response; the retardation time constant ($T = \frac{C}{K_1}$) describes the rate of creep (Burns et al., 1984).

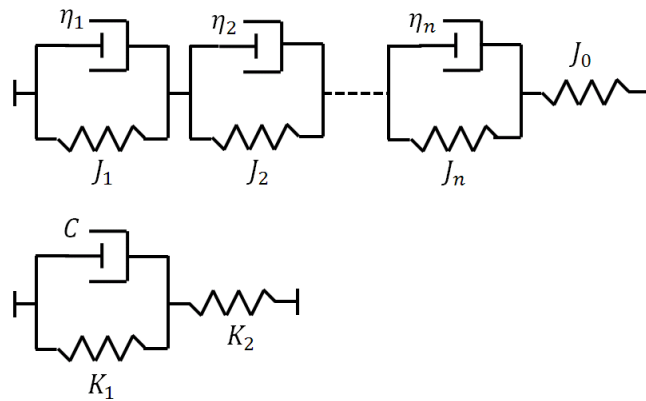


Figure 3.3: Illustration of two Kelvin-solid models: GK (top), and SNS (bottom). Each spring and damper combination in parallel represents a Kelvin model. For clarity, linear rather than rotational components are illustrated.

Model parameters were estimated for each prolonged flexion exposure, by minimizing least-squared errors in predicted lumbar flexion angles. Both models were then used to predict recovery behaviors using mean parameter values across participants for each loading condition. Using the Boltzmann Superposition Principle, the following recovery equation was derived for the GK model (Findley et al., 1989), assuming that the M_0 moment was removed at $t_1 = 6$ min (i.e., at the end of prolonged flexion period):

$$\theta(t) = M_0 \sum_{i=1}^n \frac{1}{J_i} \left(e^{-\frac{t}{\tau_i}} \right) \left(e^{\frac{t_1}{\tau_i}} - 1 \right), \text{ (for } t > t_1 \text{)} \quad (3.3)$$

Similarly, the recovery equation for the SNS model is:

$$\theta(t) = \frac{M_0}{K_1} \left(e^{-\frac{t}{T}} \right) \left(e^{\frac{t_1}{T}} - 1 \right), \text{ (for } t > t_1 \text{)} \quad (3.4)$$

3.2.5 Data analysis

After testing for normality of distribution, separate mixed-factor analyses of variance (ANOVAs) were performed to evaluate the effects of external moment and gender on the outcome measures. Only the relevant SNS model parameters (K_1 , K_2 , and C) were analyzed in this way, to assess potential nonlinearity in elastic and viscous properties, since their interpretation is relatively straightforward vs. parameters within the GK model. Post-hoc comparisons between flexion exposure levels were done, where relevant, using Tukey's HSD. Effects of external moment on initial angle, creep angle, and SNS model parameters were also explored using linear and nonlinear curve fits to mean values, and these were evaluated based on coefficients of determination (R^2). Model predictions of creep deformation during both prolonged flexion and recovery were then compared with measured angles. These predictions were evaluated using the mean, across participants, of coefficients of determination (R^2) and root-mean-square errors (RMSE) obtained from linear regressions within each exposure. Throughout, statistical significance was concluded when $p < 0.05$, and all analyses were performed using JMP (Version 9, SAS Institute Inc., Cary, NC, USA). All summary statistics are given as means (SDs).

3.3 Results: Prolonged Flexion

There were significant effects of external moment on initial angle and creep angle (Table 3.2). Both outcome measures were larger with increased external moment (Figure 3.4), and were well characterized by exponential functions ($R^2 > 0.96$). External moment did not affect residual

Table 3.2: Effects of external moment and gender on direct and derived outcome measures following prolonged flexion. The symbol * indicates a significant effect.

Measure	Moment	Gender	Moment × Gender
Initial angle	$F_{(4,28)}=3.0, p=0.037^*$	$F_{(1,8)}=0.08, p=0.79$	$F_{(4,28)}=0.6, p=0.65$
Creep angle	$F_{(4,28)}=18.86, p<0.0001^*$	$F_{(1,8)}=0.3, p=0.63$	$F_{(4,28)}=0.5, p=0.71$
Residual creep	$F_{(4,26)}=0.05, p=0.99$	$F_{(1,7)}=1.2, p=0.31$	$F_{(4,26)}=0.7, p=0.63$
K_1	$F_{(4,28)}=7.3, p=0.0004^*$	$F_{(1,8)}=1.4, p=0.27$	$F_{(4,28)}=0.4, p=0.81$
K_2	$F_{(4,28)}=0.6, p=0.67$	$F_{(1,8)}=9.8, p=0.014^*$	$F_{(4,28)}=0.2, p=0.93$
C	$F_{(4,28)}=5.2, p=0.0029^*$	$F_{(1,8)}=0.2, p=0.65$	$F_{(4,28)}=0.5, p=0.73$

creep, however, and which was 3.2 (7.1) deg across exposure conditions. External moment significantly affected the K_1 and C parameters within the SNS model (Table 3.2), and both decreased with increasing external moment (Figure 3.5). Gender had a significant effect only on the K_2 parameter, which was larger for males than females at 2.40 (0.38) and 1.84 (0.36) Nm/deg, respectively.

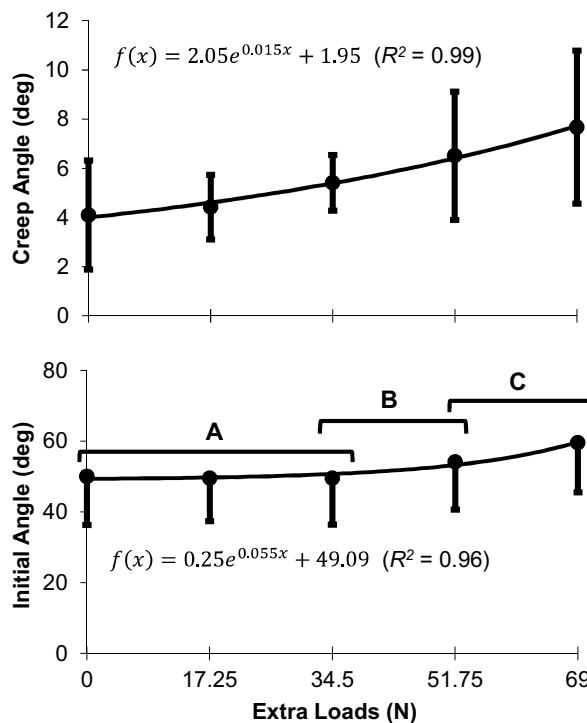


Figure 3.4: Effects of external moment, induced using extra loads (at the wrists), on initial and creep angles. Post-hoc groupings are indicated by brackets and letters, and best-fit exponential relationships are provided. Mean values of extra loads (across genders) are presented.

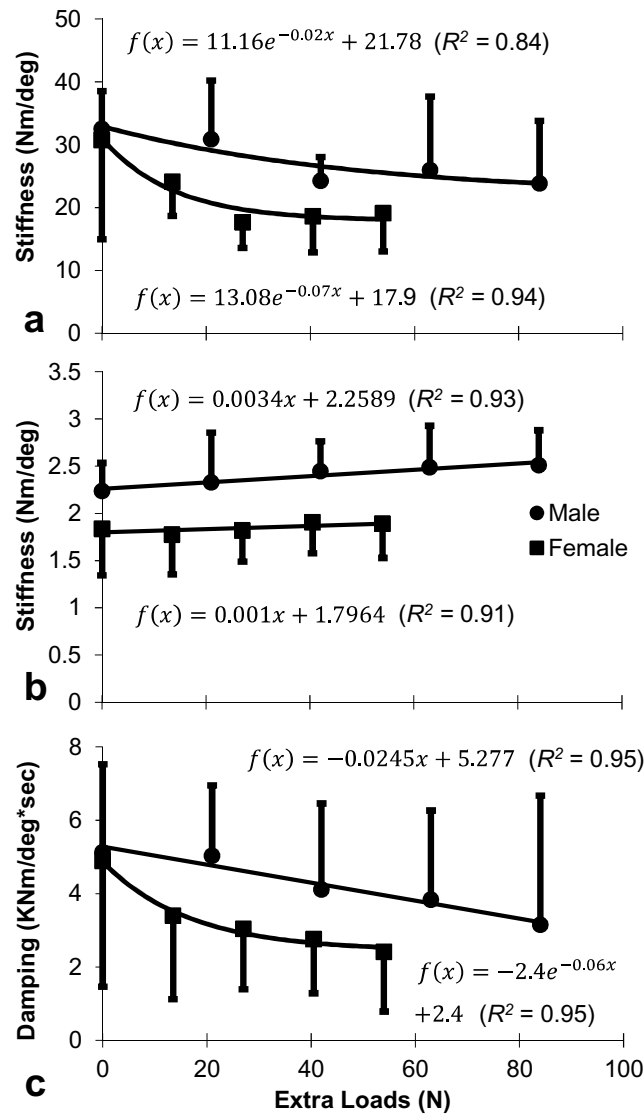


Figure 3.5: Effects of external moment on SNS model parameters for both genders: a) stiffness of Kelvin component (K_1); b) in-series (instantaneous) stiffness (K_2); and c) damping of Kelvin component (C). Best-fit relationships (linear or exponential) are provided.

The viscoelastic models exhibited different levels of prediction quality during creep exposures. Compared to the SNS model (Eqn 3.2), adding an extra retardation time constant (GK model; $n = 2$, Eqn 3.1) improved R^2 and RMSE by 0.7% and ~23%, respectively, across all exposure conditions. Respective values of R^2 and RMSE across all exposure conditions were 0.98 (0.02) and 0.22 (0.13) deg for the SNS model, and 0.99 (0.02) and 0.17 (0.12) deg for the GK model.

Use of additional retardation time constants (i.e., $n = 3$ or 4) had only minor effects on R^2 and RMSE. Therefore, only the GK model with $n = 2$ was maintained (to model prolonged flexion/recovery here, and repetitive flexion in the subsequent experiment). Moreover, model prediction quality did not substantially vary across exposure conditions.

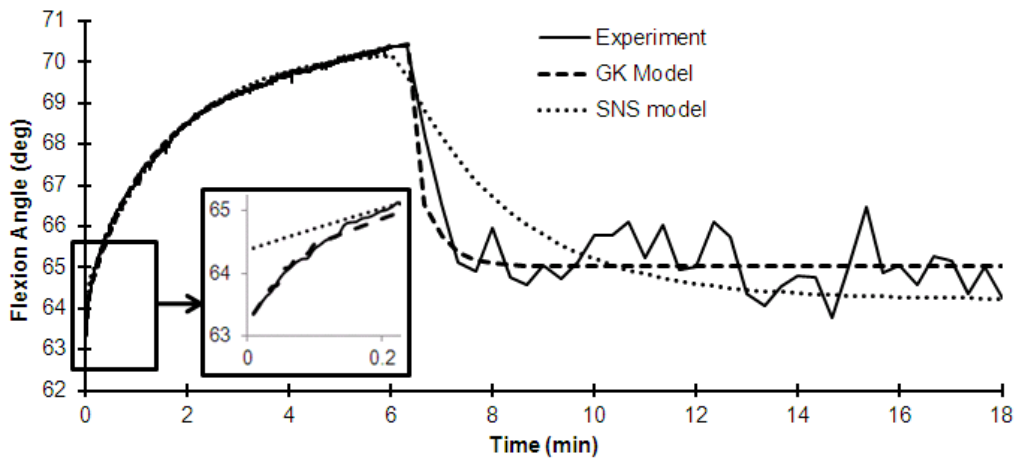


Figure 3.6: Representative data showing fast and slow phases of creep and recovery, and the, relative advantage of the GK vs. SNS models for predicting behaviors. Experimental results are mean values for exposures involving the largest external moment (i.e., largest extra load).

Prediction quality during the recovery period differed between models (Figure 3.6), and predictions of recovered angles were better using the GK vs. SNS models (Figure 3.7).

Respective R^2 and RMSE values for prediction errors across all exposure conditions were 0.64 (0.12) and 0.83 (0.16) deg for the GK model and 0.57 (0.13) and 1.01 (0.23) deg for the SNS model.

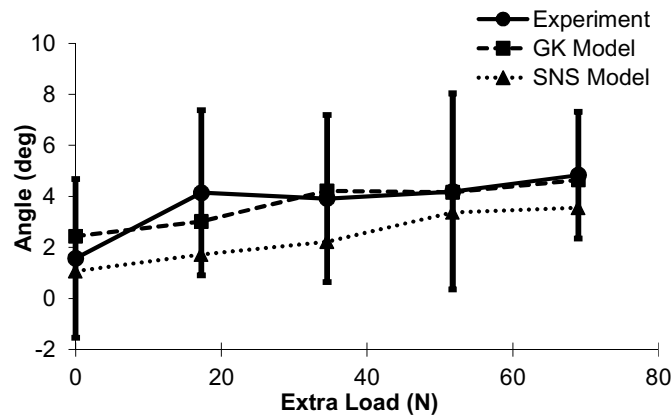


Figure 3.7: Predicted recovered angles using the GK and SNS models. Mean values of extra loads (across genders) are presented.

3.4 Methods: Repetitive Flexion

3.4.1 Participants

Twelve healthy young adults completed this experiment (Table 3.1). As in the first experiment, none had a self-reported history of low-back pain, and all completed informed consent procedures approved by the Virginia Tech Institutional Review Board.

3.4.2 Experimental design and procedure

Repetitive trunk flexion exposures were performed, to assess the effect of flexion rate and external moments on trunk mechanical behaviors, using similar instrumentation as in Experiment 1 (i.e., rigid frame, EMG, and IMUs). Each participant completed six experimental conditions involving all combinations of three flexion rates (i.e., 2, 3, and 4 flexions/min) and two external moments (i.e., extra loads of 0 and 84 N for males; 0 and 54 N for females). These rates were intended to cover a wide range of potential occupational exposures (Marras et al., 1993). As in the first experiment, the order of conditions was counterbalance, and completed in separate

sessions, in the morning, and with ≥ 3 days between sessions. Participants performed repetitive trunk flexion following similar procedures as in the recovery period described for the prior experiment, and during which lumbar flexion angle and extensor and flexor muscle activities were recorded. Isometric reference contractions were also performed, both before and after the repetitive flexion task, to assess fatigue development in trunk extensor muscles. Reference contractions involved generating a sub-maximal trunk extensor force, of 50% of maximum voluntary contraction force, for 30 seconds as in previous work (Dolan and Adams 1998; Roy et al., 1989). This force was maintained using visual feedback. For both reference and maximum contractions, a rod-harness assembly was used as described in our previous work (Bazrgari et al., 2011; Hendershot et al., 2011; Toosizadeh et al., 2012).

3.4.3 Outcome measures

Direct outcome measures for the repetitive flexion exposure were: initial angle, cumulative creep angle, and extensor muscles activity. The mean of the first three full flexion angles was obtained as the initial angle, and the difference between the mean of the last three full flexion angles and the initial angle was obtained as the cumulative creep angle (Figure 3.8). EMG of the extensor and flexor muscles during the exposures was RMS converted (time constant = 50 msec).

Changes in mean RMS values, between the last and first three flexions, were derived to indicate potential changes in muscle activity due to viscoelastic deformations. Fatigue development was assessed by changes in EMG RMS and median frequency (MF) of the trunk extensor muscles during the reference contractions.

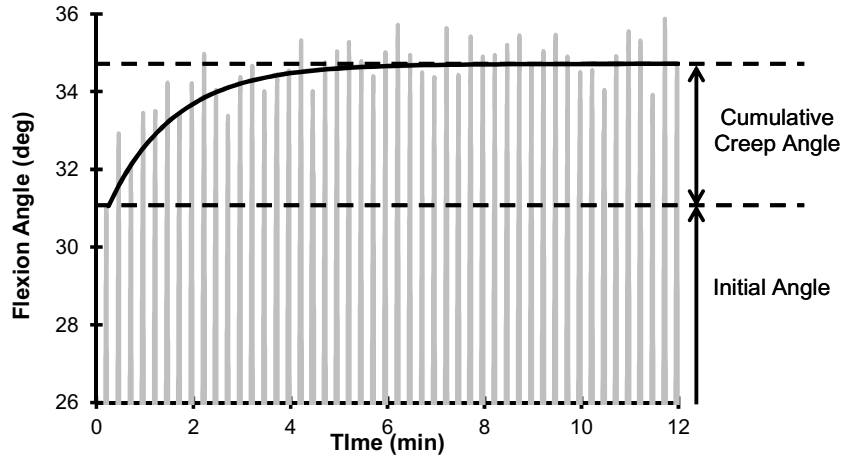


Figure 3.8: Representative results illustrating lumbar flexion angle during cumulative creep, and selected outcome measures. Experimental data are illustrated in grey for a prolonged flexion exposure with 85 N of extra load and 4 flex/min rate.

3.4.4 Viscoelastic models

Estimated model parameters from the prior experiment (prolonged flexion) were used here to predict creep behavior of the trunk in response to repetitive flexion. To achieve this, a predefined external moment history (as in Figure 3.9) was specified for each exposure condition (i.e., each combination of external moment and flexion rate), and flexion angle was calculated by solving the following equations for the GK and SNS models, respectively (Findley et al., 1989):

$$\theta(t) = \left(\sum_{i=1}^n \frac{1}{D\tau_i + J_i} + \frac{1}{J_0} \right) M \quad (3.5)$$

$$\theta(t) = \left(\frac{1}{DC + K_1} + \frac{1}{K_2} \right) M \quad (3.6)$$

where D is the differential operator with respect to time $\left(\frac{d}{dt}\right)$. To define external moment history for each exposure condition, the maximum external moment (see Figure 3.9) was estimated at the L2-L3 level (~ middle of the lumbar spine) using the multi-segment model described earlier. Mean values of participant stature and body mass from the current experiment were used to specify model anthropometry.

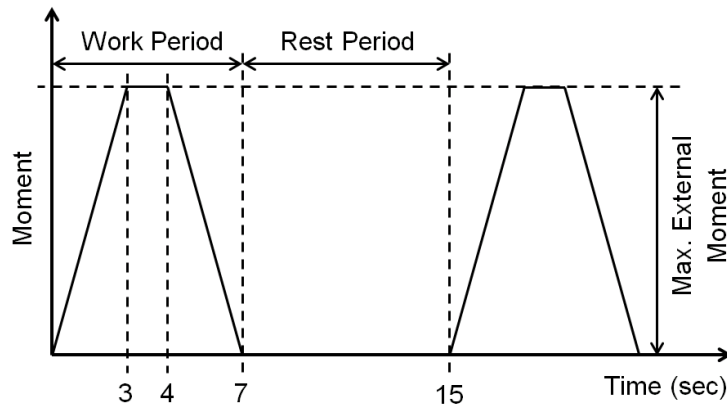


Figure 3.9: A cycle of external moment history for repetitive flexion at 4 flex/min rate. A similar moment history was applied for 2 and 3 flex/min rates, with longer rest periods.

3.4.5 Data analysis

After testing for normality of distribution, separate mixed-factor analyses of variance (ANOVAs) were performed to evaluate the effects of external moment, flexion rate, and gender on the direct outcome measures. Post-hoc comparisons between flexion exposure levels were done, where relevant, using Tukey's HSD. To assess fatigue, "time" (i.e., pre-exposure, and post-exposure) was included as an additional independent variable, and ANOVAs were used to assess changes in EMG RMS and MF of the trunk extensor muscles during the reference contractions. To evaluate the models, predicted creep deformations during repetitive flexion were compared with measured angles. For this, means of coefficients of determination (R^2) and RMSE were obtained across participants for each exposure. Statistical significance was concluded when $p < 0.05$, and all summary statistics are given as means (SDs).

3.5 Results: Repetitive Flexion

Initial angle and cumulative creep angle both increased significantly with external moment (Table 3.3). However, only cumulative creep angle increased with flexion rate (Figure 3.10).

Table 3.3: Effects of external moment and flexion rate on direct outcome measures following repetitive flexion. The symbol * indicates a significant effect.

Measure	Moment	Rate	Moment × Rate
Initial angle	$F_{(1,44)}=18.1, p=0.0001^*$	$F_{(2,44)}=0.7, p=0.52$	$F_{(2,44)}=2.7, p=0.078$
Cumulative creep	$F_{(1,44)}=5.4, p=0.025^*$	$F_{(2,44)}=8.6, p=0.0007^*$	$F_{(2,44)}=1.2, p=0.30$
Muscle activity	$F_{(1,44)}=0.1, p=0.76$	$F_{(2,44)}=1.6, p=0.22$	$F_{(2,44)}=0.4, p=0.68$

There were no main or interactive effects of external moment or flexion rate on muscle activity, and there were no main or interactive effects of gender on any of the outcome measures ($p > 0.11$). EMG RMS or MF values did not change between pre- and post-exposure reference contractions ($p > 0.32$). Cumulative creep was respectively overestimated and underestimated using the GK and SNS models (Figure 3.10).

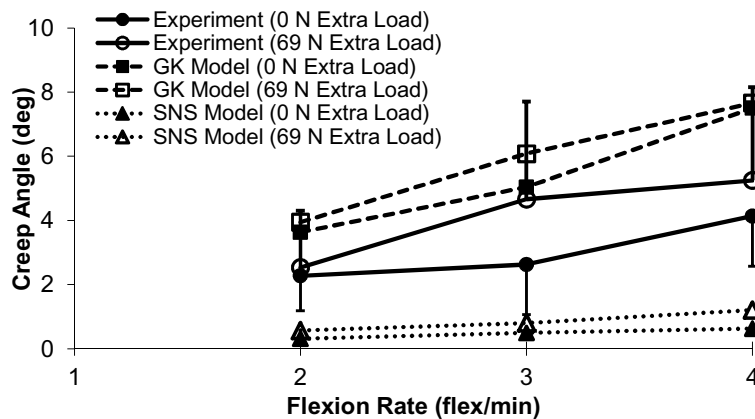


Figure 3.10: Effects of external moment and flexion rate on cumulative creep. Values are given for both experimental and model-predicted results. Mean values of extra load (across genders) are presented.

3.6 Discussion

3.6.1 Prolonged trunk flexion

In support of our first hypothesis, nonlinear viscoelastic trunk properties were observed in response to flexion exposures. This was apparent from the moment-dependency of SNS model

parameters: both K_1 and C decreased as external moment increased, while the retardation time constant (T) was consistent across the applied range of external moment. Similar changes in SNS model parameters with applied load were reported earlier for *in vivo* axial compression on porcine lumbar motion segments (Hult et al., 1995). These changes suggest reduced viscoelastic stiffness with larger external moments and consequently a nonlinear creep deformation, and which was evident here from creep angle-moment relationships (Figure 3.4). Adding to previous evidence of nonlinear viscoelastic behaviors of spinal soft tissues (Hult et al., 1995; Toosizadeh et al., 2012; Troyer and Puttlitz 2011), the current work indicates nonlinearity in the whole trunk response to flexion exposures.

During prolonged trunk flexion, the mean (SD) creep response was 4.1 (2.2) deg here without extra loads, comparable to earlier results of 2.5 and 4.2 deg of creep after 5 and 10 minutes of standing flexion, respectively (Shin and Mirka 2007, Shin et al., 2009), and a creep angle of ~3 deg after 6 minutes of flexion in a seated posture (McGill and Brown 1992). The increase in angle due to creep was ~11% here across all loading conditions, and an *in vitro* experiment (Twomey and Taylor 1982) using isolated lumbar motion segments showed similar creep behaviors (~11% increase in flexion angle after 6 minutes of loading). This indicates a predominant contribution of spinal motion segments in providing passive stiffness, though additional work is needed to facilitate an accurate estimation of the load distribution among passive muscle tissues and spinal motion segments, especially in response to prolonged loadings. Regarding trunk elastic properties, the relationship between external moment and initial angle (i.e., instantaneous moment-angle relationship) found here is similar to previous *in vivo* studies (McGill et al., 1994; Parkinson et al., 2004). Although changes in elastic stiffness (K_2) were not

significant, the same pattern of increases with external moment were found. Further, elastic stiffness was ~23% higher among males across all loading conditions, and the same gender difference has been reported previously in trunk flexion (Brown et al., 2002; Parkinson et al., 2004).

Although both Kelvin-solid models showed acceptable predictions of viscoelastic behavior (creep angle) during prolonged trunk flexion exposures, in support of our hypothesis the GK model presented some advantages. Two phases of creep deformation were evident (Figure 3.6), with an early (<1 min) rapid rate and a subsequent slower rate. Similar dual-phase creep behaviors were reported in previous *in vitro* studies using human spinal motion segments (Burns et al., 1984). As such, the improved predictions using the GK model were probably from the additional retardation time constant. This is comparable to our previous work, in which predictions of load relaxation in the trunk were improved using models with ≥ 2 constants (Toosizadeh et al., 2012). Differences in viscoelastic behaviors of trunk soft tissues (e.g., intervertebral discs, ligaments, or muscles) are a likely underlying mechanism for this dual-phase creep behavior. However, additional experimental results are again needed to characterize the distinct viscoelastic properties of different passive tissues.

Following prolonged flexion, mechanical properties recovered from the imposed creep by ~43% after 12 minutes. This suggests that a recovery period twice as long as the exposure is insufficient for full recovery. Earlier work, using both cadaver models (Little and Khalsa 2005; Twomey and Taylor 1982) and the whole human trunk (Bazrgari et al., 2011; McGill and Brown 1992), also suggested a longer required recovery period than the duration of prolonged flexion

exposure to achieve full recovery. Further, an *in vivo* study using feline lumbar spine models showed that even seven hours is not adequate to provide complete recovery of viscoelastic creep caused by 20 minutes of static flexion (Solomonow et al., 2003). Overall, results here clearly support that slower recovery vs. onset rates exist for trunk creep deformations. It was not possible here, though, to predict the time required for full recovery from creep deformations. A relatively short recovery period was used, to minimize potential confounding effects of prolonged standing and repetitive flexion on trunk behaviors (e.g., axial creep and muscle fatigue). Further, the amount of recovery (i.e., recovered angle) increased with the applied external moment during prolonged flexion (Figure 3.7), and which led to a consistent level of residual creep across exposure conditions (i.e., supporting our second hypothesis). This increase in recovery magnitude with applied external moment was also predicted by both viscoelastic models here, supporting a dependency of recovery on the external moment during exposure.

Mechanical properties recovery was roughly exponential with time (Figure 3.6); across all loading conditions ~54% of recovery occurred in the first minute. Consistent results were reported earlier (McGill and Brown 1992), specifically a rapid recovery (~50%) in the first two minutes. Studies on feline spines also showed that exponential models can describe the recovery of mechanical behaviors following prolonged or repetitive loading (Solomonow 2011; Youssef et al., 2008). This rapid initial recovery was predicted better here using the GK model, suggesting a dual-phase process similar to that for creep (see above).

3.6.2 Repetitive trunk flexion

Cumulative creep increased substantially with both external moment and flexion rate, with a larger effect of the latter within the current ranges examined. An increasing flexion rate was earlier shown to result in larger creep deformation and neuromuscular alterations such as muscle spasm and changes in reflexive behaviors (Lu et al., 2008). As such, to control the risk of WRLBDs, reducing the flexion rate might be more effective than reducing the external moment. An increase in cumulative creep with large external moment and higher flexion rate was predicted by both the GK and SNS models. However, the SNS model underestimated and GK model overestimated the actual creep responses (Figure 3.10). Such limitations in model performance should be considered when using these models for predicting viscoelastic behaviors of the trunk in response to repetitive flexion. Material properties for this purpose should be specifically derived for repetitive flexion exposure rather than using properties from prolonged flexion.

3.6.3 Limitations, implications, and conclusions

An important potential limitation of the current study is related to measuring *in vivo* viscoelastic properties. Such measurement is challenging, particularly given the relatively modest changes in creep angle during trunk flexion exposures and the unavoidable presence of uncontrolled body movements. These effects account, at least in part, for the larger variability within each exposure (larger RMSE) compared to *in vitro* studies. However, muscle activity during prolonged flexion exposures was controlled here visually (during the task) and assessed (following the task) using additional analysis of the EMG data. EMG RMS mean values were not significantly different

between the first and last minute of exposures (from paired *t*-tests, $p = 0.12$), suggesting little confounding due to uncontrolled movements.

In summary, nonlinear viscoelastic behavior of trunk soft tissues was evident. The current results, and our previous findings (Toosizadeh et al., 2012), indicate that viscoelastic properties of the trunk are influenced by exposure conditions, specifically the magnitude of external moment and flexion angle. An improved understanding of trunk soft tissue responses to prolonged or repetitive flexion exposures, including different loading magnitudes/rates, can facilitate predictions of load distributions among passive and active trunk tissues during and following such exposures. Recovery of mechanical alterations (i.e., changes in soft tissues stiffness) was prolonged, and the recovery rate depended on external moment. Residual creep, though, was comparable after equivalent recovery periods following exposures with diverse external moment. Hence, required recovery periods may be relatively independent of external moment. Kelvin-solid models were used to characterize viscoelastic responses and derive material properties in response to prolonged flexion exposures. Such material properties can be used to predict trunk behaviors and lumbar mechanics in response to prolonged flexion exposures, for example by incorporation within larger-scale biomechanical models for evaluating occupational tasks, especially those involving trunk flexion. However, use of these properties/models for predicting viscoelastic responses to repetitive trunk flexion should be done with some caution due to potential inaccuracy in predicting time-dependent trunk behaviors and the limited age range examined here.

3.7 References

- Adams, M., Dolan, P., 1995. Recent advances and their clinical in lumbar spinal mechanics significance. *Clin. Biomech.*, 10, 3-19.
- Arjmand, N., Shirazi-Adl, A., 2005. Biomechanics of changes in lumbar posture in static lifting. *Spine*, 30, 2637-2648.
- Bakker, E.W.P., Verhagen, A.P., Van Trijffel, E., Lucas, C., Koes, B.W., 2009. Spinal mechanical load as a risk factor for low back pain: A systematic review of prospective cohort studies. *Spine*, 34, E281-E293.
- Bazrgari, B., Hendershot, B., Muslim, K., Toosizadeh, N., Nussbaum, M.A., Madigan, M.L., 2011. Disturbance and recovery of trunk mechanical and neuromuscular behaviours following prolonged trunk flexion: Influences of duration and external load on creep-induced effects. *Ergonomics*, 54, 1043-1052.
- Bazrgari, B., Shirazi-Adl, A., Kasra, M., 2008. Computation of trunk muscle forces, spinal loads and stability in whole-body vibration. *J Sound Vib*, 318, 1334-1347.
- Brereton, L.C., McGill, S.M., 1999. Effects of physical fatigue and cognitive challenges on the potential for low back injury. *Hum Mov Sci*, 18, 839-857.
- Brown, M.D., Holmes, D.C., Heiner, A.D., Wehman, K.F., 2002. Intraoperative measurement of lumbar spine motion segment stiffness. *Spine*, 27, 954-958.
- Burdorf, A., Sorock, G., 1997. Positive and negative evidence of risk factors for back disorders. *Scand. J. Work. Environ. Health*, 23, 243-256.
- Burns, M., Kaleps, I., Kazarian, L., 1984. Analysis of compressive creep behavior of the vertebral unit subjected to a uniform axial loading using exact parametric solution equations of kelvin-solid models--part i. Human intervertebral joints. *J. Biomech.*, 17, 113-130.
- De Leva, P., 1996. Adjustments to zatsiorsky-seluyanov's segment inertia parameters. *J. Biomech.*, 29, 1223-1230.
- Dolan, P., Adams, M., 1998. Repetitive lifting tasks fatigue the back muscles and increase the bending moment acting on the lumbar spine. *J. Biomech.*, 31, 713-721.
- Findley, W.N., Lai, J.S., Onaran, K., 1989. Creep and relaxation of nonlinear viscoelastic materials: With an introduction to linear viscoelasticity: Dover Publications.
- Groth, K.M., Granata, K.P., 2008. The viscoelastic standard nonlinear solid model: Predicting the response of the lumbar intervertebral disk to low-frequency vibrations. *J. Biomech. Eng.*, 130, 031005.
- Guan, Y., Yoganandan, N., Moore, J., Pintar, F.A., Zhang, J., Maiman, D.J., Laud, P., 2007. Moment-rotation responses of the human lumbosacral spinal column. *J. Biomech.*, 40, 1975-1980.
- Hawkins, D., Lum, C., Gaydos, D., Dunning, R., 2009. Dynamic creep and pre-conditioning of the achilles tendon in-vivo. *J. Biomech.*, 42, 2813-2817.
- Hendershot, B., Bazrgari, B., Muslim, K., Toosizadeh, N., Nussbaum, M.A., Madigan, M.L., 2011. Disturbance and recovery of trunk stiffness and reflexive muscle responses following prolonged trunk flexion: Influences of flexion angle and duration. *Clin. Biomech.*, 26, 250-256.
- Hoogendoorn, W.E., Bongers, P.M., De Vet, H.C.W., Douwes, M., Koes, B.W., Miedema, M.C., Ariëns, G.a.M., Bouter, L.M., 2000. Flexion and rotation of the trunk and lifting at work

- are risk factors for low back pain: Results of a prospective cohort study. *Spine*, 25, 3087-3092.
- Hult, E., Ekström, L., Kaigle, A., Holm, S., Hansson, T., 1995. In vivo measurement of spinal column viscoelasticity—an animal model. *Proc Inst Mech Eng H*, 209, 105-110.
- Keller, T.S., Holm, S.H., Hansson, T.H., Spengler, D., 1990. The dependence of intervertebral disc mechanical properties on physiologic conditions. *Spine*, 15, 751-761.
- Little, J.S., Khalsa, P.S., 2005. Human lumbar spine creep during cyclic and static flexion: Creep rate, biomechanics, and facet joint capsule strain. *Ann. Biomed. Eng.*, 33, 391-401.
- Lu, D., Le, P., Davidson, B., Zhou, B.H., Lu, Y., Patel, V., Solomonow, M., 2008. Frequency of cyclic lumbar loading is a risk factor for cumulative trauma disorder. *Mus. Nerv.*, 38, 867-874.
- Machiraju, C., Phan, A.V., Pearsall, A., Madanagopal, S., 2006. Viscoelastic studies of human subscapularis tendon: Relaxation test and a wiechert model. *Comput. Methods Programs Biomed.*, 83, 29-33.
- Magnusson, S.P., Aagaard, P., Nielson, J.J., 2000. Passive energy return after repeated stretches of the hamstring muscle-tendon unit. *Med. Sci. Sports Exerc.*, 32, 1160-1164.
- Marras, W.S., Lavender, S.A., Leurgans, S., Rajulu, S., Allread, W.G., Fathallah, F.A., Ferguson, S.A., 1993. The role of dynamic three-dimensional trunk motion in occupationally-related low back disorders. *Spine*, 18, 617-628.
- Mcgill, S., Brown, S., 1992. Creep response of the lumbar spine to prolonged full flexion. *Clin. Biomech.*, 7, 43-46.
- Mcgill, S., Seguin, J., Bennett, G., 1994. Passive stiffness of the lumbar torso in flexion, extension, lateral bending, and axial rotation. Effect of belt wearing and breath holding. *Spine*, 19, 696-704.
- Mital, A., 1984. Comprehensive maximum acceptable weight of lift database for regular 8-hour work shifts. *Ergonomics*, 27, 1127-1138.
- Nussbaum, M., Chaffin, D., 1996. Development and evaluation of a scalable and deformable geometric model of the human torso. *Clin. Biomech.*, 11, 25-34.
- Olson, M.W., Li, L., Solomonow, M., 2004. Flexion-relaxation response to cyclic lumbar flexion. *Clin. Biomech.*, 19, 769-776.
- Olson, M.W., Li, L., Solomonow, M., 2009. Interaction of viscoelastic tissue compliance with lumbar muscles during passive cyclic flexion–extension. *J. Electromyogr. Kinesiol.*, 19, 30-38.
- Panjabi, M., Oxland, T., Yamamoto, I., Crisco, J., 1994. Mechanical behavior of the human lumbar and lumbosacral spine as shown by three-dimensional load-displacement curves. *J. Bone Joint Surg. Am.*, 76, 413-424.
- Panjabi, M.M., 1992. The stabilizing system of the spine. Part i. Function, dysfunction, adaptation, and enhancement. *J. Spinal Disord.*, 5, 383-383.
- Parkinson, R.J., Beach, T.a.C., Callaghan, J.P., 2004. The time-varying response of the in vivo lumbar spine to dynamic repetitive flexion. *Clin. Biomech.*, 19, 330-336.
- Prado-Leon, L.R., Celis, A., Avila-Chaurand, R., 2005. Occupational lifting tasks as a risk factor in low back pain: A case-control study in a mexican population. *Work*, 25, 107-114.
- Punnett, L., Fine, L.J., Keyserling, W.M., Herrin, G.D., Chaffin, D.B., 1991. Back disorders and nonneutral trunk postures of automobile assembly workers. *Scand. J. Work. Environ. Health*, 17, 337-346.

- Reeves, N.P., Narendra, K.S., Cholewicki, J., 2007. Spine stability: The six blind men and the elephant. *Clin. Biomech.*, 22, 266-274.
- Roy, S.H., De Luca, C.J., Casavant, D.A., 1989. Lumbar muscle fatigue and chronic lower back pain. *Spine*, 14, 992-1001.
- Ryan, E., Herda, T., Costa, P., Walter, A., Cramer, J., 2011. Dynamics of viscoelastic creep during repeated stretches. *Scand. J. Med. Sci. Sports*, 22, 179-184.
- Shin, G., D'souza, C., 2010. Emg activity of low back extensor muscles during cyclic flexion/extension. *J. Electromyogr. Kinesiol.*, 20, 742-749.
- Shin, G., D'souza, C., Liu, Y.H., 2009. Creep and fatigue development in the low back in static flexion. *Spine*, 34, 1873-1878.
- Shin, G., Mirka, G.A., 2007. An in vivo assessment of the low back response to prolonged flexion: Interplay between active and passive tissues. *Clin. Biomech.*, 22, 965-971.
- Snook, S.H., Ciriello, V.M., 1991. The design of manual handling tasks: Revised tables of maximum acceptable weights and forces. *Ergonomics*, 34, 1197-1213.
- Solomonow, M., 2011. Neuromuscular manifestations of viscoelastic tissue degradation following high and low risk repetitive lumbar flexion. *J. Electromyogr. Kinesiol.*, 22, 155-175.
- Solomonow, M., Baratta, R., Zhou, B.H., Burger, E., Zieske, A., Gedalia, A., 2003. Muscular dysfunction elicited by creep of lumbar viscoelastic tissue. *J. Electromyogr. Kinesiol.*, 13, 381-396.
- Toosizadeh, N., Nussbaum, M.A., Bazrgari, B., Madigan, M.L., 2012. Load-relaxation properties of the human trunk in response to prolonged flexion: Measuring and modeling the effect of flexion angle. *PLoS ONE*, 7, e48625.
- Troyer, K.L., Puttlitz, C.M., 2011. Human cervical spine ligaments exhibit fully nonlinear viscoelastic behavior. *Acta biomaterialia*, 7, 700-709.
- Twomey, L., Taylor, J., 1982. Flexion creep deformation and hysteresis in the lumbar vertebral column. *Spine*, 7, 116-122.
- Youssef, J., Davidson, B., Zhou, B.H., Lu, Y., Patel, V., Solomonow, M., 2008. Neuromuscular neutral zones response to static lumbar flexion: Muscular stability compensator. *Clin. Biomech.*, 23, 870-880.

4 Prolonged Trunk Flexion Can Increase Spine Loads During a Subsequent Lifting Task: An Investigation of the Effects of Trunk Flexion Duration and Angle Using a Sagittaly Symmetric Viscoelastic Spine Model

Nima Toosizadeh and Maury A. Nussbaum

Abstract

Load-relaxation of the human trunk following prolonged flexion has been observed earlier, yet the adverse effects of such viscoelastic behaviors on performing demanding tasks (e.g., lifting) remain poorly understood. Theoretically, following flexion exposures trunk stiffness reduces and this yields a compensatory increase in paraspinal muscle activation and spine loads. Here, a multi-segment model with nonlinear viscoelastic properties was developed. After evaluation, the model was used to predict changes, resulting from a range of trunk flexion exposures, in several outcome measures (i.e., peak spine load, peak axial stiffness, and absorbed energy) at L5/S1 during simulated lifting. All three measures increased (e.g., up to ~9% (~284N) increase in spine loads) following flexion exposures, and these changes were magnified by increasing flexion duration and angle. These results support prior epidemiological evidence that occupational low back injury risk is elevated when prolonged trunk flexion along with lifting are required.

4.1 Introduction

An increased risk of occupational low back disorders (LBDs) is associated with work that requires prolonged trunk flexion in combination with lifting (Hoogendoorn et al., 2000; Kuiper et al., 1999; Prado-Leon et al., 2005; Punnet et al., 1991). Trunk flexion exposures result in viscoelastic deformation of passive tissues and a consequent reduction in trunk stiffness (Hendershot et al., 2011; Kazarian, 1975; Toosizadeh et al., 2012). To achieve equilibrium, a decrease in passive stiffness may require a compensatory increase in paraspinal muscle activation (McCook et al., 2009; Olson et al., 2009; Shin and Mirka, 2007; Shin et al., 2009), in turn increasing the loads on intervertebral joints and other soft tissues. Moreover, substantial forces/intradiscal pressures develop in spinal motion segments during lifting tasks (Mientjes et al., 1999; Nachemson and Elfstrom, 1970; Wilke et al., 2001), which arise largely from the relatively small moment arms of paraspinal muscles (McGill and Norman, 1987; Tveit et al., 1994; van Dieën et al., 1999). As such, small changes in the passive stiffness of the trunk (or individual motion segments), such as due to flexion exposures, might result in important changes in spine loads (i.e., reactive compression and shear forces on spinal motion segments) during subsequent lifting tasks. One author has recommended specifically that, to reduce LBD risk, strenuous exertions should be avoided after prolonged stooping or lifting activities (McGill, 2007).

Assessing this potential injury mechanism, however, is challenging. Direct methods for measuring spine loads (e.g., intervertebral disc pressure) are invasive (Nachemson and Elfstrom, 1970; Wilke et al., 2001), and computational modeling has been used as a common alternative. However, the complex and time-dependent behavior of the human spine during prolonged task

performance has been an obstacle to estimating spine loads, particularly for tasks involving prolonged trunk flexion. Several studies have modeled the viscoelastic behavior of soft tissues to explore time-dependent kinematics/kinetics, specifically for spinal motion segments (Groth and Granata, 2008; Holmes and Hukins, 1996; Li et al., 1995; Schmidt et al., 2010; Silva et al., 2005; Wang et al., 2005) and passive muscle components (Abbott and Lowy, 1956; Glantz, 1974; Greven and Hohorst, 1975; Hedenstierna et al., 2008; Sanjeevi, 1982; Taylor et al., 1990), and primarily using poroelastic analyses and Kelvin-solid models. Poroelastic material properties of intervertebral discs can help describe/predict diverse biomechanical behaviors, such as fluid loss and pore pressure (Schmidt et al., 2010), yet these aspects are less relevant for spine load estimation and can be computationally demanding. As such, Kelvin-solid models are preferable to predict viscoelastic force-displacement behaviors of spinal motion segments and time-dependent changes in spine loads. Among several alternatives, the Standard Nonlinear Solid (SNS) and Prony Series models have best predicted viscoelastic responses under quasi-static conditions (Groth and Granata, 2008; Toosizadeh et al., 2012; Wang et al., 2005).

The current study investigated whether prolonged trunk flexion could affect spine loads during a manual lifting task, thereby providing some support for a potential injury mechanism consistent with epidemiological evidence. A viscoelastic model of the upper body was developed, based on SNS components, and used to estimate spine loads during a lifting task both prior to and following simulated flexion exposures. Muscle activities increase in response to trunk flexion exposures (McCook et al., 2009; Olson et al., 2009; Shin and Mirka, 2007; Shin et al., 2009), and the mechanical effects of exposure are task specific (Hendershot et al., 2011; Toosizadeh et al., 2012). We thus hypothesized that peak spine loads during the lifting task would increase

following flexion exposures, but that this effect would be influenced by flexion angle and duration.

4.2 Methods

4.2.1 Modeling approach

A scalable, multi-segment model of the upper body was developed initially, with viscoelastic material properties defined using SNS components. A kinematics-driven approach was used to estimate muscle forces and spine loads during a simulated lifting task. The model was then calibrated and evaluated using existing data both for predicted viscoelastic behavior and spine load. Finally, the model was used to predict spine loads during the simulated lifting task, and changes in these loads were assessed by comparing values before and after flexion exposures.

A sagittally-symmetric model was developed (Figure 4.1), containing six sagittally-deformable lumbar motion segments (T12-L1 through L5-S1) and one rigid component representing all other segments (head, neck, upper arms, forearms, hands, and thorax). As in previous work (Arjmand and Shirazi-Adl, 2006; Nussbaum and Chaffin, 1996) the thorax was considered rigid during voluntary flexion. Passive muscle components were modeled in the sagittal plane (Figure 1), with posterior muscles including 18 “local” muscles and two “global” muscles. Only passive components of posterior muscles were modeled (passive contributions of abdominal muscles were assumed negligible for trunk flexion). Muscle origins, insertions, and physiological cross-sectional areas (PCSAs) were obtained from existing reports (Bogduk et al., 1992; Marras et al., 2001; Stokes and Gardner-Morse, 1999), and a wrapping mechanism was used to represent changes in global muscle paths with trunk flexion. Similar muscle insertion locations on T12-L5

were used as in a previous report (Arjmand et al., 2006), and the wrapping reactive forces were considered as external forces in the kinematic-driven approach (see below). To facilitate comparisons of model outputs with earlier results, model anthropometry was scaled to match the latter (see Appendix A).

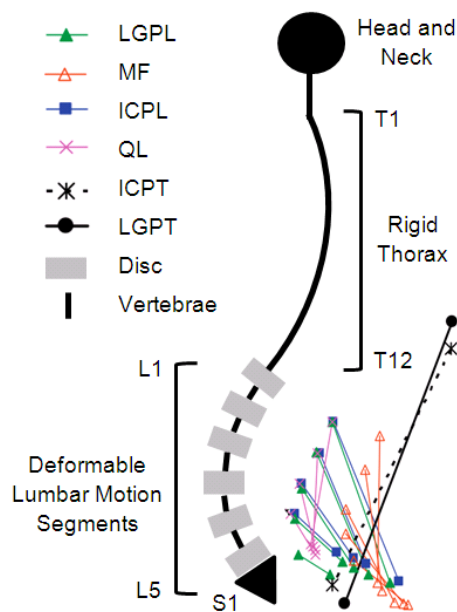


Figure 4.1: Multi-segment model in an upright posture. *Global muscles* – ICPT: iliocostalis lumborum pars thoracic, LGPT: longissimus thoracis pars thoracic. *Local muscles* – ICPL: iliocostalis lumborum pars lumborum, LGPL: longissimus thoracis pars lumborum, MF: multifidus, and QL: quadratus lumborum. Hands and arms are not illustrated in this figure, and the figure is not to scale.

Axial and rotational stiffness of each lumbar motion segment, and muscle stiffness along the line of action, were modeled using SNS components (Figure 4.2). Elastic properties ($K_1 + K_2$) of these SNS components were defined in several steps. Existing data (Bazrgari et al., 2008; Guan et al., 2007; Panjabi et al., 1994) for spinal motion segments were used to define elastic properties for axial compression and sagittal rotation (Appendix). Muscle elastic properties were

developed from McCully and Faulkner (1983), as a relationship between muscle-tendon passive force (F_P) and axial displacement (L):

$$F_P = F_{max} \left(1.066e^{-8} \times e^{17.49 \frac{L}{L_0}} \right) \quad (4.1)$$

where L_0 is the optimal length and F_{max} is the maximum contractile force. Optimal length was estimated separately for each trunk extensor muscle group, by normalizing model-estimated muscle length at 80% of full trunk flexion (L_n) to the optimal sarcomere length (L_s) as in Equation 2. Specific L_s values were obtained from Delp et al., (2001), as 2.36, 2.38, 2.37, and 2.31 μm for multifidus, quadratus, iliocostalis, and longissimus, respectively.

$$L_0 = 2.38 \times 10^{-6} \times \frac{L_n}{L_s} \quad (4.2)$$

The noted posture (80% of full trunk flexion) was selected based on previous work (Keller and Roy, 2002; Raschke and Chaffin, 1996), as estimating the optimum lengths of trunk extensor muscles. In Equation (1), F_{max} is the product of PCSA and the maximum contractile stress (MCS). Since a wide range of values have been reported for MCS, this parameter was estimated using earlier data on flexion-relaxation (FR) angles (Toosizadeh et al., 2012). Specifically, at the mean FR angle found in the noted study, MCS was estimated using static moment equilibrium (between passive and external moments) at L5/S1. Estimated MCS was 42.7 N/cm², within the range previously reported (e.g., Bean et al., 1988; Reid et al., 1987). Only the L5/S1 level was considered here, since origins of all trunk extensor muscles were at S1.

Subsequently, viscous properties were defined using previous experimental results for lumbar motion segments (Adams and Dolan, 1995; Holmes and Hukins, 1996; Johannessen et al., 2004) and trunk muscles (Abbott and Lowy, 1956; Best et al., 1994; Magnusson et al., 2000; Sanjeevi, 1982). Since these data were not sufficient to define viscoelastic properties of all spinal motion

Table 4.1: Estimated relationships between viscous (K_1 and C) and elastic (K_2) components of spinal motion segments and muscles in the model.

Spinal Level	Sagittal Rotation ($K_1/(K_1+K_2)$)	Sagittal Rotation ($C/(K_1+K_2)$)	Axial Deformation ($K_1/(K_1+K_2)$)	Axial Deformation ($C/(K_1+K_2)$)
T12-L1	0.264599	0.000231	0.827198	0.000185
L1-L2	0.300003	0.000243	0.802620	0.000103
L2-L3	0.332149	0.000254	0.826371	0.000116
L3-L4	0.351766	0.000272	0.761870	0.000296
L4-L5	0.370069	0.000301	0.856839	0.000191
L5-S1	0.387462	0.000315	0.856839	0.000191
Muscles	-	-	0.792644	0.019917

segments and muscle groups at different loading magnitudes, they were only used to approximate the relationships between viscous (K_1 and C) and elastic ($K_1 + K_2$) components (Table 4.1). First, ($K_1 + K_2$) values were estimated for each SNS segment of the model (as above), second, separate SNS equations were fit to load-relaxation data of spinal motion segments and muscles from available *in vitro* studies. Finally, using the elastic properties ($K_1 + K_2$) and fitted SNS models, relationships between viscous and elastic components for each spinal motion segment and muscle in the current model were derived.

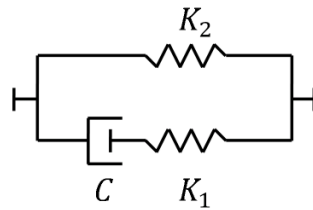


Figure 4.2: SNS model representation of intervertebral discs and passive muscles. Here, K_1 and C are the respective stiffness and damping of a torsional/linear spring and damper components in series (Maxwell component), and K_2 is the stiffness of a parallel torsional/linear spring (Roylance, 2001). K_1 and C represent viscous responses to deformation, K_2 is the steady-state stiffness once the material is totally relaxed, and $K_1 + K_2$ is the instantaneous stiffness. The moment-time equation for the SNS model at a constant flexion angle of θ_0 is

$$M(t) = \theta_0 \left(K_2 + K_1 e^{-\frac{K_1 t}{C}} \right).$$

An inverse dynamics algorithm was used to estimate muscle forces and spine loads during simulated lifting. Kinematics and external kinetics of the pelvis, trunk, and lumbar motion segments during lifting were obtained from a previous study (Bazrgari et al., 2007), and were entered into the viscoelastic model to estimate the required moment (i.e., for equilibrium corresponding to prescribed kinematics) at each lumbar level. Using these moments, a separate algorithm estimated active muscle forces with an objective of minimizing the sum of cubed muscle stresses (as in Arjmand and Shirazi-Adl, 2006 and Raikova and Prilutsky, 2001). A similar posterior muscle architecture was used as in the passive model, but with the inclusion here of abdominal muscles (i.e., rectus abdominus, internal oblique, and external oblique; origin/insertion in Appendix A). Using an iterative procedure, muscle forces were estimated that satisfied moment equilibrium at each lumbar level, with iterations continued at each time step until convergence of estimated forces. Otherwise, the muscle forces were treated as external forces and iterations were continued. ABAQUS (SIMULIA Inc., Version 8.5) implicit dynamics, with a 0.01 sec time step, was used to predict required moment and spine loads at each lumbar level using the described viscoelastic multi-segment model. Optimization analyses were performed in Python (Python IDLE, Version 3.1.2).

4.2.2 Model calibration and evaluation

Experimental load-relaxation results (Toosizadeh et al., 2012) were used to adjust the model's viscoelastic behavior in response to prolonged trunk flexion. Mean values of participant body mass, stature, and FR angles from that study were used to update scalable model properties (i.e., model geometry, muscle PCSAs, segment masses, and MCS). A period of 16 minutes of load-relaxation was then simulated in the model, for five levels of trunk flexion specified relative to

the mean observed FR angle (specifically, 30, 40, 60, 80, and 100% of FR angle). Moment-time curves of the trunk from the model and experiments were compared using fitted SNS models, and the following correction ratios were determined:

$$P_1 = \frac{K_1^{Experiment}}{K_1^{Model}}, P_2 = \frac{K_2^{Experiment}}{K_2^{Model}}, \text{ and } P_3 = \frac{C^{Experiment}}{C^{Model}} \quad (4.3)$$

Model-predicted material properties of spinal motion segments in sagittal rotation and passive muscle components were modified using these correction ratios (P_1 , P_2 , and P_3), and the same procedure was repeated until convergence of the ratios. Finally, coefficients of determination (R^2) and root-mean-square errors (RMSE) were obtained at each flexion angle, from linear regression of moment-time curves from the model vs. earlier results regarding load-relaxation (Toosizadeh et al., 2012).

Estimated spine loads were then compared to reported in vivo values for several quasi-static tasks (Wilke et al., 2001); for this, peak estimated loads (i.e., resultant compression and antero-posterior shear forces) at L4/L5 were converted into intradiscal pressures (Sato et al., 1999; Shirazi-Adl and Drouin, 1988). Different model settings, involving muscle wrapping and levels of abdominal muscle co-activity, were used to explore the influence of these model settings. Abdominal muscle co-activity was assigned as a percentage of maximum contractile force of each muscle group (El-rich et al., 2004). For these evaluations, anthropometry in the current model was scaled based on earlier participant data.

4.2.3 Prolonged flexion exposures

Effects of flexion angle and duration on spine loads during lifting were assessed for 15 combinations of three flexion durations (2, 4, and 16 minutes) and five trunk flexion angles (30,

40, 60, 80, and 100% of FR angle). These conditions were intended to represent a wide range of occupational exposures. Two lifting tasks were simulated, before and after each of the 15 exposure combinations. The lifting task involved a 180 N object and a peak trunk flexion of ~65 deg, and was performed quasi-statically over 5 sec (kinematics/kinetics data from Bazrgari et al., 2007). Both the wrapping mechanism and co-activation were included in all simulated lifting tasks as they provided the best model predictions (see Results). Several parameters associated with motion segment failure were estimated during the lifting tasks, as percentage increases (after vs. before flexion exposure) in: peak load, peak axial stiffness, and absorbed energy (i.e., areas under the loading and unloading moment-angle curves) at L5/S1 (Yoganandan et al., 1989). Only results for the lowest motion segment (L5/S1) are reported here, since most low back problems occur at this level and mechanical loads were expected to be the highest (Kingma et al., 1996).

4.3 Results

4.3.1 Calibration and evaluation results

Comparisons of viscoelastic responses between model and experimental results for 30%, 40%, 60%, 80% and 100% of FR yielded respective R^2 values of 0.92, 0.90, 0.96, 0.76, and 0.86 and RMSEs of 1.22, 2.28, 5.14, 8.47, and 7.81 Nm. Comparisons of measured and predicted intradiscal pressures indicated that prediction quality could be altered using different model settings (Figure 4.3). For flexion tasks with no hand load, simulations with muscle wrapping and no abdominal muscle co-activity provided reasonable predictions of intradiscal pressure. For load lifting, in contrast, intradiscal pressure was underestimated using these same settings, though model predictions were improved by adding abdominal muscle co-activity. Model

predictions with no wrapping mechanism overestimated intradiscal pressure for tasks involving greater flexion angles, and these overestimations were improved by adding global muscle wrapping.

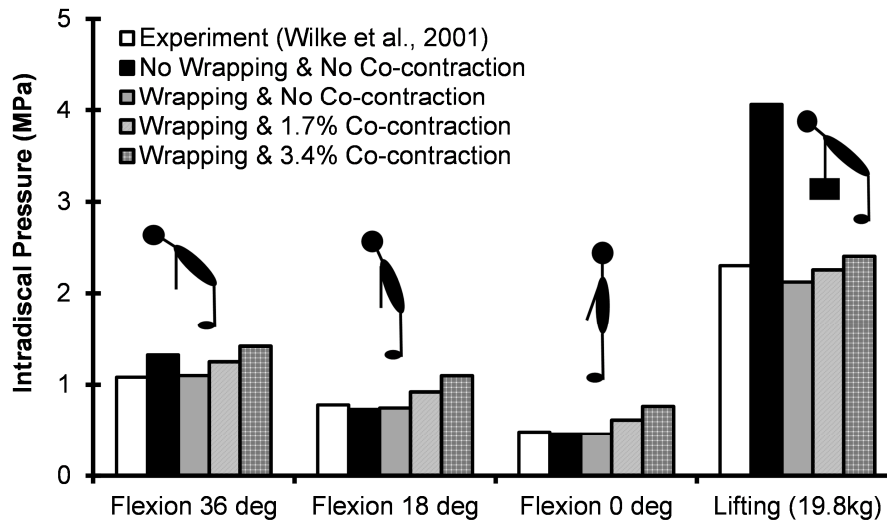


Figure 4.3: Peak intradiscal pressure at L4/L5 in several tasks from an *in vivo* experiment (Wilke et al., 2001) and predicted by the current model. Model predictions were made under different conditions of muscle wrapping and specified levels of abdominal muscle (RA, EO, and IO) co-activity.

4.3.2 Results from prolonged flexion exposures

Prior to exposure, respective values of L5/S1 peak load, peak axial stiffness, and absorbed energy during the lifting task were 3201N, 708.7N/mm, and 10.2J; all values for lifting tasks before and after flexion occurred at the maximum trunk flexion angle. These measures were predicted to increase following flexion exposures, and these increases were magnified with flexion angle and duration (Figure 4.4). Increases in all three measures were small (<2%), however, for flexion angles less than 60% FR, even after 16 min of load-relaxation exposure.

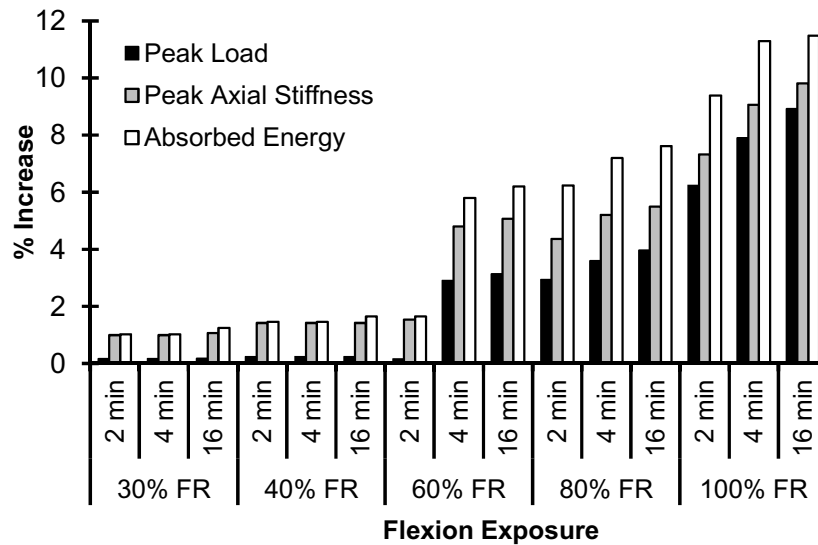


Figure 4.4: Increases in peak load, peak axial stiffness, and absorbed energy at L5/S1, following trunk flexion exposures of different durations and angles (as a % of flexion-relaxation angle = FR).

4.4 Discussion

Good agreement between model-based and experimental results was evident overall, both for viscoelastic behavior and spine load estimation. Comparing the viscoelastic behavior of the model and experimental results demonstrated reduced accuracy in predicting load-relaxation at larger flexion angles, likely resulting from the bi-phasic viscoelastic behavior of soft tissues (Toosizadeh et al., 2012). Across a range of flexion angles, however, total moment drops predicted by the model were comparable with experimental results, and suggest that spine load estimations were not substantially affected by this bi-phasic behavior. Direct validation of predicted time-dependent changes in spine loads was infeasible, since the available literature for this purpose is not sufficient; as such, only tasks with no prior flexion exposure were evaluated. However, acceptable moment drop predictions (load-relaxation behavior) and spine load estimations support the ability of the model in estimating changes in spine loads.

Increased peak spine loads were predicted following trunk flexion exposures, an effect that increased with the flexion angle. An increase in peak spine loads is consistent with our previous experimental results, wherein the magnitude of load-relaxation was more substantial following exposures to larger trunk flexion angles (Toosizadeh et al., 2012). Some additional understanding of the viscoelastic behavior of spinal soft tissues can be gained by investigating the model predictions in some additional detail (Table 4.2), particularly for the most severe flexion/lifting condition (i.e., prolonged flexion at 100% FR for 16 minutes in combination with 180N load lifting). Changes in peak muscle forces following flexion exposures were primarily in the active components, with an ~11% increase in total active muscle forces across all levels of the lumbar spine. Moreover, flexion exposure increased peak compression (~9.5%) and reduced peak shear forces (~8.5%) at L5/S1 during lifting, and these changes, especially in shear forces, were smaller at more superior spinal levels.

A previous study (Bazrgari and Shirazi-Adl, 2007) predicted peak spine loads to increase by 11.8 and 6.8% with 40 and 20% reductions in passive rotational stiffness of motion segments, respectively. Here, the passive moment reduction was ~35%, and caused an 8.9% increase in peak spine loads, roughly comparable with the noted study. Approximately 0.6 Nm of the moment drop here was caused by load-relaxation in passive muscles, which is only ~3% of the total moment drop. This supports a predominant contribution of spinal motion segments to measured viscoelastic behavior, specifically in load-relaxation. Results from our previous load-relaxation experiments (Toosizadeh et al., 2012) also supported predominant contributions of spinal motion segments (rather than passive muscle components), and we suggested that the viscoelastic behavior of the whole trunk in response to prolonged flexion was more comparable

Table 4.2: Predicted reactive moment changes, and changes in compression and antero-posterior shear forces and muscle forces (passive and active) when performing lifting task prior to (Pre) and immediately following (Post) a simulated flexion exposure of 16 min at 100%FR angle. Peak values are reported at each spinal level, for lifting 180N. Muscles are listed at the level of insertion. (See Figure 4.1 caption for a list of muscles.)

Spinal level	Reactive Moment Reduction (Nm)	Compression (N)		Shear (N)		Passive Muscle (N)		Active Muscle (N)	
		Pre	Post	Pre	Post	Pre	Post	Pre	Post
T12/L1	1.6	2165	2290	648	649	ICPT: 122	120	667	685
						LGPT: 167	162	1158	1188
L1/L2	4.5	2527	2743	454	473	ICPL: 23	22	53	79
						LGPL: 14	14	38	57
						MF: 41	39	63	94
						QL: 20	19	42	63
L2/L3	6.0	2818	3128	288	289	ICPL: 34	33	42	72
						LGPL: 16	16	24	41
						MF: 30	30	49	84
						QL: 18	18	21	36
L3/L4	4.0	2973	3277	227	195	ICPL: 41	40	0	0
						LGPL: 19	19	0	0
						MF: 47	47	0	0
						QL: 17	17	0	0
L4/L5	1.9	3105	3399	452	399	ICPL: 43	42	7	3
						LGPL: 21	21	4	2
						MF: 42	42	8	3
						QL: 16	16	2	1
L5/S1	3.0	3136	3436	648	593	LGPL: 22	22	0	0
						MF: 30	30	0	0

to isolated spinal motion segments rather than passive muscles. As such, most of the moment drop was likely compensated by additional muscle activities, and which caused the increased spinal loads.

Increases in peak spine loads depended on the duration of flexion exposure. These changes were similar for 4 and 16 minutes of exposure, however, indicating that most of the moment drop occurred within 4 minutes. Similarly, we reported earlier that a mean (SD) duration of 5.9 (3.7) minutes was required for a 90% drop relative to the initial moment (Toosizadeh et al., 2012).

Regarding occupational safety in tasks requiring prolonged trunk flexion, the risk of LBDs may thus be relatively independent of flexion duration for exposures longer than ~4-6 minutes.

In parallel with changes in peak spine load, peak axial stiffness and absorbed energy were also increased by ~10-12% during lifting following flexion exposure. In work by Yoganandan et al., (1989), spine load, axial stiffness, and absorbed energy at the initiation of trauma were measured to be 9kN, 2850Nmm⁻¹, and 10.2J for normal segments, respectively. From results here, only absorbed energy approached/exceeded the respective criterion, while other aspects (i.e., spine loads and axial stiffness) remained substantially below. Specifically, absorbed energy was ~10.2J for lifting prior to prolonged flexion, and ~11.4J following the extreme flexion exposure, indicating that an increased risk of spinal motion segment failure might exist when lifting following prolonged trunk flexion at extreme angles. Moreover, a common occupational limit for spinal compression is ~3400 N (Waters et al., 1993), and predicted peak compression force while lifting 180N was in the safe region (3136 N). Yet, performing the same task following 16 minutes of trunk flexion led to a value slightly above this limit (3436 N). Although available compression limits and estimated spinal loads here can vary substantially between individuals, in the context of job design the present results suggest that prior exposures should be considered, especially for demanding tasks such as lifting that involve high spine loads.

There are several limits in the current modeling approach that warrant discussion. Due to inadequate experimental data regarding the nonlinear viscoelastic behavior of passive tissues, some assumptions were required to define material properties of different muscle groups. Here, mean load-relaxation properties were derived from human hamstring, rat tail, and tibialis anterior

and extensor digitorum longus of rabbit muscle-tendon units (Best et al., 1994; Magnusson et al., 2000; Sanjeevi, 1984). Although viscoelastic load-relaxation behaviors of these different types of muscles are similar, and relatively small compared to the load-relaxation of spinal motion segments, the assumption of identical properties for all trunk extensor muscles might introduce some errors. Further, no previous experimental study, to our knowledge, has provided viscoelastic properties of soft tissues under different loading conditions (i.e., load-relaxation at different displacements/rotations). As such, assuming identical relationships between elastic and viscous SNS components in different loading conditions (as in Table 4.1) can also introduce errors in allocating load-relaxation to passive muscle components and spinal motion segments during flexion exposures. Lack of experimental data led to the assumption of negligible shear viscoelastic deformation of spinal motion segments, which can also introduce some errors. Another limitation was related to viscoelastic modeling of soft tissues, where the SNS model with a single relaxation time constant was used for this purpose. Previous work has identified distinct fast and slow phases of load-relaxation (creep), with the transition occurring in roughly the first 30-60 seconds of exposure (Burns et al., 1984; Toosizadeh et al., 2012). Such dual-phase behavior can be predicted by more complex models, such as Prony Series, by adding an additional relaxation (creep) time constant (Toosizadeh et al., 2012). For the current work, however, sufficient experimental data were not available. While using more complex models can improve predictions of load-relaxation, predictions of moment drop are quantitatively similar for Kelvin-solid models with differing complexity.

Here, identical kinematics were used when simulating lifting tasks prior to and following flexion exposures, though relative rotational displacements of spinal motion segments during the lifting

task could be affected by the prolonged flexion exposure, and might lead to inaccuracy in estimating spine loads. Further, load distribution among different components of spinal motion segments was not assessed here, and therefore contribution of ligaments in time-dependent spine load changes was not considered. However, previous investigations reported small load bearing from ligaments during lifting tasks (Cholewicki and McGill 1992; Potvin et al., 1991), and it can be assumed that their time-dependent contribution is negligible. Further, the dependency of motion segment stiffness in sagittal rotations on the compression force magnitude was not considered here. Our estimates of time-dependent changes in spine loads are not expected to be substantially influenced by this effect, though, since the increase in stiffness with compression force reaches an asymptotic level at forces >1000 N (Stokes and Gardner-Morse 2003). Finally, while alternative approaches exist to estimate redundant muscle forces, the optimization approach used here allowed us to simulate changes in spine load following viscoelastic deformation. However, underlying mechanisms of the neuromuscular system may be more complex and variable within/between individuals. Also, spine rotational stiffness and stability are closely related (Bazrgari and Shirazi-Adl 2007, Graham and Brown 2012), and the reduction in passive stiffness observed here could compromise trunk stability and increase the risk of LBDs (Hoogendoorn et al., 2000). To stabilize the trunk, an increase in paraspinal muscle activation and co-contraction may be required to compensate for reductions in passive stiffness (Marras and Granata 1997; Shin et al., 2009). As such, in future studies electromyography (EMG) of trunk muscles can alternatively be collected in future work and used in EMG-assisted models to estimate spine load changes in response to flexion exposures.

In summary, the current work sought to help understand how the load distribution among passive and active trunk components changes as a result of prolonged flexion exposures. There was a predicted increase in the contribution of active components required to complete a lifting task following load-relaxation exposures, consistent with available epidemiological evidence and recommendations (McGill, 2007). Of note, there are also physiological influences of prolonged (or repetitive) flexion exposure, such as fatigue, muscle inflammation, and alterations in the reflexive responses of trunk extensor muscles (Hendershot et al., 2011; Rogers and Granata, 2006; Solomonow, 2011). Such influences might further accentuate the risk of LBDs related to flexion exposure, and should be investigated in future work. Ultimately, such studies can help determine the appropriateness of diverse flexed postures during prolonged tasks and jobs, both from mechanical and physiological perspectives. Such results have potential future application in evaluating diverse occupational tasks based on time-dependent lumbar mechanics and could help control occupationally-related LBDs.

4.5 Appendix

Mass and mass center locations for model segments (Table 4.3) were derived from Bazrgari et al., (2008) and de Leva et al., (1996).

Table 4.3: Mass centers (z): vertical locations of mass centers with respect to S1 in the vertical direction, Mass centers (x): horizontal distance from corresponding vertebral centers in the antero-posterior direction, with positive indicating posterior to S1.

Spinal level	%Body mass	Mass center (z) (%Stature)	Mass center (x) (%Stature)
Head-neck	6.94	41.82	-0.70
Upper arms	2x2.8	31.31	2.10
Forearms	2x1.6	29.87	2.10
Hands	2x0.6	28.40	2.10
T1	1.28	32.72	-0.56
T2	1.38	31.31	-0.84
T3	1.47	29.87	-1.40
T4	1.58	28.40	-1.96
T5	1.68	26.88	-2.31
T6	1.78	25.31	-2.73
T7	1.88	23.68	-3.01
T8	1.99	21.98	-3.15
T9	2.10	20.22	-3.36
T10	2.19	18.40	-3.36
T11	2.30	16.47	-3.22
T12	2.39	14.31	-3.08
L1	2.50	11.97	-2.59
L2	2.59	9.45	-2.03
L3	2.70	6.83	-1.19
L4	2.79	4.12	-0.70
L5	2.91	1.44	-0.42
S1	0.00	0.00	0.00

Muscle moment arms and physiological cross section areas (PCSAs; Table 4.4) were obtained from previous work (Bogduk et al., 1992; Marras et al., 2001; Stokes et al., 1999).

Table 4.4: Physiological cross section area (PCSA), and muscle origins and insertions. “z” and “x” values are vertical and horizontal locations with respect to S1, with positive indicating superior and posterior to S1, respectively. PCSA values from this table were multiplied by two to account for bilateral muscle pairs.

Spinal level	Muscle	PCSA (%Stature ²)	Insertion (%Stature)		Origin (%Stature)	
			z	x	z	x
T12/L1	ICPT	0.000240	14.18	5.11	-0.60	2.10
	LGPT	0.000435	15.84	5.16	-1.81	2.41
	RA	0.000206	16.26	7.63	-4.82	-4.82
	IO	0.000569	12.05	0.78	1.20	-2.41
	EO	0.000488	10.06	-4.82	2.41	-2.41
L1/L2	ICPL	0.000039	9.60	2.15	-0.42	3.80
	LGPL	0.000029	9.61	2.11	-0.51	3.55
	MF	0.000035	8.74	3.31	-0.45	3.25
	QL	0.000032	9.60	2.10	1.93	1.57
L2/L3	ICPL	0.000056	7.64	1.79	0.72	2.95
	LGPL	0.000033	7.73	1.71	0.01	3.01
	MF	0.000050	6.63	2.94	-0.99	3.37
	QL	0.000029	7.64	1.72	1.81	1.63
L3/L4	ICPL	0.000066	5.74	1.32	1.08	2.65
	LGPL	0.000037	5.43	1.33	0.44	2.65
	MF	0.000077	4.12	2.45	-1.71	3.68
	QL	0.000027	5.74	1.27	1.57	1.69
L4/L5	ICPL	0.000069	3.85	1.17	1.39	2.23
	LGPL	0.000040	3.53	1.16	0.80	2.35
	MF	0.000067	2.61	2.45	-1.78	3.92
	QL	0.000025	3.85	1.03	1.27	1.69
L5/S1	LGPL	0.000042	1.24	1.55	0.00	2.35
	MF	0.000049	0.91	2.65	-1.83	4.04

Abdominal muscles – RA = rectus abdominus, IO = internal oblique, and EO = external oblique
Global muscles – ICPT: iliocostalis lumborum pars thoracic and LGPT: longissimus thoracis pars thoracic. *Local muscles* – ICPL: iliocostalis lumborum pars lumborum, LGPL: longissimus thoracis pars lumborum, MF: multifidus, and QL: quadratus lumborum.

Mean values for sagittal rotation and axial compression were derived from Bazrgari et al., (2008), Guan et al., (2007) and Panjabi et al., (1994). Since the model is two-dimensional, only axial compression and sagittal rotation values are presented here (Figure 4.5).

The same elastic properties (force/displacement and moment/rotational displacement) were entered into the model to estimate axial and rotational stiffness of spinal motion segments.

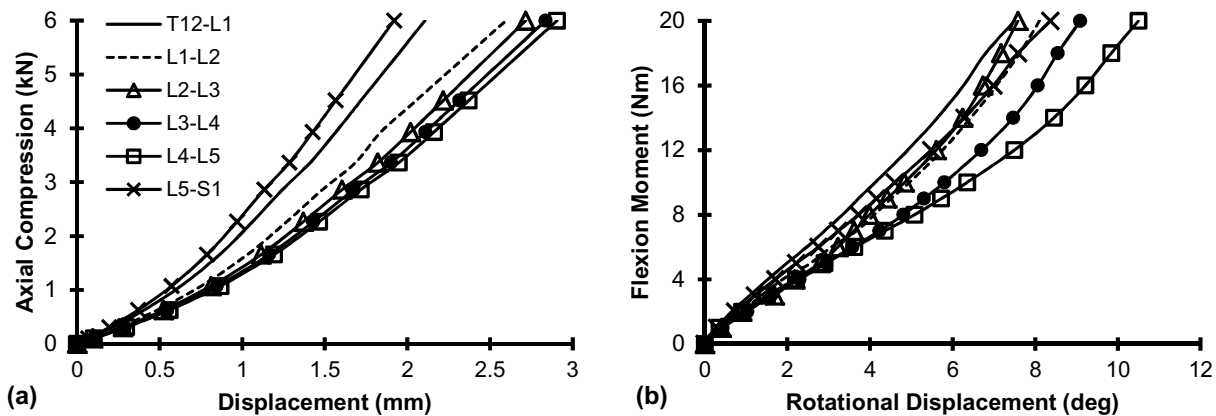


Figure 4.5: Elastic properties of lumbar motion segments in (a) axial compression, and (b) sagittal rotation.

4.6 References

- Abbott, B., Lowy, J., 1957. Stress relaxation in muscle. *Proceedings of the Royal Society of Lond. B-Biol. Sci.* 146, 281-288.
- Adams, M., Dolan, P., 1996. Time-dependent changes in the lumbar spine's resistance to bending. *Clin. Biomech.* 11, 194-200.
- Arjmand, N., Shirazi-Adl, A., 2006. Sensitivity of kinematics-based model predictions to optimization criteria in static lifting tasks. *Med. eng., phys.* 28, 504-514.
- Arjmand, N., Shirazi-Adl, A., Bazrgari, B., 2006. Wrapping of trunk thoracic extensor muscles influences muscle forces and spinal loads in lifting tasks. *Clin. Biomech.* 21, 668-675.
- Bazrgari, B., Shirazi-Adl, A., 2007. Spinal stability and role of passive stiffness in dynamic squat and stoop lifts. *Comput. Methods Biomech. Biomed. Engin.* 10, 351-360.
- Bazrgari, B., Shirazi-Adl, A., Arjmand, N., 2007. Analysis of squat and stoop dynamic liftings: muscle forces and internal spinal loads. *Eur. Spine J.* 16, 687-699.

- Bazrgari, B., Shirazi-Adl, A., Kasra, M., 2008. Computation of trunk muscle forces, spinal loads and stability in whole-body vibration. *J. Sound Vib.* 318, 1334-1347.
- Best, T.M., McElhaney, J., Garrett Jr, W.E., Myers, B.S., 1994. Characterization of the passive responses of live skeletal muscle using the quasi-linear theory of viscoelasticity. *J. Biomech.* 27, 413-419.
- Bean, J.C., Chaffin, D.B., Schultz, A.B., 1988. Biomechanical model calculation of muscle contraction forces: A double linear programming method. *J. Biomech.* 21:59-66.
- Bogduk, N., Macintosh, J.E., Pearcy, M.J., 1992. A universal model of the lumbar back muscles in the upright position. *Spine* 17, 897-913.
- Burns, M., Kaleps, I., Kazarian, L., 1984. Analysis of compressive creep behavior of the vertebral unit subjected to a uniform axial loading using exact parametric solution equations of Kelvin-solid models-Part I. Human intervertebral joints. *J. Biomech.* 17, 113-130.
- De Leva, P., 1996. Adjustments to Zatsiorsky-Seluyanov's segment inertia parameters. *J. Biomech.* 29, 1223-1230.
- Delp, S.L., Suryanarayanan, S., Murray, W.M., Uhlir, J., Triolo, R.J., 2001. Architecture of the rectus abdominis, quadratus lumborum, and erector spinae. *J. Biomech.* 34, 371-375.
- El-rich, M., Shirazi-adl, A., Arjmand, N., 2004. Muscle activity, internal loads, and stability of the human spine in standing postures: Combined model and in vivo studies. *Spine.* 29:2633-2642.
- Glantz, S.A., 1974. A constitutive equation for the passive properties of muscle. *J. Biomech.* 7, 137-145.
- Greven, K., Hohorst, B., 1975. Creep after loading in relaxed and contracted (KC1 or K 2 SO 4 depolarized) smooth muscle (taenia coli of the guinea pig). *Pflügers Arch.* 359, 111-125.
- Groth, K.M., Granata, K.P., 2008. The viscoelastic standard nonlinear solid model: Predicting the response of the lumbar intervertebral disk to low-frequency vibrations. *J. Biomech. Eng.* 130, 031005.
- Guan, Y., Yoganandan, N., Moore, J., Pintar, F.A., Zhang, J., Maiman, D.J., Laud, P., 2007. Moment-rotation responses of the human lumbosacral spinal column. *J. Biomech.* 40, 1975-1980.
- Hedenstierna, S., Halldin, P., Brodin, K., 2008. Evaluation of a combination of continuum and truss finite elements in a model of passive and active muscle tissue. *Comput. Methods Biomech. Biomed. Engin.* 11, 627-639.
- Hendershot, B., Bazrgari, B., Muslim, K., Toosizadeh, N., Nussbaum, M.A., Madigan, M.L., 2011. Disturbance and recovery of trunk stiffness and reflexive muscle responses following prolonged trunk flexion: Influences of flexion angle and duration. *Clin. Biomech.* 26, 250-256.
- Holmes, A., Hukins, D., 1996. Analysis of load-relaxation in compressed segments of lumbar spine. *Medical engineering, physics* 18, 99-104.
- Hoogendoorn, W.E., Bongers, P.M., de Vet, H.C.W., Douwes, M., Koes, B.W., Miedema, M.C., Ariëns, G.A.M., Bouter, L.M., 2000. Flexion and rotation of the trunk and lifting at work are risk factors for low back pain: Results of a prospective cohort study. *Spine* 25, 3087-3092.
- Johannessen, W., Vresilovic, E.J., Wright, A.C., Elliott, D.M., 2004. Intervertebral disc mechanics are restored following cyclic loading and unloaded recovery. *Ann. Biomed. Eng.* 32, 70-76.

- Kazarian, L., 1975. Creep characteristics of the human spinal column. *Orthop. Clin. North Am.* 6, 3-18.
- Keller, T.S., Roy, A.L., 2002. Posture-dependent isometric trunk extension and flexion strength in normal male and female subjects. *J. Spinal Disord.* 15, 312-318.
- Kingma, I., de Looze, M.P., Toussaint, H.M., Klijnsma, H.G., Bruijnen, T., 1996. Validation of a full body 3-D dynamic linked segment model. *Hum. Mov. Sci.* 15, 833-860.
- Kuiper, J.I., Burdorf, A., Verbeek, J.H.A.M., Frings-Dresen, M.H.W., van der Beek, A.J., Viikari-Juntura, E.R.A., 1999. Epidemiologic evidence on manual materials handling as a risk factor for back disorders: a systematic review. *Int. J. Ind. Ergon.* 24, 389-404.
- Li, S., Patwardhan, A.G., Amirouche, F.M.L., Havey, R., Meade, K.P., 1995. Limitations of the standard linear solid model of intervertebral discs subject to prolonged loading and low-frequency vibration in axial compression. *J. Biomech.* 28, 779-790.
- Magnusson, S.P., Aagaard, P., Nielson, J.J., 2000. Passive energy return after repeated stretches of the hamstring muscle-tendon unit. *Med. Sci. Sports Exerc.* 32, 1160-1164.
- Marras, W.S., Granata, K.P., 1997. Changes in trunk dynamics and spine loading during repeated trunk exertions. *Spine* 22, 2564-2570.
- Marras, W., Jorgensen, M., Granata, K., Wiand, B., 2001. Female and male trunk geometry: size and prediction of the spine loading trunk muscles derived from MRI. *Clin. Biomech.* 16, 38-46.
- McCook, D.T., Vicenzino, B., Hodges, P.W., 2009. Activity of deep abdominal muscles increases during submaximal flexion and extension efforts but antagonist co-contraction remains unchanged. *J. Electromyogr. Kinesiol.* 19, 754-762.
- McCully, K., Faulkner, J., 1983. Length-tension relationship of mammalian diaphragm muscles. *J. Appl. Physiol.* 54, 1681-1686.
- McGill, S., 2007. *Low back disorders: evidence-based prevention and rehabilitation.* Human Kinetics Publishers.
- McGill, S.M., Norman, R.W., 1987. Effects of an anatomically detailed erector spinae model on disc compression and shear. *J. Biomech.* 20, 591-600.
- Mientjes, M.I.V., Norman, R.W., Wells R.P., McGill, S.M., 1999. Assessment of an EMG-based method for continuous estimates of low back compression during asymmetrical occupational tasks. *Ergonomics* 42, 868-879.
- Nachemson, A., Elfstrom, G., 1970. Intravital dynamic pressure measurements in lumbar discs. *Scand. J. Rehabil. Med.* 2, 1-40.
- Nussbaum, M., Chaffin, D., 1996. Development and evaluation of a scalable and deformable geometric model of the human torso. *Clin. Biomech.* 11, 25-34.
- Olson, M.W., Li, L., Solomonow, M., 2009. Interaction of viscoelastic tissue compliance with lumbar muscles during passive cyclic flexion-extension. *J. Electromyogr. Kinesiol.* 19, 30-38.
- Panjabi, M., Oxland, T., Yamamoto, I., Crisco, J., 1994. Mechanical behavior of the human lumbar and lumbosacral spine as shown by three-dimensional load-displacement curves. *J. Bone Joint Surg. Am.* 76, 413-424.
- Prado-Leon, L.R., Celis, A., Avila-Chaurand, R., 2005. Occupational lifting tasks as a risk factor in low back pain: a case-control study in a Mexican population. *Work*, 25, 107-114.
- Punnett, L., Fine, L.J., Keyserling, W.M., Herrin, G.D., Chaffin, D.B., 1991. Back disorders and nonneutral trunk postures of automobile assembly workers. *Scand. J. Work Environ. Health*, 17, 337-346.

- Raikova, R.T., Prilutsky, B.I., 2001. Sensitivity of predicted muscle forces to parameters of the optimization-based human leg model revealed by analytical and numerical analyses. *J. Biomech.* 34, 1243-1255.
- Raschke, U., Chaffin, D.B., 1996. Support for a linear length-tension relation of the torso extensor muscles: an investigation of the length and velocity EMG-force relationships. *J. Biomech.* 29, 1597-1604.
- Reid J.G., Costigan P., 1987. Trunk muscle balance and muscular force. *Spine*, 12:783-786.
- Rogers, E.L., Granata, K.P., 2006. Disturbed paraspinal reflex following prolonged flexion-relaxation and recovery. *Spine* 31, 839-845.
- Roylance, D., 2001. Engineering viscoelasticity. Department of materials science and engineering. Massachusetts Institute of Technology. Cambridge, MA 2139, 24.
- Sanjeevi, R., 1982. A viscoelastic model for the mechanical properties of biological materials. *J. Biomech.* 15, 107-109.
- Sato, K., Kikuchi, S., Yonezawa, T., 1999. In vivo intradiscal pressure measurement in healthy individuals and in patients with ongoing back problems. *Spine* 24, 2468-2474.
- Schmidt, H., Shirazi-Adl, A., Galbusera, F., Wilke, H.J., 2010. Response analysis of the lumbar spine during regular daily activities-A finite element analysis. *J. Biomech.* 43, 1849-1856.
- Shin, G., D'Souza, C., Liu, Y.H., 2009. Creep and fatigue development in the low back in static flexion. *Spine* 34, 1873-1878.
- Shin, G., Mirka, G.A., 2007. An in vivo assessment of the low back response to prolonged flexion: interplay between active and passive tissues. *Clin. Biomech.* 22, 965-971.
- Shirazi-Adl, A., Drouin, G., 1988. Nonlinear gross response analysis of a lumbar motion segment in combined sagittal loadings. *J. Biomech. Eng.* 110, 216- 222.
- Silva, P., Crozier, S., Veidt, M., Pearcy, M.J., 2005. An experimental and finite element poroelastic creep response analysis of an intervertebral hydrogel disc model in axial compression. *J. Mater. Sci. Mater. Med.* 16, 663-669.
- Solomonow, M., 2011. Neuromuscular manifestations of viscoelastic tissue degradation following high and low risk repetitive lumbar flexion. *J. Electromyogr. Kinesiol.* 22, 155-175.
- Stokes, I.A.F., Gardner-Morse, M., 1999. Quantitative anatomy of the lumbar musculature. *J. Biomech.* 32, 311-316.
- Stokes, I.A.F., Gardner-Morse, M., 2003. Spinal stiffness increases with axial load: Another stabilizing consequence of muscle action. *J. Electromyogr. Kinesiol.* 13:397-402.
- Taylor, D.C., Dalton, J.D., Seaber, A.V., Garrett, W.E., 1990. Viscoelastic properties of muscle-tendon units. *Am. J. Sports Med.* 18, 300-309.
- Thomas, R.W., Putz-Anderson, V., Garg, A., Lawrence, J., 1993. Revised NIOSH equation for the design and evaluation of manual lifting tasks. *Ergonomics* 36, 749-776.
- Toosizadeh, N., Nussbaum, M.A., Bazrgari, B., Madigan, M.L., 2012. Load-relaxation properties of the human trunk in response to prolonged flexion: Measuring and modeling the effect of flexion angle. *PLoS ONE* 7, e48625
- Tveit, P., Daggfeldt, K., Hetland, S., Thorstensson, A., 1994. Erector spinae lever arm length variations with changes in spinal curvature. *Spine* 19, 199-204.
- van Dieën, J.H., de Looze, M.P., 1999. Sensitivity of single-equivalent trunk extensor muscle models to anatomical and functional assumptions. *J. Biomech.* 32, 195-198.
- Wang, J.L., Shirazi-Adl, A., Parnianpour, M., 2005. Search for critical loading condition of the

- spine-A meta analysis of a nonlinear viscoelastic finite element model. *Comput. Methods Biomech. Biomed. Engin.* 8, 323-330.
- Wilke, H.J., Neef, P., Hinz, B., Seidel, H., Claes, L., 2001. Intradiscal pressure together with anthropometric data-a data set for the validation of models. *Clin. Biomech.* 16, S111-S126.
- Yoganandan, N., Ray, G., Pintar, F., Myklebust, J., Sances Jr, A., 1989. Stiffness and strain energy criteria to evaluate the threshold of injury to an intervertebral joint. *J. Biomech.* 22, 135-142.

5 Trunk Tissue Creep Can Increase Spine Forces During a Subsequent Lifting Task: An Investigation of the Effects of Trunk Flexion on Spine Mechanical Behaviors Using Experimental and Viscoelastic Modeling Approaches

Nima Toosizadeh and Maury A. Nussbaum

Abstract

Prolonged trunk flexion decreases soft tissue stiffness due to viscoelastic deformations and can also lead to altered kinematics when performing a subsequent lifting task. Yet, it remains to determine if or how these changes and alterations might increase spine forces. Here, a previously-developed viscoelastic model was used, along with experimental data, to predict changes in peak spine forces during a lifting task performed following a prolonged flexion exposure (creep). Model inputs were obtained from an experiment, using 10 participants, in which lifting kinematics and muscle activity were measured both before and after creep exposure. Two sets of simulations were performed; one in which kinematics were assumed to be unchanged by creep exposure, and the other incorporating measured changes in kinematics following exposure. Post-exposure changes in lifting kinematics involved a reduction in the peak relative sagittal-plane flexion of superior lumbar motion segments and an increase in these flexion among inferior lumbar motion segments. Creep exposure caused increases in predicted peak spine forces during lifting, at all levels of the lumbar spine (77-241N). A portion (~25%) of this increase was estimated to be the result of muscular compensations for reduced passive tissue stiffness. The current study demonstrates that both changes in lifting kinematics and viscoelastic deformations, resulting from creep exposures, can lead to increased trunk muscle forces and spine forces during a lifting task. This evidence suggests a potential mechanical basis

for previous epidemiological evidence that indicates an increased risk of low back disorders for jobs involving both trunk flexion and lifting.

5.1 Introduction

Several authors have found evidence that trunk flexion combined with lifting tasks have stronger associations with low back disorder (LBD) risk compared to other occupationally-related physical exposures (Burdorf and Sorock 1997; Hoogendoorn et al., 1999; Marras 2000; Nelson and Hughes 2009). However, it is difficult to specify the separate effects of such exposures, since many occupational tasks involve combinations of exposures. With respect to trunk flexion and lifting, one author has suggested that performing a lifting task following a period of trunk flexion can expose the trunk to a substantially higher risk of a LBD (McGill 2007). This suggestion was based on the reported viscoelastic behavior of trunk soft tissues and muscle spasms following prolonged trunk flexion. To improve our understanding of LBD risk, it is important to investigate the potential interactions between risk factors. Of specific interest here is the effect of creep exposure on trunk muscle activity and trunk mechanical behaviors when performing a subsequent lifting task.

Previous work has indicated that alterations in both mechanical and neuromuscular behaviors of trunk tissues occur following creep exposures. These alterations include a reduction in passive stiffness of the trunk (Bazrgari et al., 2011; McGill and Brown 1992; Shin and Mirka 2007; Chapter3), changes in trunk kinematics, specifically the relative sagittal flexion of the lumbar spine and hip (Marras and Granata 1997), and an increase in trunk muscle activity (Bazrgari et al., 2011; Shin and Mirka 2007; Shin et al., 2009). These changes may, in turn, result in additional loads on spinal motions segments and other soft tissues, and a consequent increase in the risk of LBDs. Yet, assessing spine forces is challenging, especially using direct methods,

and computational biomechanical modeling is used as a common alternative (Arjmand and Shirazi-Adl 2006; Stokes and Gardner-Morse 1995).

Use of biomechanical models becomes challenging, however, when predicting time-dependent changes in spine forces, since such predictions require that the viscoelastic properties of soft tissues be accurately characterized. Several studies have modeled soft tissues viscoelastic behavior to explore time-dependent kinematics/kinetics, specifically for spinal motion segments (Holmes and Hukins 1996; Groth and Granata 2008; Li et al., 1995; Silva et al., 2005; Schmidt et al., 2010; Wang et al., 2005) and passive muscle components (Abbott and Lowy 1957, Hedenstierna et al., 2008; Glantz 1974; Greven and Hohorst 1975; Sanjeevi 1982; Taylor et al., 1990). Among these, Kelvin-solid models are preferable for predicting viscoelastic behaviors of trunk soft tissues and time-dependent changes in spine forces, due to the convenient definition of material properties for these models and their relatively lower computational costs (compared to more complex models such as poroelastic ones). Yet, it remains to incorporate these approaches into a biomechanical model of the trunk to allow for an assessment of time-dependent changes in spine forces (e.g., during lifting, as of interest here).

To explore time-dependent changes in spine forces, we developed and evaluated a viscoelastic model of the upper body in a previous study (Chapter 4), with the goal of investigating the effect of angle and duration of prolonged trunk flexion at constant flexion angle (load-relaxation) on spine forces during a subsequent lifting task. Results from the noted study indicated an increase in peak spine forces during lifting following trunk flexion inducing load relaxation, and these changes were magnified with flexion duration and angle. The current study aimed to investigate

the effect of prolonged flexion at constant external moment (creep) on spine forces. To achieve this, the previously developed viscoelastic, multi-segment model of the upper body was used to simulate lifting tasks before and after prolonged trunk flexion, and changes in spine forces and trunk muscle forces were estimated. One limitation of our previous approach (Chapter 4) was using identical kinematics for lifting tasks before and after creep exposures. Here, data were obtained from participants during actual lifting, to assess any alterations in the kinematics of lifting and trunk muscle activity before vs. after prolonged trunk flexion; these kinematics data were also used for model-based simulations. We hypothesized an increase in spine forces and trunk muscle activity (from both the model simulations and experiments) during a lifting task due to creep exposures. We also explored whether changes in lifting kinematics occur after trunk creep exposure, in terms of the peak relative flexion of the lumbar spine and hip, and/or the peak relative flexion of lumbar motion segments. Overall, the current study aimed to provide evidence for a potential low back injury mechanism involved during occupational tasks that require both trunk flexion and lifting.

5.2 Methods

The scalable, multi-segment model of the upper body (developed previously) was modified to account for creep responses, and was then used to estimate muscle forces and spine forces during simulated lifting tasks before and after prolonged trunk flexion. A kinematics-driven approach was again used to estimate muscle and spine forces during the simulated lifting tasks. For this, kinematics were obtained experimentally and used as model input. Below, the model development and evaluation procedure is explained briefly; for more details, readers are referred to Chapter 4.

5.2.1 Modeling approach

A sagittally-symmetric scalable model was used (Chapter 4), containing six sagittally-deformable lumbar motion segments (T12-L1 through L5-S1) and passive muscle components (18 “local” and two “global” muscles). Axial and rotational stiffness of each lumbar motion segment, and muscle stiffness along the line of action, were modeled using SNS components (Figure 5.1). Elastic properties (K_2 as in Figure 5.1) were defined using existing data (Bazrgari et al., 2008; Guan et al., 2007; McCully and Faulkner 1983; Panjabi et al., 1994) for each SNS component. Viscous properties were defined using previous experimental results for lumbar motion segments (Little and Khalsa 2005; Oliver and Twomey 1995; Twomey and Taylor 1982) and trunk muscles (Glantz 1974; Ryan et al., 2010; Ryan et al., 2011; Sanjeevi 1982). These data were subsequently used to relate viscous parameters (K_1 and C) of each SLS component with elastic parameters (K_2) within the current model (Table 5.1). Of note, this approach was used to approximate the viscoelastic properties of SLS components, since available data were not sufficient to define creep behaviors of all spinal motion segments and muscle groups at different loading magnitudes. The developed viscoelastic model was then used in combination with a kinematics-driven approach and an optimization algorithm to estimate muscle and spine forces.

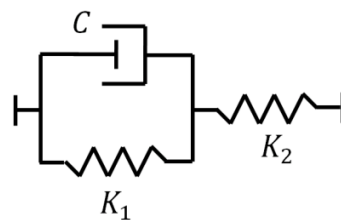


Figure 5.1: SNS model representation of intervertebral discs and passive muscles. Here, K_1 and C are the respective stiffness and damping of a torsional/linear spring and damper components in parallel (Kelvin component), and K_2 is the stiffness of a parallel torsional/linear spring (Roylance, 2001). K_1 and C represent viscous responses to deformation, $K_1 + K_2$ is the steady-state stiffness once the material is totally relaxed, and K_2 is the instantaneous stiffness. The creep angle-time equation for the SNS model at a constant external moment of M_0 is:

$$\theta(t) = \frac{M_0}{K_1} \left(\frac{K_1 + K_2}{K_2} - e^{-\frac{t}{T}} \right).$$

Table 5.1: Estimated relationships between viscous (K_1 and C) and elastic (K_2) components of spinal motion segments and muscles used in the biomechanical model.

Spinal Level	Sagittal flexion (K_1/K_2)	Sagittal flexion (C/K_2)	Axial Deformation (K_1/K_2)	Axial Deformation (C/K_2)
T12-L1	2.8	303.0	4.8	3703.7
L1-L2	2.3	370.4	4.1	6250.0
L2-L3	2.0	434.8	4.8	5882.4
L3-L4	1.8	454.6	3.2	1960.8
L4-L5	1.7	454.6	6.0	3846.2
L5-S1	1.6	476.2	6.0	3846.2
Muscles	-	-	3.8	31.5

5.2.2 Model calibration and evaluation

Experimental creep results (Chapter 3) were used to calibrate/evaluate model-predicted viscoelastic behaviors. Briefly, a 6-minute period of prolonged trunk flexion with extra loads in the hand (overall weight of 84 N for males, and 54 N for females) was simulated in the model. Creep angle-time curves of the trunk from the model and the experiment were compared, using fitted SNS models and material properties of spinal motion segments in sagittal flexion, and passive muscle components were modified within an iterative procedure. Coefficients of determination (R^2) and root-mean-square errors (RMSE) were obtained for the 6-minute prolonged trunk flexion, from linear regression of creep angle-time curves from the model vs. the experiment. In addition, estimated spine forces were compared to reported *in vivo* values for several sagittally-symmetric, quasi-static tasks (see Chapter 4 for details).

5.2.3 Flexion/lifting kinematics

Kinematics and external kinetics of the pelvis, trunk, lumbar motion segments, and upper extremities were obtained from participants when performing dynamic, stoop lifting tasks, both before and after controlled creep exposures. Ten healthy young adults, with no self-reported history of low-back pain or any current medical conditions, completed the study after providing

informed consent. All experimental procedures were approved by the Virginia Tech Institutional Review Board. Participants included six males, with respective mean (SD) age, stature, and body mass of 24 (3) yr, 183.7 (6.1) cm, and 81.2 (6.7) kg; corresponding values for the four females were 25 (3) yr, 166.9 (5.6) cm, and 66.1 (7.4) kg. A relatively young group of participants (from 18-30 yr) was included to avoid potential influences related to advanced age. Prolonged full flexion (i.e., creep exposure) was induced by participant's flexing their trunk slowly to full passive trunk flexion, remaining in this flexed posture for six minutes, and then slowly returning to the upright standing posture. During this, two additional loads (total weight of 84 N for males, and 54 N for females) were attached to their wrists. Flexion tasks were performed while participants stood in a rigid metal frame, and straps were used to restrain the pelvis.

During the lifting tasks, participants were asked to lift a box, with weight set to 25% of individual body mass, from an adjustable platform at the knee height. Five lifts were done before the creep exposure, with 2 minutes rest between lifts, and one immediately after the creep exposure. The first four pre-exposure lifts were used to provide warm up and familiarization to the task; only the final (fifth) pre-exposure lifts were used as described below. During the lifting tasks, kinematics were tracked via reflective markers, at 120 Hz, using a 7-camera motion capture system (Vicon MX, Vicon Motion Systems Inc., Denver, CO, US). Markers were placed in the mid-sagittal plane over the T12, L1, L2, L3, L4, L5, and S1 vertebrae processes, and bilaterally over ASIS, the acromial processes, lateral humeral epicondyles, radialis, styloid processes, and second metacarpal heads. Markers were also placed on the box to track the mass center. An existing transformation model was then used to estimate lumbar curvature using skin

markers (Lee et al., 1995). By connecting the centers of adjacent motion segments, an initial angle for adjacent vertebrae were estimated; changes in these angles were determined over time.

Electromyography (EMG) of the paraspinal muscles (trunk extensors) and trunk flexors on the right side were measured, using bipolar Ag/AgCl surface electrodes, to explore the force distribution among superficial trunk muscles. Electrode placements followed earlier protocols (El-Rich et al., 2004, McGill 2005), targeting the iliocostalis lumborum pars thoracic, longissimus thoracis pars thoracic, iliocostalis lumborum pars lumborum, longissimus thoracis pars lumborum, multifidus, rectus abdominus, internal oblique, and external oblique. Prior to applying electrodes, the skin was prepared using abrasion and cleaned with alcohol; raw EMG signals were pre-amplified ($\times 100$) near the collection site, then bandpass filtered (10–500 Hz), amplified, and converted to root-mean-square (RMS) in hardware (Measurement Systems Inc., Ann Arbor, MI, USA). Values were then normalized (nEMG) to peak EMG obtained from maximum voluntary contractions (MVC) performed by each participant. Six trials of MVC (three trials each in extension and flexion) were performed in standing posture. During MVCs, a rigid frame was used to constrain the lower limbs, pelvis, and trunk. Participants pulled back/pushed forward maximally for 5 seconds. Paired *t* tests were used to assess changes, before vs. after creep exposure, in peak values relative lumbar motion segment flexion (sagittal plane, as % of total lumbar flexion), total lumbar flexion, hip flexion and trunk muscle nEMG. Statistical analyses were done using JMPTM (Version 8, SAS Institute Inc., Cary, NC), and significance was concluded when $p < 0.05$.

5.2.4 Flexion/lifting simulations

Both the prolonged trunk creep exposure and the lifting tasks were simulated in the model. Two sets of lifting simulations were performed. The first assumed similar kinematics for the lifting tasks done prior to and after creep exposure (identical kinematics), by using the pre-exposure kinematics as input. Specifically, mean lifting kinematics, across participants, from the final pre-exposure lifting tasks were used as input to the model. The second considered (accounted for) changes in kinematics due to the creep exposure (modified kinematics). In this, kinematics from the final pre-exposure lifting task were used, along with kinematics from the one post-exposure lift. These two sets of simulations, using the two data sets, were performed to explore the separate effects of creep deformation and altered kinematics on any changes in spine forces following creep exposure. An additional set of simulations was done, using the modified kinematics and with only elastic (rather than viscoelastic) properties incorporated in the model. These latter simulations were used to isolate the effects of creep deformation on spine forces. From these three sets of simulations, the separate contributions of kinematic changes and creep deformation, and the joint contribution of both factors, were identified. Outcome measures obtained from the model, for a given lifting task, were peak spine forces at each level of the lumbar spine (T12-L1 through L5-S1) and peak muscle forces.

5.3 Results

5.3.1 Experiment results: kinematics and nEMG

Peak relative flexion of the lumbar motion segments changed between lifting tasks performed before versus after creep exposure. Post-exposure, the flexion of superior (i.e., T12-L1 and L1-L2) and inferior motion segments (i.e., L4-L5 and L5-S1) of the lumbar spine significantly

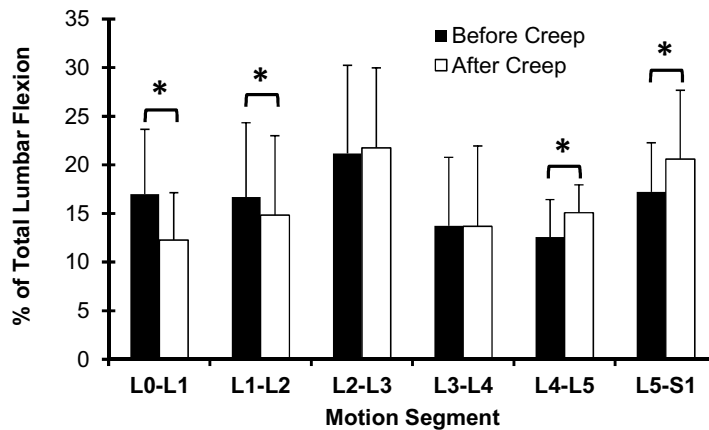


Figure 5.2: Changes in peak relative flexion of lumbar motion segments during lifting tasks performed before and after creep exposure. The symbol * indicates a significant post-exposure change.

decreased ($p < 0.025$) and increased ($p < 0.027$), respectively (Figure 5.2). No significant changes, however, were observed for the L2-L3 and L3-L4 motion segments ($p > 0.54$). Overall lumbar flexion (T12-S1) decreased post-exposure (from 64.1 to 61.1 deg, $p = 0.029$), whereas hip flexion increased (from 37.4 to 39.8 deg, $p = 0.0031$). Peak nEMG increased in all muscle groups following creep exposures (Figure 5.3), though only some of these changes were statistically significant.

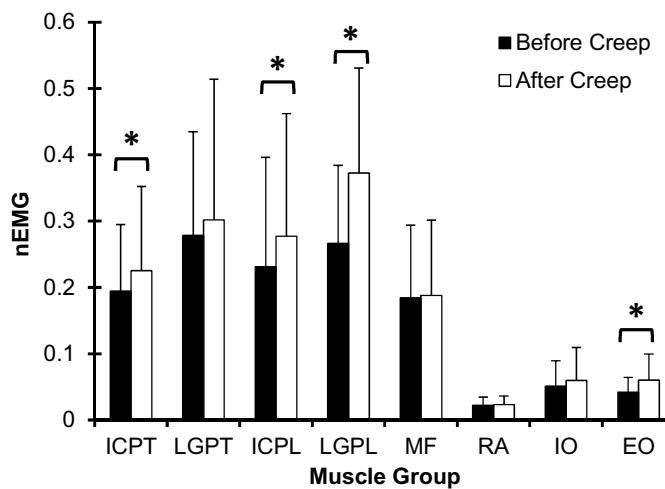


Figure 5.3: Increase in muscle activity (nEMG) during lifting tasks performed before and after creep exposure. The symbol * indicates a significant post-exposure change.

Table 5.2: Predicted changes in peak passive and active muscle forces (all values in Newton) during lifting tasks performed prior to (Pre) and immediately following (Post) a simulated 6-minute creep exposure. Muscles are listed at the level of origin.

Spinal Level	Muscle Group	Before Creep			After Creep (Identical Kinematics)			After Creep (Modified Kinematics)		
		Active	Passive	Total	Active	Passive	Total	Active	Passive	Total
T12-L1	ICPT	666	70	669	696	70	700	764	68	767
	LGPT	1156	60	1158	1209	60	1211	1329	59	1331
L1-L2	ICPL	53	20	57	57	20	60	42	20	46
	LGPL	38	12	40	41	12	43	30	12	32
	MF	63	30	70	67	35	76	50	37	62
L2-L3	QL	42	17	45	45	17	48	33	17	38
	ICPL	42	20	47	42	30	52	9	31	32
	LGPL	24	12	27	24	14	28	5	15	16
	MF	49	28	56	49	27	57	10	29	30
L3-L4	QL	21	17	27	21	16	26	4	16	17
	ICPL	0	37	37	0	36	36	34	38	51
	LGPL	0	17	17	0	17	17	19	18	26
	MF	0	44	44	0	44	44	52	45	69
L4-L5	QL	0	15	15	0	15	15	14	15	21
	ICPL	7	39	40	0	39	39	0	42	42
	LGPL	4	19	20	0	19	19	0	21	21
	MF	8	39	40	1	39	39	0	43	43
L5-S1	QL	2	14	14	0	14	14	0	15	15
	LGPL	0	20	20	0	20	20	0	22	22
	MF	0	29	29	0	29	29	0	31	31

Global muscles – ICPT: iliocostalis lumborum pars thoracic, LGPT: longissimus thoracis pars thoracic. *Local muscles* – ICPL: iliocostalis lumborum pars lumborum, LGPL: longissimus thoracis pars lumborum, MF: multifidus, and QL: quadratus lumborum.

5.3.2 Model-based results: creep, spine forces, and muscle forces

Comparison between the creep angle-time curves from the model and experimental results during creep exposure yielded respective R^2 and RMSE values of 0.99 and 0.35 deg. Peak spine forces, specifically compression and antero-posterior shear forces, were predicted to increase following creep exposure; such increases were found using both “identical” and “modified” lifting kinematics (Figure 5.4). Across all lumbar levels, respective increases in peak spine forces were 3.4 and 24.2% larger in compression and shear, when using the modified vs. identical kinematics. The largest increase in compression force occurred at the L5-S1 motion

segment, which increased by 233N following creep exposure; antero-posterior shear force had the largest increase (177 N) at the L1-L2 motion segment. Peak muscle forces (i.e., summation of passive and active forces) increased when performing the lifting task following creep exposures (Table 5.2). Post-exposure increases in peak muscles forces were larger when the modified (9.7%) vs. identical (4.1%) kinematics were used, and this increase mainly resulted from additional activity predicted in the global muscles. When using the model with elastic properties and modified kinematics, a 4% (133N) increase in compression and 7% (~49N) increase in antero-posterior shear forces were predicted at L5/S1 following creep exposure.

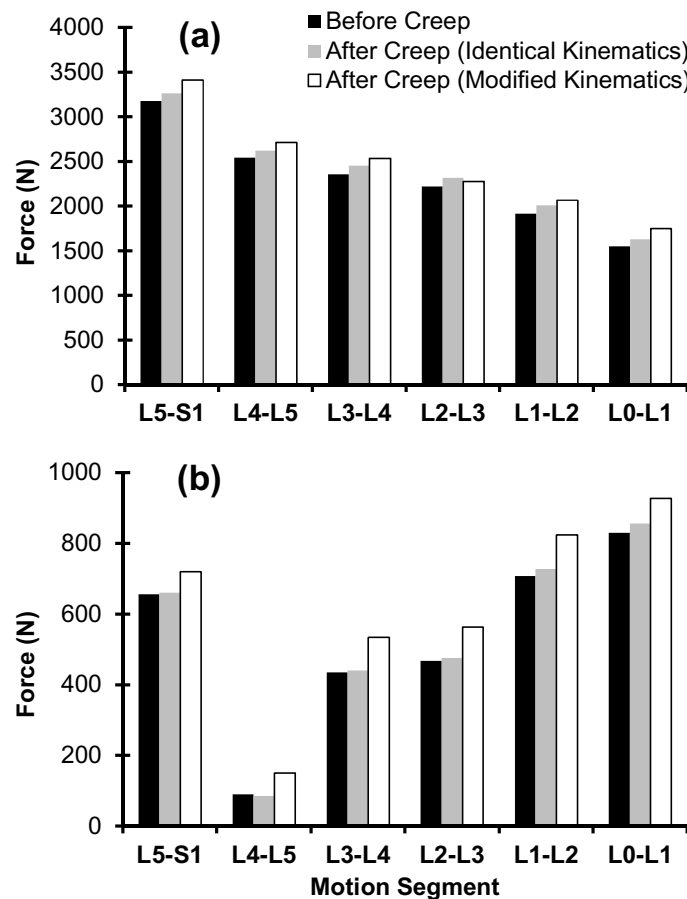


Figure 5.4: Increases in predicted peak compression force (a) and antero-posterior shear force (b) during lifting tasks performed before and after creep exposures; the latter predictions were done using identical and modified kinematics.

5.4. Discussion

Viscoelastic deformation predicted by the model had a high level of correspondence with experimental results. For example, the difference between model predicted and experimental values of total creep angle during 6 minutes of flexion was ~ 0.5 deg, which was only 8% of the total creep angle. As such, it is expected that estimated decreases in stiffness within trunk passive components was reasonably well predicted using the model. Direct evaluation of time-dependent changes in spine forces was infeasible due to the lack of available literature, and for this reason the model was only evaluated for specific tasks without prior creep exposure. However, earlier comparisons of spine forces (Chapter 4) and viscoelastic behaviors between experimental studies and model predictions support the ability of the model to estimate time-dependent changes in spine forces.

In support of the study hypotheses, alterations in kinematics and spine forces during lifting were observed as a result of prolonged trunk flexion exposure. After such exposures, the contribution of hip flexion total trunk flexion during lifting increased, while the total lumbar flexion decreased. This effect of flexion exposure is consistent with previous work that reported qualitatively similar changes in hip and lumbar flexion when performing a lifting task following repetitive lifting (Marras and Granata 1997). As suggested by these authors, this trade-off between hip and lumbar flexion may be used to help decrease trunk external moments via reducing the moment arm between L5-S1 and the load and/or trunk masses. However, as was apparent here from the model results, these kinematic changes did not fully compensate for other mechanical alterations induced by flexion exposure, and predicted spine forces were larger following these exposures. Also, within the lumbar spine there was a post-exposure reduction in

the peak relative flexion of superior lumbar motion segments and an opposite increase in flexion of inferior lumbar motion segments. Although between-subject variability of the magnitude of these kinematic changes was substantial, a similar qualitative pattern of kinematics changes was observed among almost all participants. While an increase in peak spine forces was found as a result of changes in the peak relative flexion of lumbar motion segments, the underlying mechanisms responsible for these changes, and/or any physiological benefits (or disadvantages), are not obvious.

For compression forces, predicted increases in peak values were 2.5% (81N) for identical kinematics and 7.3% (233N) for modified kinematics. Of note, accounting for changes in lifting kinematics increased the levels of predicted antero-posterior shear force in superior levels of lumbar spine up to ~16% (117N). Overall, these changes following flexion exposure emphasize the importance of considering both viscoelastic deformations and kinematics alterations for task assessment. Accordingly, to explore the effect of viscoelasticity on model estimates of spine forces, the simulation was performed with only elastic material properties. Without viscoelasticity, model outputs indicated a 4.3% increase in total spine forces (i.e., summation of compression and antero-posterior forces) only as a result of changes in lifting kinematics. As such, using elastic biomechanical models may lead to underestimation of changes in spine forces following flexion exposures. Such errors would be of particular importance when assessing tasks involving prolonged (or repetitive) loading.

An increase in peak predicted muscle forces was evident during lifting tasks following the flexion exposure; such increases were found for all model simulations. Passive muscle forces

during lifting tasks were predicted to decrease by only 0.7% (~4N) when using identical kinematics. These observations suggest a predominant contribution of spinal motion segments in providing viscoelastic deformation, rather than passive muscle components. A similar conclusion regarding the relative contribution of motion segments and muscles was drawn in our previous investigation of responses to load-relaxation exposures (Toosizadeh et al., 2012; Chapter 4). Additional trunk muscle activity was also directly observed here, during lifting tasks performed before and after a flexion exposure. Active muscle forces from the model and experimental results (nEMG) indicated comparable levels of increased activity in global muscles post-exposure (overall respective increases of 14.8 and 12.3%). However, model predictions of local muscle activity were inconsistent with the nEMG measured. Specifically, model predictions indicated a 9% decrease in active muscle forces post-exposure, while nEMG increased by a mean of 21% across participants. As such, the model-based predictions of spine forces are likely underestimates of actual values. However, since the maximum force capacity of local muscles is relatively small (Marras et al., 2001), the magnitude of this underestimation is likely modest.

An increased level of co-activity was observed when participants performed the lifting task following flexion exposure, with mean 22% increase of nEMG across all abdominal muscle groups. This increase, though, was statistically significant only for external oblique, perhaps due to the large variability in observed muscle activity levels. Additional co-activity can impose additional forces on lumbar motion segments, and may therefore be an additional mechanism whereby flexion exposure increases the risk of a LBD during a subsequent lifting task. This increase in co-activity post-exposure, however, was not predicted by the model, and likely is a

second contribution to underestimates of actual spine forces. In future studies, alternative approaches, such as EMG-assisted and optimization hybrid models or coupled objective approaches (using stability criterion), could be implemented to provide better predictions of changes in muscle activity.

As noted, there was substantial between-subject variability in observed changes of muscle activity (nEMG) when performing a lifting task following flexion exposure. At the extremes, one participant had slightly reduced muscle activity (~4%) following creep exposure, while for another muscle activity increased more substantially (~40%). Notable differences in kinematics changes were evident when comparing the lifting kinematics for these particular individuals. The former had more substantial changes in lumbar motion segment flexion compared to other participants, specifically the highest post-exposure reduction in peak relative flexion in superior levels and the largest increase in peak relative flexion of inferior levels. For the latter participant (with a 40% increase in muscle activity), an increase in peak relative flexion in superior levels and a reduction in inferior levels was observed that was in contrast to other participants. In terms of LBD pathology, both types of flexion-induced alterations (i.e., increase in muscle activity and changes in lumbar motion segment flexion) may contribute to soft tissues injury (McGill 2007). Thus, the risk of LBD development may involve different mechanisms that result from individual differences in mechanical and neuromuscular responses to prolonged flexion.

There are several limitations in the current work that merit discussion. First, assumptions were made to define viscoelastic material properties for passive muscles, due to the lack of sufficient experimental results. Viscoelastic material properties in response to prolonged loading were

derived here from human hamstring, rat tail, and papillary muscles (Glantz 1974, Sanjeevi 1982, Ryan et al., 2010, Ryan et al., 2011). The assumption of identical viscoelastic properties for all trunk extensor muscle groups likely introduced some errors. Further, viscoelastic responses of soft tissue under prolonged loading have not been reported for different loading magnitudes, and assumptions made here that identical relationships exist between elastic and viscous SNS components in different loading magnitudes (as in Table 5.1) contributed to inaccuracy in predicting trunk viscoelastic behaviors. These properties were, however, evaluated and calibrated based on empirical measures (responses to creep exposures), and are considered to provide the best predictions of viscoelastic behaviors given available evidence. Second, use of an SNS model with a single retardation time constant does not capture the dual-phase creep responses of spinal motion segments (Chapter 4). This limitation could be addressed using more complex models, such as Generalized-Kelvin Solid models (Chapter 3), though relevant experimental data are not available for defining material properties in such models. Third, predictions of the load distribution among different components of spinal motion segments were not evaluated here, and would be quite difficult to achieve in a non-invasive manner. Among these components, the contributions of ligaments to changes in spine forces were not considered. However, previous investigations have reported relatively small magnitudes of load bearing from ligaments during lifting tasks (Cholewicki and McGill 1992; Potvin et al., 1991), and time-dependent changes in such load bearing are likely even smaller.

In summary, the current study, consistent with earlier reports, provides evidence that exposure to trunk flexion changes kinematics and mechanical loading during a subsequent lifting task. An adjustment between the load sharing between active and passive tissues was apparent, and was

likely an adaptation to viscoelastic deformation. This adjustment led to increased contributions from active muscle force, and consequently additional forces on spinal motion segments. As such, the current study provides evidence consistent with previous epidemiological studies that a combination of risk factors (here, prolonged trunk flexion and lifting) may contribute to the risk of LBD development. Models accounting for time-dependent effects of task demands, and associate tissue responses, may thus be of future benefit for job evaluation and design.

5.5 References

- Abbott, B., Lowy, J., 1957. Stress relaxation in muscle. *Proc. R. Soc. Lond. B. Biol. Sci.*, 146, 281-288.
- Arjmand, N., Shirazi-Adl, A., 2006. Sensitivity of kinematics-based model predictions to optimization criteria in static lifting tasks. *Med. Eng. Phys.*, 28, 504-514.
- Bazrgari, B., Hendershot, B., Muslim, K., Toosizadeh, N., Nussbaum, M.A., Madigan, M.L., 2011. Disturbance and recovery of trunk mechanical and neuromuscular behaviours following prolonged trunk flexion: Influences of duration and external load on creep-induced effects. *Ergonomics*, 54, 1043-1052.
- Bazrgari, B., Shirazi-Adl, A., Kasra, M., 2008. Computation of trunk muscle forces, spinal loads and stability in whole-body vibration. *J Sound Vib*, 318, 1334-1347.
- Burdorf, A., Sorock, G., 1997. Positive and negative evidence of risk factors for back disorders. *Scand. J. Work. Environ. Health*, 23, 243-256.
- Cholewicki, J., McGill, S., 1992. Lumbar posterior ligament involvement during extremely heavy lifts estimated from fluoroscopic measurements. *J. Biomech.*, 25, 17-28.
- El-Rich, M., Shirazi-Adl, A., Arjmand, N., 2004. Muscle activity, internal loads, and stability of the human spine in standing postures: Combined model and in vivo studies. *Spine*, 29, 2633-2642.
- Glantz, S.A., 1974. A constitutive equation for the passive properties of muscle. *J. Biomech.*, 7, 137-145.
- Greven, K., Hohorst, B., 1975. Creep after loading in relaxed and contracted (kcl or k 2 so 4 depolarized) smooth muscle (taenia coli of the guinea pig). *Pflugers Arch.*, 359, 111-125.
- Groth, K.M., Granata, K.P., 2008. The viscoelastic standard nonlinear solid model: Predicting the response of the lumbar intervertebral disk to low-frequency vibrations. *J. Biomech. Eng.*, 130, 031005.
- Guan, Y., Yoganandan, N., Moore, J., Pintar, F.A., Zhang, J., Maiman, D.J., Laud, P., 2007. Moment-rotation responses of the human lumbosacral spinal column. *J. Biomech.*, 40, 1975-1980.
- Hedenstierna, S., Halldin, P., Brodin, K., 2008. Evaluation of a combination of continuum and truss finite elements in a model of passive and active muscle tissue. *Comput Methods Biomech Biomed Engin*, 11, 627-639.

- Holmes, A., Hukins, D., 1996. Analysis of load-relaxation in compressed segments of lumbar spine. *Med. Eng. Phys.*, 18, 99-104.
- Hoogendoorn, W.E., Van Poppel, M.N.M., Bongers, P.M., Koes, B.W., Bouter, L.M., 1999. Physical load during work and leisure time as risk factors for back pain. *Scand. J. Work. Environ. Health*, 25, 387-403.
- Lee, Y., Chiou, W., Chen, W., Lee, M., Lin, Y., 1995. Predictive model of intersegmental mobility of lumbar spine in the sagittal plane from skin markers. *Clin. Biomech.* 10, 413-420.
- Li, S., Patwardhan, A.G., Amirouche, F.M.L., Havey, R., Meade, K.P., 1995. Limitations of the standard linear solid model of intervertebral discs subject to prolonged loading and low-frequency vibration in axial compression. *J. Biomech.*, 28, 779-790.
- Little, J.S., Khalsa, P.S., 2005. Human lumbar spine creep during cyclic and static flexion: Creep rate, biomechanics, and facet joint capsule strain. *Ann. Biomed. Eng.*, 33, 391-401.
- Marras, W., 2000. Occupational low back disorder causation and control. *Ergonomics*, 43, 880-902.
- Marras, W.S., Granata, K.P., 1997. Changes in trunk dynamics and spine loading during repeated trunk exertions. *Spine*, 22, 2564-2570.
- Marras, W., Jorgensen, M., Granata, K., Wiand, B., 2001. Female and male trunk geometry: size and prediction of the spine loading trunk muscles derived from MRI. *Clin. Biomechanics*. 16, 38-46.
- McCully, K., Faulkner, J., 1983. Length-tension relationship of mammalian diaphragm muscles. *J. Appl. Physiol.*, 54, 1681-1686.
- McGill, S., 2007. *Low back disorders: Evidence-based prevention and rehabilitation: Human Kinetics Publishers.*
- McGill, S., Brown, S., 1992. Creep response of the lumbar spine to prolonged full flexion. *Clin. Biomech.*, 7, 43-46.
- McGill, S.M., 2005. Electromyographic activity of the abdominal and low back musculature during the generation of isometric and dynamic axial trunk torque: Implications for lumbar mechanics. *J. Orthop. Res.*, 9, 91-103.
- Nelson, N.A., Hughes, R.E., 2009. Quantifying relationships between selected work-related risk factors and back pain: A systematic review of objective biomechanical measures and cost-related health outcomes. *International Journal of Industrial Ergonomics*, 39, 202-210.
- Oliver, M., Twomey, L., 1995. Extension creep in the lumbar spine. *Clin. Biomech.*, 10, 363-368.
- Panjabi, M., Oxland, T., Yamamoto, I., Crisco, J., 1994. Mechanical behavior of the human lumbar and lumbosacral spine as shown by three-dimensional load-displacement curves. *J. Bone Joint Surg. Am.*, 76, 413-424.
- Potvin, J., McGill, S., Norman, R., 1991. Trunk muscle and lumbar ligament contributions to dynamic lifts with varying degrees of trunk flexion. *Spine*, 16, 1099-1107.
- Ryan, E., Herda, T., Costa, P., Walter, A., Cramer, J., 2011. Dynamics of viscoelastic creep during repeated stretches. *Scand. J. Med. Sci. Sports*, 22, 179-184.
- Ryan, E.D., Herda, T.J., Costa, P.B., Walter, A.A., Hoge, K.M., Stout, J.R., Cramer, J.T., 2010. Viscoelastic creep in the human skeletal muscle-tendon unit. *Eur. J. Appl. Physiol.*, 108, 207-211.

- Sanjeevi, R., 1982. A viscoelastic model for the mechanical properties of biological materials. *J. Biomech.*, 15, 107-109.
- Schmidt, H., Shirazi-Adl, A., Galbusera, F., Wilke, H.J., 2010. Response analysis of the lumbar spine during regular daily activities—a finite element analysis. *J. Biomech.*, 43, 1849-1856.
- Shin, G., D'souza, C., Liu, Y.H., 2009. Creep and fatigue development in the low back in static flexion. *Spine*, 34, 1873-1878.
- Shin, G., Mirka, G.A., 2007. An in vivo assessment of the low back response to prolonged flexion: Interplay between active and passive tissues. *Clin. Biomech.*, 22, 965-971.
- Silva, P., Crozier, S., Veidt, M., Percy, M.J., 2005. An experimental and finite element poroelastic creep response analysis of an intervertebral hydrogel disc model in axial compression. *J. Mater. Sci. Mater. Med.*, 16, 663-669.
- Stokes, I.a.F., Gardner-Morse, M., 1995. Lumbar spine maximum efforts and muscle recruitment patterns predicted by a model with multijoint muscles and joints with stiffness. *J. Biomech.*, 28, 173-186.
- Taylor, D.C., Dalton, J.D., Seaber, A.V., Garrett, W.E., 1990. Viscoelastic properties of muscle-tendon units. *Am. J. Sports Med.*, 18, 300-309.
- Toosizadeh, N., Nussbaum, M.A., Bazrgari, B., Madigan, M.L., 2012. Load-relaxation properties of the human trunk in response to prolonged flexion: Measuring and modeling the effect of flexion angle. *PLoS ONE*, 7, e48625.
- Twomey, L., Taylor, J., 1982. Flexion creep deformation and hysteresis in the lumbar vertebral column. *Spine*, 7, 116-122.
- Wang, J.L., Shirazi-Adl, A., Parnianpour, M., 2005. Search for critical loading condition of the spine—a meta analysis of a nonlinear viscoelastic finite element model. *Comput. Methods Biomech. Biomed. Engin.*, 8, 323-330.

6 Conclusions

6.1 Effects of Task Conditions on Trunk Viscoelastic Behaviors

Results from *in vivo* flexion exposures of the human trunk showed important effects of flexion angle on viscoelastic behaviors, which were indicated by the magnitude of moment drop during the load-relaxation period and also changes in derived viscoelastic material properties. Smaller viscoelastic stiffness was evident with exposure to larger angles of trunk flexion, where there was an exponential increase in moment drop with flexion angle (Chapter 2). Similarly, viscoelastic stiffness decreased with external moment (achieved by additional extra loads attached to wrists) during prolonged trunk flexion. An exponential relationship was again evident, specifically for the increase in creep angle with external moment (Chapter 3).

Regarding recovery behaviors from viscoelastic deformation, a slower rate of recovery from creep was observed compared to creep deformation; even a rest period twice as long as the exposure period (to trunk flexion) was not sufficient to provide full recovery. Similar to creep development, recovery from viscoelastic deformation depended on external moment. This resulted in comparable levels of residual creep at the end of the recovery period when the trunk was exposed to flexion exposures involving different external moments. Cumulative creep resulting from repetitive flexion was influenced by external moment and flexion rate, though the latter effect was more pronounced. All of these observations support the existence of nonlinear viscoelastic behaviors of the intact trunk across exposure to different flexion conditions.

Accordingly, nonlinear viscoelastic models (such as the SNS model), instead of linear models (such as SLS model), are recommended for predicting the angle- or moment-dependency of trunk viscoelastic behaviors.

6.2 Characterizing Trunk Viscoelastic Behaviors Using Kelvin-solid Models

For both load-relaxation and creep deformations, a dual-phase behavior was observed, with more rapid changes in moment drop or creep angle during the first minute of exposure. Accordingly, more complex Kelvin-solid models, with ≥ 2 relaxation or retardation time constants, predicted this dual-phase behavior more effectively. As mentioned above, nonlinear material properties were required for these models to estimate viscoelastic behaviors in response to different trunk flexion angles and external moments. Overall, good predictions of both viscoelastic behaviors in response to prolonged trunk flexion exposures and recovery behaviors were achieved using the Kelvin-solid models. However, some limitations were apparent when fitted models were used to predict trunk viscoelastic behaviors in response to repetitive flexion. As such, material properties obtained using static conditions may not be appropriate for describing quasi-static or dynamic flexion exposures.

6.3 Changes in Spine Loads due to Prolonged Trunk Flexion

Peak spine loads when performing a lifting task increased following prolonged trunk flexion, and these increases were magnified by increasing angles and durations of flexion. Only relatively minor effects of external moment on spine loads were evident, however, though only a limited range of extra loads were investigated. Changes in lifting kinematics due to trunk flexion exposures were also evident (Chapter 5), and which caused additional changes in spine loads in a lifting task. In model-based simulations, viscoelastic deformations occurred in both spinal motion segments and passive muscle components; yet, the spinal motion segments were predicted to provide the predominant contribution to overall viscoelastic behaviors. Consequently, changes in spinal motion segment stiffness led to additional muscle activities.

These effects of flexion exposure can be considered to contribute to an increased risk of LBDs, which is consistent with epidemiological and experimental studies. Overall the present work and results can help, such as in future task evaluations, improve predictions of force distributions among active and passive components of the trunk, and also among different passive component (i.e., passive muscle components and spinal motion segments).

6.4 Limitations and Future Direction

In vivo measurement of viscoelastic properties during prolonged trunk flexion is challenging because of uncontrolled body movement. Although some level of control and assessment of such movements were done in the current work, some errors were unavoidable. These movements likely contributed to the rather large variability in measured viscoelastic properties within each exposure condition. Furthermore, material properties from the current experiments were used only to calibrate viscoelastic behaviors of the model; initial estimations of passive viscoelastic properties were derived from previous *in vitro* data. These latter data were not sufficient for developing material properties of each component in each of the different loading conditions. Therefore, some assumptions were made, and which likely contributed to errors in defining viscoelastic properties of trunk soft tissues. To avoid this in future work, additional experimental data are required to provide better predictions of load allocation among different passive components. Using such evidence, more complex models (e.g., with exact geometry) can be developed to explore stresses in intervertebral discs, ligaments, and facet joints, thereby more completely describing/characterizing spinal motion segments. Neuromuscular alterations such as changes in reflexive responses and muscle activation patterns, due to trunk flexion

exposures and stretches in ligaments, can also be added to the model to improve spine load estimations.

6.5 Summary

The main goal of the current research was to explore the potential increased risk of LBD resulting from performing tasks that require prolonged or repetitive trunk flexion. In support of previous epidemiological studies, evidence was found for increased spine loads when performing a lifting task following flexion exposure. This research is considered an initial step towards providing more accurate guidelines by incorporating time-dependent spine loading, and with the ultimate goal of reducing occupational LBD risks. However, more investigations are required in this area to provide more basic data, especially regarding the recovery of viscoelastic deformations and the effects of repetitive trunk flexion exposures.

Appendix A: Informed Consent Form

VIRGINIA POLYTECHNIC INSTITUTE AND STATE UNIVERSITY

Informed Consent for Participants

In Research Projects Involving Human Subjects

Title of Project: Musculoskeletal Biomechanics of Movement and Control
Investigator(s): Babak Bazrgari, Brad Hendershot, Michael Madigan, Khoirul Muslim, Maury Nussbaum, Nima Toosizadeh

Purpose of this Research

To understand musculoskeletal injury and improve clinical diagnoses of injury, it is necessary to understand how muscles control force and movement. The purpose of this study is to measure the relationship between human movement, force generation, and muscle activity. We are also interested in observing how gender, posture and work-task factors influence this relationship. More than 128 healthy individuals will participate throughout the course of this project, ranging in age from 18-49 years.

Procedures

We will tape adhesive markers and sensors on your skin around your abdomen and back. These sensors are EMG electrodes that measure the activity of your muscles and position sensors to measure how you move. After some preliminary warm up stretches, we may ask you to push and/or pull as hard as you can against a resistance. We may also ask you to hold or lift a weight or weighted-box and to bend forward and back. You may be requested to return for repeated testing. We may also apply quick but small perturbations to record reflexes. You may be requested to return for repeated testing. Between test sessions you may be asked to participate in specified physical conditioning as per the American College of Sports Medicine recommended guidelines.

Risks

The risks of this study are minor. However, they include a potential skin irritation to the adhesives used in the tape and electrode markers. You may also feel some temporary muscle soreness such as might occur after exercising. Subjects participating in physical conditioning may experience muscle soreness and/or musculoskeletal injury associated with inherent risks of cardiovascular, strength training and therapeutic exercise. To minimize these risks you will be asked to warm-up before the tasks and tell us if you are aware of any history of skin-reaction to tape, history of musculoskeletal injury, cardiovascular limitations. During prolonged testing, you may feel dizzy or light-headed, and there is a small risk that you could faint. To minimize these risks, you will be asked several times if you are experiencing such symptoms; if so, you will be asked to walk around or sit down as appropriate. In addition, hunger may exacerbate such risks, so you will be asked to not come to experimental sessions hungry, and small snacks will be made available should you become hungry.

Benefits

By participating in this study, you will help to increase our understanding of time-course mechanics of the spine and musculoskeletal injury mechanisms of the lower back. We hope to make this research experience interesting and enjoyable for you where you may learn experimental procedures in biomechanical sciences. We do not guarantee or promise that you will receive any of these benefits, and no promise of benefits has been made to encourage your participation.

Anonymity and Confidentiality

Experimental data collected from your participation will be coded and matched to this consent form so only members of the research team can determine your identity. Your identity will not be divulged to unauthorized people or agencies. Digital video recorded during the experimental trials will be used to track the movement of sensors by means of computer analyses and is sufficient video quality to observe individual participant characteristics. Secondary VHS-style video may be recorded to validate the digital motion data. The camera angle is placed to avoid facial or other identifying characteristics. Sometimes it is necessary for an investigator to break confidentiality if a significant health or safety concern is perceived or the participant is believed to be a threat to himself/herself or others.

Compensation

Participants required to return for multiple test sessions or participate in physical conditioning for this protocol will receive payment per the number of test sessions completed. Subjects participating in experiments as part of course or laboratory procedures will receive appropriate credit for analysis of specified data as described in the course syllabus but not for personal performance during the experimental session.

Freedom to Withdraw

You are free to withdraw from a study at any time without penalty. If you choose to withdraw, you will be compensated for the portion of the time of the study (if financial compensation is involved). You are free not to answer any questions or respond to experimental situations that they choose without penalty.

There may be circumstances under which the investigator may determine that you should not continue as a subject. You will be compensated for the portion of the project completed.

Approval of Research

This research project has been approved, as required, by the Institutional Review Board for Research Involving Human Subjects at Virginia Polytechnic Institute and State University, by the Department of Engineering science and Mechanics.

Subject's Responsibilities

I voluntarily agree to participate in this study. I have the following responsibilities:

- Inform the investigators of all medical conditions that may influence performance or risk
- Comply to the best of my ability with the experimental and safety instructions
- Inform the investigator of any physical and mental discomfort resulting from the experimental protocol
- Inform the investigator of any feelings of dizziness, light-headedness, or fainting

Subject's Permission

I have read and understand the Informed Consent and conditions of this project. I have had all my questions answered. I hereby acknowledge the above and give my voluntary consent:

Subject Name (Print): _____

Subject signature: _____ Date _____
_____ Date _____

Witness (Optional except for certain classes of subjects)

Should I have any pertinent questions about this research or its conduct, and research subjects' rights, and whom to contact in the event of a research-related injury to the subject, I may contact:

Faculty Advisor: Maury A. Nussbaum E-mail: nussbaum@vt.edu Phone 231-6053
Ishwar Puri 231-3243
Departmental Reviewer/Department Head Telephone/e-mail

David M. Moore
Chair, IRB
Office of Research Compliance
Research, Graduate Studies
540-231-4991 / moored@vt.edu

This Informed Consent is valid from January 21, 2011 to January 20, 2012.

Subjects must be given a complete copy (or duplicate original) of the signed Informed Consent

PARTICIPANT INFORMATION AND SCREENING FORM

Participant #: _____ (filled out by the experimenter)

Date: _____

Part I

Name: _____ (Last), _____ (First)

Phone: _____ Email: _____

Address: _____

Birth date (mm/dd/yyyy): _____ Age: _____

Gender (please circle): Male - Female

Race:

Caucasian

African American

Asian

American Indian/Alaska Native

Native Hawaiian/Pacific Islander

Other: _____

Occupation: _____ (Current) _____ (Previous)

Length of time at present occupation: _____ years _____

Part II

Frequency of physical exercise of 15 min or more: _____ days/week

Please describe types of exercise:

Please list any current medical conditions and/or use of medications:

Part III

Have you had any history of the following (Please circle 'Y' or 'N')?

1. Y – N : Shoulder and upper extremity problems during the past year
2. Y – N : Upper/lower back problems during the past year
3. Y – N : Falls in the past three years
4. Y – N : Lower extremity injuries in the past three years
5. Y – N : Joint replacement or joint fusion.
6. Y – N : Being treated with corticosteroids for any condition
7. Y – N : Problems caused by arthritis, muscle problems, or broken bones, etc. that limit your ability to walk or bend your joints
8. Y – N : Ear infection or drainage from the ear in the past 6 months
9. Y – N : Severe head injury, concussion, or been 'knocked out'.
10. Y – N : Problems with coordination, dizziness, or loss of balance (in the past 12 months) that seemed to occur frequently or lasted for an extended period of time.
11. Y – N : Neuromuscular/neuromotor problems
12. Y – N : Any other disorders, illnesses or injuries that you feel might interfere with this study.

For any 'yes' answer above, please describe the time, type, extent, duration, and limitations on your daily activities.

Part IV

Availability (including evening hours)

Monday: _____

Tuesday: _____

Wednesday: _____

Thursday: _____

Friday: _____

Weekends: _____

Filled out by experimenter:

Height: _____ (cm)

Weight: _____ (kg)

Torso Depth: _____ (cm)

Torso Width: _____ (cm)

L5/S1 Height: _____ (cm)

T10 distance: _____ (cm)

Subject #: _____

Date: _____

Gender: M F

Age: _____

MMH exp: _____

Height (cm): _____

Weight (kg): _____

Harness Height from L5/S1 (cm): _____

Laser Height from L5/S1 (cm): _____

L3 Height (cm): _____

L1 Height (cm): _____

T12 Height (cm): _____

S1 Height (cm): _____

FR-Angle: _____

